Reproduced by

DOCUMENT SERVICE CENTER

ARMED SERVICES TECHNICAL INFORMATION AGENCY

U. B. BUILDING, DAYTON, 2, OHIO

REEL-C 5905

A.T.I 134 246

"NOTICE: When Government or other drawings, specifications or other data are used for any purpose other than in connection with a definitely related Government procurement operation, the U.S. Government thereby incurs no responsibility, nor any obligation whatsoever; and the fact that the Government may have formulated, furnished, or in any way supplied the said drawings, specifications or other data is not to be regarded by implication or otherwise as in any manner licensing the holder or any other person or corporation, or conveying any rights or permission to manufacture, use or sell any patented invention that may in any way be related thereto."

UNCLASSIFIED

UNCLASSIFIED (CORR. CARD 1)

ATI 134 246 (COPIES OBTAINABLE FROM ASTIA-DSC)

PRINCETON UNIVERSITY, AERONAUTICAL ENGINEERING LAB., N.J.
(REPORT NO. 187)

A MIXING THEORY FOR THE INTERACTION BETWEEN DISSIPATIVE FLOWS AND NEARLY-ISENTROPIC STREAMS

CROCCO, LUIGI; LEES, LESTER 15 JAN'52 108PP TABLES, DIAGRS, GRAPHS

USN CONTR. NO. N6-ORI-270

FLOW, ISENTROPIC
PRESSURE, BASE
BOUNDARY LAYER, TURBULENT

AERODYNAMICS (2)
FLUID MECHANICS (9)

UNCLASSIFIED

FORMERLY ATI 134 264

ATI No. 134
CADO FILE COPY
2446

A MIXING THEORY FOR THE INTERACTION BETWEEN DISSIPATIVE FLOWS AND NEARLY-ISENTROPIC STREAMS

By

LUIGI CROCCO and LESTER LEES

PRINCETON UNIVERSITY

AERONAUTICAL ENGINEERING LABORATORY

Report No. 187

January 15, 1952

UNITED STATES NAVY

Office of Naval Research
Mechanics Branch, Mathematical Sciences Division

and

UNITED STATES AIR FORCE

Air Research and Development Command

(Contract N6-ori-270, Task Order #6,

roject Number NR 061-049)

A MIXING THEORY FOR THE INTERACTION BETWEEN DISSIPATIVE FLOWS AND NEARLY-ISENTROPIC STREAMS

By

Luigi Crocco and Lester Lees

PRINCETON UNIVERSITY

AERONAUTICAL ENGINEERING LABORATORY

Report No. 187

January 15, 1952

ACKNOWLEDGEMENT

A major portion of the support for the present study was furnished jointly by the Office of Naval Research (U.S.N.), Mechanics Branch, and by the United States Air Force Research and Development Command, as part of a broad program of theoretical and experimental research on viscous effects in supersonic flow being conducted by the Department of Aeronautical Engineering, Princeton University.

The authors are grateful for the valuable assistance of Mr. C. E. Cohen, Daniel and Florence Guggenheim Fellow in Jet Propulsion.

The numerical computations were carried out by Mrs. Alberta J. Mozley, and the Misses Carol Knoderer, Margaret Liptak and Shirley Itter, Assistants in Research.

TABLE OF CONTENTS

	Page
SUMMARY	
LIST OF SYMBOLS	
1. Introduction	1
2. General Theory	5
2.1 Basic Equations of Motion	5
2.2 Expression for the Mean Temperature: the F-χ Curve	10
2.3 Mixing Rate and Friction Coefficient	20
2.4 Reduction of Equations of Motion to a Single Equation for Constant Mixing Coefficient	24
2.5 Critical Point of the Equation for $\frac{dF}{d\omega_2}$ and its Significance	27
3. Application to Base Pressure Problem in Plane Supersonic Flow	30
4. "Simplified" Mixing Theory for Separated and Reattaching Flows and Wakes	40
4.1 Basic Assumptions and Equations	40
4.2 Characteristics of Separated and Reattaching Flows and Recompression in Wakes (Simplified Theory)	47
5. Application of Simplified Mixing Theory to Base Pressure Problem in Plane Supersonic Flow	53
5.1 Methods and Assumptions	53
5.2 Effect of Reynolds Number on Base Pressure: The Various Flow Regimes	60
6. Future Investigations	68

	Page
CONCLUSIONS	70
REFERENCES	74
Table 1. The Function J(M)	76
Figures	

SUMMARY

By means of a simplified theoretical "model", the present paper treats the general class of flow problems characterized by the interaction between a viscous, or dissipative flow near the surface of a solid body, or in its wake, and an "outer" nearly-isentropic stream. For the present the external flow is taken to be a plane, steady, supersonic flow, which makes a small angle with a plane surface, or plane of symmetry, although the methods used can be extended to curved surfaces, to axially-symmetric supersonic flows, and also to subsonic flows. The internal dissipative flow is regarded as quasi-one dimensional, and parallel to the surface on the average, with a properly defined mean velocity and mean temperature. The non-uniformity of the actual velocity distribution is taken into account only approximately, by means of a relation between mean temperature and mean velocity. Mixing, or the transport of momentum from outer stream to dissipative flow, is considered to be the fundamental physical process determining the pressure rise that can be supported by the flow. With the aid of this concept a large number of flow problems are shown to be basically similar, such as boundary layer-shock wave interaction, wake flow behind blunt-based bodies (base pressure problem), flow separation in overexpanded supersonic nozzles, separation on wings and bodies, etc.

When the mixing rate is taken to be proportional to the mass flux density of the isentropic stream, the equations of motion are reduced to a single, non-linear ordinary differential equation that can be integrated numerically. An important property of this equation is the existence

of a "critical point" for supersonic wake flows, and also, under certain conditions, for supersonic flows directed toward a solid surface. This critical point acts very much like the "throat" of a nozzle in determining the base pressure, for example, or in some cases the surface pressure distribution in a boundary layer-shock wave interaction. One important reason for the marked difference between laminar and turbulent flows is the fact that the turbulent mixing rates are from 5 to 10 times larger than the laminar mixing rates.

By introducing several reasonable physical assumptions, a "simplified" form of the mixing theory is developed particularly for separated and reattaching flows, and wake flows. Separating flows as well as reattaching flows are found to be capable of supporting considerable pressure increases at high velocities. The maximum compression, as measured by the isentropic flow deflection, is roughly proportional to the square root of the mixing coefficient, and also to $(M^2 - 1)^{\frac{1}{4}}$, where M is some average Mach number. Thus the pressure ratio increases rapidly with Mach number, or the base pressure ratio, for example, decreases rapidly with increasing Mach number. In separated flows the pressure gradient along the surface is a maximum at separation, and drops off steeply downstream; in reattaching flows, or wake flows, the pressure gradient is negligible some distance upstream of the "reattachment point", and increases very rapidly toward a maximum as this point is approached. The inflected surface pressure distribution observed in laminar boundary layer-shock wave interactions with flow separation is now understandable, and the distribution itself can be calculated approximately.

When the present mixing theory is applied to the problem of determining the base pressure for a supersonic airfoil with a blunt trailing edge, it gives the correct fluid-mechanical explanation of the observed phenomena. Qualitative agreement is found between the theoretical calculations of the curve of base pressure versus Reynolds number and the data of Chapman and Bogdonoff on bodies of revolution, and Chapman's data on blunt trailing-edge airfoils. The theory is now being extended to axially-symmetric supersonic flows.

The results obtained in the base pressure problem for a supersonic airfoil with a blunt trailing edge open the way for application of the mixing theory to boundary layer-shock wave interactions, boundary layer separation, and many other phenomena. However, the dependence of the mixing rate and the mean velocity-mean temperature relation for the dissipative flow region on the flow parameters must be carefully investigated experimentally and theoretically, and the results incorporated into the analysis.

LIST OF SYMBOLS

The subscript "e" denotes quantities in the nearly-isentropic flow; the subscript "1" denotes mean quantities for the dissipative flow; the subscript "cr" signifies values taken at the critical point of the basic differential equation. Except where otherwise noted, the subscript "s" denotes stagnation conditions. In addition, the subscript "i" applies to quantities of the equivalent incompressible flow in the Stewartson transformation; the subscript "b" denotes quantities in the airfoil boundary layer just upstream of the trailing edge; the subscript "b'" denotes quantities evaluated in the mixing zone just aft of the trailing edge, while the subscript "j" applies to the mixing zone in general.

x,y	coordinates parallel and normal to surface, or plane of symmetry.
δ	thickness of dissipative flow region.
p	pressure
ρ	density
T	temperature
h	enthalpy
a	speed of sound
μ	ordinary coefficient of viscosity
γ	ratio of specific heats, c_p/c_v
R	gas constant
u_e	magnitude of local velocity of nearly-isentropic stream at $y = \delta$

M	Mach number, u_e/a_e
θ	local angle between external stream and x-axis at $y = \delta$
ν	characteristic angle variable of plane, isentropic supersonic flow.
$\bar{p}$, $\bar{M}$, $\bar{w}_e$, $\bar{\nu}$, etc.	"Free-stream" pressure, Mach number, reduced velocity, etc. far from body.
u	component of velocity parallel to surface in internal flow.
$\bar{m}$	mass flux, $\int_0^\delta \rho u \, dy$
I	momentum flux, $\int_0^\delta \rho u^2 \, dy$
δ^*	displacement thickness, $\int_0^\infty \left(1 - \frac{\rho}{\rho_e}\frac{u}{u_e}\right) dy$
δ^{**}	momentum thickness, $\int_0^\infty \frac{\rho}{\rho_e}\frac{u}{u_e}\left(1 - \frac{u}{u_e}\right) dy$ +
u_1	mean velocity of internal flow, $I/\bar{m}$
T_1	mean temperature of internal flow, defined by $\bar{m} = \frac{p}{RT_1} u_1 \delta$
w_1	u_1/a_s
w_e	u_e/a_s
m	$\bar{m}\ a_s$
ϕ_e	$\frac{T_e}{T_s}\frac{1}{\gamma w_e} = \frac{1 - \frac{\gamma-1}{2} w_e^2}{\gamma w_e}$
ϕ_1	$\frac{T_1}{T_s}\frac{1}{\gamma w_1}$

+ The symbol δ^{**} is used in order to avoid confusion with the local angle, θ.

$\varkappa$	$u_1/u_e = w_1/w_e$
f	parameter appearing in mean temperature-mean velocity relation $T_1/T_s = f - \frac{\gamma-1}{2} w_1^2$
F	$\frac{f}{\varkappa^2} - 1$
k	mixing coefficient, defined by relation $\frac{d\bar{m}}{dx} = k \rho_e u_e$
τ_W	viscous shear stress at solid surface.
c_f	local skin-friction coefficient, $\frac{\tau_W}{\frac{1}{2}\rho_e u_e^2}$
C_f	total skin-friction coefficient, $\frac{1}{X}\int_0^X c_f \, dx$
σ	$c_f/2k\,(1-\varkappa)$
δ_s, θ_s, X_s / δ_R, θ_R, X_R	thickness of dissipative flow, local angle of inclination of external stream, and coordinate of separation point (s), or reattachment point (R)
$\bar{X}$	$\frac{X}{\delta_R}$ OR $\frac{X}{\delta_s}$
$\bar{\delta}$	$\frac{\delta - \varkappa_j(\delta_j - \delta_j^*)}{\delta_R}$ OR $\frac{\delta - \varkappa_j(\delta_j - \delta_j^*)}{\delta_s}$
$\bar{\delta}_R$ OR $\bar{\delta}_s$	$1 - \varkappa_j\left(1 - \frac{\delta^*}{\delta}\right)_j$
θ_w	flow deflection across incident oblique shock.
c	airfoil chord
h	airfoil thickness at trailing edge

Re_c Reynolds number, $\frac{\bar{\rho}_e \bar{u}_e C}{\mu_{el}}$

Re_{tr} transition Reynolds number, $\frac{\rho_e u_e x_{TR}}{\mu_e}$, where x_{TR} is defined in the text where needed.

Re_{x_s} $\frac{\rho_e u_e x_s}{\mu_e}$, Reynolds number based on location of separation point.

1. Introduction.

One of the least understood phenomena in fluid mechanics is the interaction between a viscous or dissipative flow near the surface of a solid body, or in its wake, and an "outer" nearly-isentropic stream with varying static pressure. This phenomenon is observed in all types of boundary layer-shock wave interactions, in the wake behind blunt-based bodies and airfoils with blunt trailing edges at supersonic speeds (base-pressure problem), in flow separation associated with recompression in an overexpanded supersonic nozzle, in flow separation from the surface of airfoils and bodies at high angles of incidence, etc. Apart from its theoretical interest, the problem is of considerable technical importance, because of the widespread occurrence of such interactions in compressors, rocket nozzles, supersonic and subsonic diffusers and on supersonic wings and bodies.

In all these interactions, the "external flow" cannot be regarded as a known datum for the calculation of the "internal" dissipative flow. In contrast to the usual Prandtl boundary layer theory, and its extension to wakes and jets, the development of the dissipative flow itself helps to determine the external flow, and it is now generally recognized that this interplay must be made the basis of any valid theoretical treatment. It is the aim of this paper to bring out the importance of the transport of momentum from outer stream to dissipative flow (turbulent "mixing" or laminar diffusion) in determining the flow pattern and pressure rise in these interactions, and to formulate this concept in quantitative terms. By means of this concept a large number of seemingly diverse flow problems are shown to be basically similar, and therefore capable of being treated by one general theory.

Previous theoretical treatments of the interaction between an internal dissipative flow and an outer, nearly-isentropic stream do not seem to have recognized the importance of mixing. For example, in the case of the boundary layer-shock wave interaction problem, Tsien and Finston[1], Lighthill[2] and others regard the interaction between the subsonic flow field adjacent to the surface and the outer supersonic stream as paramount, and treat the problem by means of a linearized non-viscous flow theory. Their calculations show only a negligible upstream spreading of the interaction near the surface, and this result corresponds to the facts only for a turbulent boundary layer and a weak shock. Even in this case the mechanism is not correct, because it does not include the mixing between external and internal flows, and does not take into account the non-linear character of the external flow and of the interaction. The importance of mixing in determining the pressure rise that can be supported by the turbulent boundary layer in an adverse pressure gradient has already been recognized by Schubauer and Klebanoff[3] for low speed flows.

Treatments of the boundary layer-shock wave interaction problem which regard viscous effects as important, such as those of the junior author[4], utilize the ordinary Prandtl boundary layer theory to determine the rate of growth of the displacement thickness, $\frac{d\delta^*}{dx}$, in terms of the (unknown) pressure variation in the external stream. (Here, mixing is taken into account approximately). The wall is then replaced by a streamline of slope $\frac{d\delta^*}{dx}$, and the pressure variation in the external stream is obtained in terms of the curvature $\frac{d^2\delta^*}{dx^2}$ by means of the Prandtl-Meyer relation. The solution obtained for the laminar boundary layer shows an

extensive region of upstream influence and an exponential decay of the upstream pressure rise along the surface away from the shock, and predicts separation of the boundary layer ahead of the shock. While these predictions now seem to be qualitatively correct, the theory is unable to deal with the flow downstream of separation, and tells us nothing about the subsequent reattachment of the flow downstream of the reflected expansion fan, where most of the pressure rise along the surface apparently occurs. Ritter[5] recently attempted to improve upon this treatment, but the basic difficulty has not been overcome, because of the inability of the usual boundary layer theory to deal with this type of dissipative flow. Since the characteristics of the compressible turbulent boundary layer in an adverse pressure gradient are largely unknown, this technique has not been applied to the turbulent layer at all.

In the case of the base pressure problem, it has long been recognized that mixing in the wake just aft of the body must determine the amount of recompression that can be supported by the flow, and, hence, the base pressure, but this concept has never been precisely formulated. Recently Chapman[6] reviewed the entire problem, and found that existing data on base pressure could be correlated in terms of the ratio of the boundary layer thickness at the base to the base diameter. No mechanism is advanced to explain the correlation. The ordinary theory of wakes and jets, which is usually restricted to uniform pressure, is of little assistance in this problem.

Another important phenomenon involving the interaction between a dissipative flow near a surface and an "external" flow with increasing pressure in the flow direction is observed in an overexpanded supersonic

nozzle. When the ratio of chamber pressure to receiver pressure is reduced below a certain critical value, it is observed experimentally[7,8] that the oblique shocks at the nozzle exit move upstream into the nozzle. The streamlines near the nozzle wall are deflected through these shocks and the flow separates from the wall. For the conditions investigated, the flow deflection angle is remarkably constant ($\approx 14^\circ$), and the pressure ratio across the shock is about 3.0, virtually independent of nozzle divergence half-angle, in the range from 5° to 30°. The flow deflection and pressure ratio lie well below the possible maxima corresponding to the local Mach number ahead of the shock. Non-viscous flow theory establishes certain limits for the flow deflection angle and shock pressure ratio, but otherwise the problem is indeterminate without the introduction of viscosity. No theoretical explanation of this phenomenon has as yet been advanced.

It seems hopeless to attempt to solve the complete Navier-Stokes equations in detail, or these equations including the Reynolds stresses, for these interactions between an internal dissipative flow and an external, nearly-isentropic stream. What is required is a generalization of the concept of the von Kármán momentum integral for the dissipative flow region, where, however, this internal flow is treated as quasi-one-dimensional with properly defined mean velocity and mean temperature. It is essential to retain the non-linear character of the external flow and of the interaction itself. The non-uniformity of the actual velocity distribution across the internal flow is taken into account only approximately, by means of a relation between mean temperature and mean velocity. Mixing between the external and internal streams is admitted as a fundamental

physical process, which will furnish the mechanism for the pressure rise. While some of the details of the flow are undoubtedly lost, it is believed that this simplified theoretical "model" preserves the main features of the interaction with the external stream. The loss of detail is outweighed for the present by the generality of the results, and the fact that flows are treated which cannot be analyzed at all by the classical boundary layer theory.

2. General Theory.

2.1. Basic Equations of Motion.

Suppose that the flow along a plane surface or a plane of symmetry (x-axis) is characterized by two more or less distinct regions (Figure 1):* (1), an internal dissipative region of local thickness δ, in which the non-uniform velocity u is essentially parallel to the x-axis, on the average; (2), an external isentropic flow, making the local angle θ with the x-axis at $y = \delta$. For the moment θ is assumed to be sufficiently small so that $\tan\theta \approx \theta$ and $\cos\theta \approx 1$. Because of the mass transfer, or "mixing", between the external and internal streams, $\frac{d\delta}{dx} > \theta$.

In order to bring out the main aspects of the theory without becoming too involved in mathematical difficulties, the treatment is restricted for the present to plane, steady, isentropic, supersonic external flows, for which the Prandtl-Meyer relation $\frac{dp}{p} = \frac{\gamma M^2}{\sqrt{M^2-1}}\, d\theta$ holds. Actually, the analysis can be extended to axially-symmetric supersonic

---

* The treatment can be extended to the more general case of a curved surface.

flows by the method of characteristics, and shock-wave losses in the external flow can also be taken into account. In principle, subsonic external flows can also be treated by conformal mapping techniques.

The following assumptions are introduced:

(i) The static pressure p is constant across the internal flow and equal to the local pressure p_e in the external stream at $y = \delta$.

(ii) Heat transfer between the fluid and surface (if a solid surface is present) is zero, and the stagnation enthalpy h_s is constant across the flow and equal to h_{se} at $y = \delta$. The applicability of these assumptions will be discussed briefly later. (Section 6).

For the internal stream the mass flux is given by $\bar{m} = \int_0^\delta \rho u \, dy$, the momentum flux is $I = \int_0^\delta \rho u^2 \, dy$, and the flux of enthalpy is $H = \int_0^\delta h_s \rho u \, dy = \bar{m} h_{se}$. By referring to Figure 1, one sees that the angle between the streamline and the outer boundary of the dissipative flow at $y = \delta$ is $\frac{d\delta}{dx} - \theta$; therefore the rate at which mass is transported to the internal flow is

$$\frac{d\bar{m}}{dx} = \rho_e u_e \left(\frac{d\delta}{dx} - \theta\right). \tag{2.1}$$

A momentum balance yields

$$\frac{dI}{dx} = u_e \frac{d\bar{m}}{dx} - \delta \frac{dp}{dx} - \tau_w , \tag{2.2}$$

where τ_w is the frictional stress at the surface (if a surface is present). Since h_{s_e} is constant the energy equation is automatically satisfied under the assumption (ii) above.

The momentum equation (E . 2.2) represents the integral of the exact equations of motion across the flow, except that the gradients of the viscous or Reynolds stresses in the flow direction are considered to be negligible in comparison with the pressure gradient. Up to this point the approach does not differ essentially from the von Kármán momentum integral method of ordinary boundary layer theory.

Let an average velocity of the internal flow be defined by the relation

$$(2.3) \qquad u_1 = \frac{I}{\overline{m}} \quad ,$$

i.e. the ratio of the momentum flux to the mass flux. Let us also define, without attributing any particular physical meaning to the definition, a mean density ρ_1 , or a mean temperature T_1 through the mass flow relation

$$(2.4) \qquad \overline{m} = \rho_1 u_1 \delta = \frac{p}{RT_1} u_1 \delta$$

Introducing the displacement and momentum thicknesses of ordinary boundary layer theory *

$$(2.5a) \qquad \delta^* = \int_0^\delta \left(1 - \frac{\rho u}{\rho_e u_e}\right) dy = \delta - \int_0^\delta \frac{\rho u}{\rho_e u_e}\, dy = \delta - \frac{\overline{m}}{\rho_e u_e}$$

$$(2.5b) \qquad \delta^{**} = \int_0^\delta \frac{\rho u}{\rho_e u_e}\left(1 - \frac{u}{u_e}\right) dy = \delta - \delta^* - \int \frac{\rho u^2}{\rho_e u_e^2}\, dy = \delta - \delta^* - \frac{I}{\rho_e u_e^2}$$

---

* δ^{**} has been used here to indicate the momentum thickness in order to avoid confusion with the angle of flow, θ .

From these equations $\overline{m}$ and I can be derived and replaced in (2.3) and (2.4) to obtain the following expressions for the mean quantities in terms of the thicknesses:

$$\text{(2.6a)} \quad \frac{u_1}{u_e} = \mathcal{H} = \frac{\delta - \delta^* - \delta^{**}}{\delta - \delta^*}$$

$$\text{(2.6b)} \quad \frac{\rho_1}{\rho_e} = \frac{T_e}{T_1} = \frac{(\delta - \delta^*)^2}{\delta(\delta - \delta^* - \delta^{**})}$$

where $\mathcal{H} = \frac{I}{\overline{m} u_e}$ is an important parameter always less than 1. The definition of the thickness δ will be discussed in Section 2.2.

Non-dimensional reduced velocities $w = u/a_s$ are now introduced by dividing through by the stagnation speed of sound a_s. The auxiliary quantities

$$\text{(2.6c)} \quad \varphi_1 = \frac{T_1}{T_s}\frac{1}{\gamma w_1}, \qquad \varphi_e = \frac{T_e}{T_s}\frac{1}{\gamma w_e} = \frac{1 - \frac{\gamma - 1}{2} w_e^2}{\gamma w_e}$$

are defined, in terms of which the Bernoulli equation can be written as

$$\text{(2.6d)} \quad \frac{dp}{p} = -\frac{dw_e}{\varphi_e}$$

Useful relations are also

$$\text{(2.6e)} \quad \rho_e u_e a_s = \frac{p}{\varphi_e}; \qquad \rho_e u_e^2 = \frac{p w}{\varphi_e}$$

The reduced mass flow is then given by

$$(2.7)\quad \overline{m} = m a_s = \frac{p\delta}{\varphi_1} = \frac{I}{w_1},$$

and Equations (2.1) and (2.2) become

$$(2.8)\quad \frac{dm}{dx} = \rho_e u_e a_s \left(\frac{d\delta}{dx} - \theta\right) = \frac{p}{\varphi_e}\left(\frac{d\delta}{dx} - \theta\right)$$

$$(2.9)\quad \frac{d}{dx}(m w_1) = w_e \frac{dm}{dx} - \delta \frac{dp}{dx} - \tau_w = w_e \frac{dm}{dx} - \delta \frac{dp}{dx} - \frac{p w_e}{\varphi_e}\frac{c_f}{2},$$

where the wall friction $\tau_w = \frac{1}{2}\rho_e u_e^2 c_f$ has been expressed through the friction coefficient c_f. Suppose now that c_f can be related directly to the unknowns m, δ, w_e, and w_1. Suppose also that $\frac{T_1}{T_s}$ can be expressed explicitly in terms of the unknowns through a more general formula than the ordinary one-dimensional energy relation $\frac{T_1}{T_s} = 1 - \frac{\gamma-1}{2} w_1^2$ (correct for a uniform velocity distribution <u>only</u>). Then since $p = p(w_e)$ and $\theta = \theta(\nu_e)$ are known by the Prandtl-Meyer relation, Equations (2.7), (2.8) and (2.9) furnish three relations between the four variables m, δ, w_e and w_1. An additional relation between these variables is introduced by means of an assumption regarding the mixing rate dm/dx, which will be discussed in Section 2.3. It is at this point, with the introduction of an approximate

expression for the mean temperature and for the mixing rate, that the present approach departs from the usual boundary layer theory.

2.2 Expression for the Mean Temperature: The $F-\mathcal{H}$ Curve.

In any given flow the mean temperature can be computed from the defining relations, Equations (2.6) and (2.7). But since the solution is not known the exact evaluation cannot be obtained a priori. Therefore, if any progress is to be made toward a solution of the equations an approximate relationship must be introduced, which depends on some average properties of the flow and involves the minimum possible number of parameters.

Laminar Flow. In the laminar case such a relationship can be established from the following considerations: Stewartson[9] has shown that for Prandtl number unity, $\mu \sim T$ and an insulated wall, any compressible boundary layer flow with prescribed variation of external velocity can be reduced to an equivalent incompressible boundary layer flow with a transformed external velocity distribution. This means that from a given incompressible flow a family of compressible flows can be generated, whose solutions are related in a simple way to the incompressible solution. The Stewartson transformation is represented completely by the relations

$$(2.10)\quad \rho_0 a_0\, d\eta = \rho a_e\, dy; \quad \rho_0 a_0\, d\xi = \rho_e a_e\, dx; \quad \frac{\rho}{\rho_0} u = \psi_y; \quad \frac{\rho}{\rho_0} v = -\psi_x;$$
$$u_i = \psi_\eta; \quad v_i = -\psi_\xi,$$

where the subscript "o" denotes some fixed reference condition, and the subscript "i" denotes the quantities of the equivalent incompressible flow with the constant density ρ_0, with coordinates ξ, η, and with

the same stream function ψ as in the compressible case. From the relations (2.10) the two following additional relations can be written

$$(2.10a)\quad \frac{u_i}{a_o} = \frac{u}{a_e} \quad ; \quad \rho_o u_i \, d\eta = \rho u \, dy$$

It follows that at corresponding stations the relative velocities in the compressible and incompressible flows coincide:

$$(2.11)\quad \frac{u_i}{u_{ie}} = \frac{u}{u_e}$$

By utilizing the first two relations in Equation (2.10), the expressions corresponding to Equations (2.5a) and (2.5b) can be written as follows.

$$(2.12)\quad \delta_i - \delta_i^* = \int_0^{\delta_i} \frac{u_i}{u_{ie}} \, d\eta = \frac{\rho_e a_e}{\rho_o a_o} \int_0^{\delta} \frac{\rho u}{\rho_e u_e} \, dy = \frac{\rho_e a_e}{\rho_o a_o} (\delta - \delta^*)$$

$$(2.13)\quad \delta_i - \delta_i^* - \delta_i^{**} = \int_0^{\delta_i} \frac{u_i^2}{u_{ie}^2} \, d\eta = \frac{\rho_e a_e}{\rho_o a_o} \int_0^{\delta} \frac{\rho u^2}{\rho_e u_e^2} \, dy = \frac{\rho_e a_e}{\rho_o a_o} (\delta - \delta^* - \delta^{**})$$

Also,

$$(2.14)\quad \delta = \int_0^{\delta} dy = \int_0^{\delta_i} \frac{\rho_o}{\rho} \frac{u_i}{u} \, d\eta = \frac{\rho_o a_o}{\rho_e a_e} \int_0^{\delta_i} \frac{T}{T_e} \, d\eta = \frac{\rho_o a_o}{\rho_e a_e} \frac{T_s}{T_e} \int_0^{\delta_i} \frac{T}{T_s} \, d\eta$$

But, from the constancy of the stagnation enthalpy, $\frac{T}{T_s} = 1 - \frac{\gamma-1}{2} w^2$.

Therefore, utilizing Equations (2.11) and (2.13), one finds

$$(2.15) \quad \int_0^{\delta_i} \frac{T}{T_s}\, d\eta = \int_0^{\delta_i} \left(1 - \frac{\gamma-1}{2} w_e^2 \frac{u_i^2}{u_{ie}^2}\right) d\eta = \delta_i - \frac{\gamma-1}{2} w_e^2 \left(\delta_i - \delta^* - \delta^{**}\right)$$

Finally, by employing Equations (2.12) and (2.13), Equation (2.6a) can be written as follows:

$$(2.16) \quad \mathcal{H} = \frac{u_1}{u_e} = \frac{\delta_i - \delta_i^* - \delta_i^{**}}{\delta_i - \delta_i^*}$$

By means of Equations (2.14) and (2.15), Equation (2.6b) is transformed into

$$\frac{T_1}{T_s} = \frac{\delta_i - \delta_i^* - \delta_i^{**}}{(\delta_i - \delta_i^*)^2} \left[\delta_i - \frac{\gamma-1}{2} w_e^2 \left(\delta_i - \delta_i^* - \delta_i^{**}\right)\right],$$

or, utilizing Equation (2.16), into

$$(2.17) \quad \frac{T_1}{T_s} = f - \frac{\gamma-1}{2} \mathcal{H}^2 w_e^2 = f - \frac{\gamma-1}{2} w_1^2 ,$$

where

$$(2.18) \quad f = \frac{(\delta_i - \delta_i^* - \delta_i^{**})\delta_i}{(\delta_i - \delta_i^*)^2}$$

This mean temperature-mean velocity relationship differs from that for a one-dimensional isoenergetic flow only in that the quantity f

appears, rather than unity. It is to be observed that for every incompressible boundary layer flow f (Equation (2.18)), and $\mathcal{H}$ (Equation (2.16)), can be related to each other, so that the given incompressible flow, and the corresponding complete family of compressible boundary layer flows obtained through the Stewartson transformation, are characterized by a certain $f(\mathcal{H})$ relation. All the effects of Mach number for the compressible family are contained in the second term of the right hand side of Equation (2.17). Of course in general this $f(\mathcal{H})$ relation is different for every flow. However at this point it should be observed that certain classes of low-speed laminar boundary layer flows, such as those investigated by Falkner and Skan[10,11] ($u_{i_e} = C_\beta \xi^{s}$), are described completely in terms of a single parameter. Each flow corresponds to a point in the f-$\mathcal{H}$ plane and the whole class of flows is represented by a single f-$\mathcal{H}$ curve. By means of the Stewartson transformation this one-parameter description is extended to the corresponding compressible flows as well.

The $f(\mathcal{H})$ relation can be evaluated for known incompressible solutions once the thickness δ_i of the dissipative region is suitably defined. Now the thickness of a laminar boundary layer is not a sharply defined quantity, because of the asymptotic transition from dissipative to non-dissipative conditions. Too large a value of δ_i would result in the inclusion of too much of the nearly isentropic flow in the dissipative region, while for too small δ_i appreciable viscous effects could be lost. Clearly the choice of δ_i is influenced by the relative importance of the transversal pressure variations in the flow (see Section 6). For comparison two different values of δ_i are employed in what follows.

corresponding to $\frac{u(\delta)}{u_e} = 0.99$ and 0.95. Once δ_i is defined, $\mathcal{H}$ and f can be obtained from Equations (2.16) and (2.18) by utilizing the ordinary values of δ_i^* and δ_i^{**} computed for $y \to \infty$, which corresponds to concentrating all of the actual mass and momentum defect of the boundary layer in the conventionally defined dissipative region. Observe that the definition of δ follows immediately from that of δ_i because of Equation (2.11).

In Figure 2a the $f-\mathcal{H}$ curves are shown for two laminar incompressible boundary layer solutions: the Howarth[12] solution for a linearly decelerated velocity distribution; and the Falkner-Skan[10,11] family $\left(u_{ie} = C\xi^{\alpha}\right)$ of solutions. The first curve corresponds to the development of a specific boundary layer flow, with $\mathcal{H}$ going from an initial maximum value to a final minimum value where separation occurs; this curve passes through the $f-\mathcal{H}$ point corresponding to the Blasius solution on a flat plate, which is characterized by constant values of f and $\mathcal{H}$. On the other hand, each point of the second curve corresponds to a different boundary layer flow evolving in such a way that f and $\mathcal{H}$ remain constant, and the "position" of the flow with respect to separation remains fixed. Here again the Blasius solution is included; all the points on the right of the Blasius point correspond to acceleration, those on the left to deceleration. The minimum $\mathcal{H}$ corresponds to a flow which is continuously on the verge of separation.

All of the curves show a common qualitative behavior: going toward separation $\mathcal{H}$ decreases and f increases steadily, the slope becoming steeper and steeper, until at separation, the slope is practically

vertical, i.e. $\mathcal{H}$ varies but little as f increases. This fact has a clear physical interpretation. The increase in thickness near separation is caused mainly by an increase in the extent of the low velocity portion of the boundary layer, the high velocity region being pushed away from the wall, while the velocity distribution in the high velocity region remains approximately similar to itself. In the extreme case when the velocities near the wall are very low, the effect of this region on I and $\bar{m}$ is negligible, and $\mathcal{H}$ is nearly constant at the value computed from the high velocity region alone. On the other hand f increases steadily because of the increase in total thickness of the dissipative flow. This fact can also be expressed in the following way: with approaching separation the effect of the wall on the high velocity portion becomes less and less marked and the conditions in this portion, which determines the value of $\mathcal{H}$, become more and more similar to those of a "free" half-jet with a constant $\mathcal{H}$ value. This physical picture is essential, since it gives a clue to the qualitative prediction of what happens after separation, where no theoretical solutions are known. It is to be expected that in the separated region the jet-like behavior is still more pronounced, and therefore $\mathcal{H}$ undergoes only small variations, while all the variations in the flow will be reflected in f. The f-$\mathcal{H}$ curve will have therefore a nearly vertical extension beyond the separation point.

An interesting case is that of a flow which after having undergone separation in the way just described, is brought to reattach itself to the wall, and to build up a regular boundary layer again. A compressible flow of this type is observed, for example, in the laminar boundary layer-shock wave interaction. Again, despite the absolute lack of theoretical

information on flows of this kind, the qualitative behaviour of a reattaching flow in the f-$\mathcal{H}$ plane can be predicted to follow a path analogous to the one observed for separating and separated flows, but in the opposite direction. The f-$\mathcal{H}$ curve, after having described some loop with small $\mathcal{H}$ variation and large f-variation, reaches a reattachment point, generally distinct from the separation point, after which $\mathcal{H}$ starts increasing again. If, for instance, the conditions are uniform after reattachment, a Blasius flow will finally be reached and the f-$\mathcal{H}$ curve passes through the Blasius point again.

Consider finally the case of a wake formed behind a body, where the velocity distribution across the dissipative flow region passes from a typical boundary layer profile just upstream of the base of the body to a necessarily uniform distribution in the wake far behind the body (e.g. Figure 7). Far beyond the body $\delta_i^* = \delta_i^{**} = 0$, and $\mathcal{H} = f = 1$. In the f-$\mathcal{H}$ plane the path of the flow will be represented by a smooth line connecting the initial f-$\mathcal{H}$ point (say the Blasius point) with the point $\mathcal{H} = f = 1$. For a blunt-based body, as in the compressible base pressure problem, conditions in the wake just aft of the body are similar to those of a separated flow, the low velocity region being in this case represented by the "dead-water" region. The path in the f-$\mathcal{H}$ plane will be developed at first as in the case of reattachment (where, however, the wall influence is negligible) through a line of nearly constant $\mathcal{H}$. Then $\mathcal{H}$ will start increasing, until far beyond the body $\mathcal{H}$ and $f \to 1$. The f-$\mathcal{H}$ curve for this flow does not necessarily pass through the Blasius point, but it is not likely to pass too far from it.

From this discussion it follows that every incompressible dissipative flow involving separating, separated, reattached regions and wakes can be described as a particular curve in the f-$\mathcal{H}$ plane having qualitatively the shape just discussed. Supposing that the Stewartson transformation still holds in the separated regions, the family of corresponding compressible dissipative flows is described by the same curve. The exact determination of this curve requires the complete solution of the flow, which can be obtained only in the case of unseparated flows, since no known method is available for the other cases. The next step is therefore to replace the exact curve with a suitable approximation.

Based on the preceding qualitative considerations it appears that the loop characterizing the separation-reattachment case can be replaced with a single representative mean curve, extended vertically ($\mathcal{H}$ = const.) beyond the separation point (jet-like behaviour in separated region). For instance the single mean curve can be the theoretical f-$\mathcal{H}$ curve for the Falkner-Skan solutions. Moreover, this curve can be extended up to f = $\mathcal{H}$ = 1, and in this way it includes also the wake-like flows. However the value of $\mathcal{H}$ at separation given by the Falkner-Skan solutions does not coincide with the $\mathcal{H}_j$ value for the free jet given by Chapman's solution[13], as shown in Figure 2a. One could neglect this small difference in $\mathcal{H}$, and extend the Falkner-Skan curve vertically, or, as we have done in Figure 2a for $\frac{u(\delta)}{u_e} = 0.95$, utilize an extrapolation between the Falkner-Skan f ($\mathcal{H}$) curve and the line $\mathcal{H} = \mathcal{H}_j$ given by Chapman's solution. (In order not to complicate the figure we have not included the curve for $\frac{u(\delta)}{u_e} = 0.99$)

With the assumption of this general relation between f and $\mathcal{H}$ the character of the flow, even if slightly distorted, is certainly preserved.

Thus f ($\mathcal{H}$) in Equation (2.17) becomes a general function* for all types of incompressible flows, and therefore for all types of compressible flows covering the cases of separation, reattachment and wake flow. In other words, the assumption is made that a single parameter, $\mathcal{H}$, or better f, is sufficient to characterize the state of the flow through all its possible development. Of course, all the assumptions and quantitative considerations regarding the f-$\mathcal{H}$ curve should be thought of as preliminary, and may be subject to some revisions after analysis of existing (and new) experimental data.

It proves to be more convenient later to work with the quantity F, which is related to f by

$$(2.19) \quad F = \frac{f}{\mathcal{H}^2} - 1 = \frac{\delta_i^* + \delta_i^{**}}{\delta_i - \delta_i^* - \delta_i^{**}}$$

In Figure 2b the corresponding F-$\mathcal{H}$ curves for laminar flows are shown. (Note that in wake-like flows, when f and $\mathcal{H} \rightarrow 1$, $F \rightarrow 0$).

Turbulent Flows. While the laminar case gives the possibility of determining the important relation (2.17) and the approximate behavior of the quantities involved from theoretical considerations, nothing of this kind can be done in the turbulent case, because of the almost complete lack of theoretical knowledge on the effect of compressibility, and because even

---

*This procedure may recall to a certain extent the method of Thwaites[14], who used a single mean function derived by comparison between known solutions in his successful treatment of incompressible laminar boundary layers with a pressure gradient.

the empirical information in the incompressible case is very meager. The possibility of considering the velocity profiles for an incompressible boundary layer as a one-parameter family has been discussed many times, but it is not yet clear if this assumption is even approximately correct in general. If the velocity profile is not changing too fast then this assumption may be correct. In that case the quantity $\mathcal{H}$ defined by Equation (2.16) can again be chosen as the parameter representing the state of the flow, and the function f is computed from Equation (2.19) by using known incompressible values of δ_i^* and δ_i^{**}. The curve of Figure 3a has been computed from the low-speed data of Schubauer and Klebanoff[3] (It should be observed that in the turbulent case it is possible to take δ such that $\frac{u(\delta)}{u_e} = 1.0$, because the thickness is a quite sharply defined quantity). Points calculated from the von Doenhoff-Tetervin semi-empirical relation[15] are also shown. The behavior of this f-$\mathcal{H}$ curve, which corresponds to boundary layers going toward separation, is similar to that of the laminar case, and the same qualitative discussion can be applied. The f-$\mathcal{H}$ path corresponding to any given low-speed case involving separation, reattachment, or wakes can be represented approximately by a single curve, consisting of the curve just described extended vertically beyond separation ($\mathcal{H} = \mathcal{H}_j$),* and extrapolated toward $f = \mathcal{H} = 1$ to cover the case of wakes. The curve passes through the point corresponding to zero pressure gradient (flat plate).

---

* For a semi-infinite "half-jet" at constant pressure $\mathcal{H}_j = 0.720$, by direct calculation from the theoretical (Tollmien) velocity distribution. So little is known about turbulent flows after separation that the vertical extension of the f-$\mathcal{H}$ curve at this value of $\mathcal{H}$ should be regarded only as a first approximation.

Finally, the additional bold assumption is made that the effect of compressibility can be taken into account exactly as in the laminar case by utilizing Equation (2.17). As a preliminary test of this assumption, good qualitative correlation is observed between the Schubauer low-speed f-$\mathcal{H}$ curve and the points calculated from turbulent boundary layer profiles measured through a shock wave interaction region at M = 3.0 by Bogdonoff and Solarski[16] in this laboratory (Figure 3a). Some of these points correspond to the region preceding the incident shock wave, where $\mathcal{H}$ is decreasing, and some to the region downstream of the incident shock, where the velocity profile is gradually returning to its undisturbed form.

2.3 Mixing Rate and Friction Co-efficient

Again, the laminar case can be treated by eliminating compressibility effects with the aid of the Stewartson transformation, and examining known incompressible solutions. By integrating the second relation of Equation (2.10a) across the boundary layer it appears that $\overline{m}_i = \overline{m}$. Therefore, using the second relation of Equation (2.10) the compressible and the incompressible mixing rates are connected by the following equation:

$$(2.20) \qquad \frac{d\overline{m}}{dx} = \frac{a_e \rho_e}{a_o \rho_o} \frac{d\overline{m}_i}{d\xi}$$

Now for an incompressible flow (Equation 2.5a).

$$(2.21) \qquad \overline{m}_i = \rho_o u_{ie} (\delta_i - \delta_i^*)$$

and on a flat plate

$$(2.21a) \qquad \delta_i - \delta_i^* = \left(\frac{2C\mu_o \xi}{\rho_o u_{ie}} \right)^{\frac{1}{2}} ,$$

where C is a constant whose value depends on the definition of δ_i . The expression for $\frac{d\bar{m}_i}{d\xi}$ can be found from Equations (2.21) and (2.21a) and substituted into Equation (2.20) to obtain the value of $\frac{d\bar{m}}{dx}$. If a mixing coefficient k is introduced such that

$$(2.22) \quad \frac{d\bar{m}}{dx} = k \rho_e u_e ,$$

the result for the flat plate is $k = C \frac{\mu_e}{\bar{m}}$. The analogous expression for the incompressible case is $k_i = C \frac{\mu_o}{\bar{m}_i}$, and the non-dimensional expression $\frac{\bar{m}_i}{\mu_o}$ here replaces the square root of the Reynolds number (see Equations (2.21) and (2.21a)). The quantity k_i can also be evaluated for various other solutions of the laminar boundary layer; the form of the relation giving k_i remains the same, except that C is now a function of the parameter determining the conditions of the boundary layer. If the parameter $\mathcal{H}$ is chosen, then $C = C(\mathcal{H})$ is the same for the incompressible case and for the corresponding compressible family, and therefore the mixing rate is given by Equation (2.22) with

$$(2.23) \quad k = \frac{\mu_e}{\bar{m}} C(\mathcal{H})$$

The values of $C(\mathcal{H})$ depend of course on the definition of δ_i ; for the theoretical solutions already discussed, $C(\mathcal{H})$ is given in Figure 4 for the two definitions already used in the f-$\mathcal{H}$ computations.

A similar treatment can be given for the friction coefficient. From Equation (2.10a) the following relation is derived between the viscous stresses

$$\tau = \mu u_y = \frac{\rho_e}{\rho_o} \frac{T_e}{T_o} \mu_o u_{i\eta} = \frac{\rho_e}{\rho_o} \frac{T_e}{T_o} \tau_i$$

where the assumption $\mu \sim T$ has been used. On the other hand

$$\rho_e u_e^2 = \frac{p_e}{p_o} \rho_o u_{ie}^2$$

therefore,

$$c_f = \frac{2\tau}{\rho_e u_e^2} = \frac{T_e}{T_o} \frac{2\tau_i}{\rho_o u_{ie}^2} = \frac{\mu_e}{\mu_o} c_{f_i}$$

Now for the flat plate, remembering the relations between $\frac{\overline{m}_i}{\mu_o}$ and Reynolds number, one finds that $c_{f_i} = D \frac{\mu_o}{\overline{m}_i}$, with constant D. For the other incompressible solutions the same relation can be written, with $D = D(\mathcal{H})$, the function being generally different for different solutions. Finally, the relation

$$(2.24) \quad c_f = \frac{\mu_e}{\overline{m}} D(\mathcal{H})$$

gives the friction coefficient for the corresponding compressible families. $D(\mathcal{H})$ is plotted in Figure 4 for the Howarth and Falkner-Skan solutions.

The next step now is to replace the particular functions $C(\mathcal{H})$, $D(\mathcal{H})$ representing particular solutions with two general functions, which moreover have to be extended beyond separation and into the wake region, and must also cover the reattachment case. Provisionally, $C(\mathcal{H})$ and $D(\mathcal{H})$ obtained from the Falkner-Skan solutions are chosen as "universal" functions. However, further study is required to determine the mixing coefficient for the jet-like flow beyond separation and prior to reattachment, and also for wake flows with a pressure gradient. Of course $D(\mathcal{H}) = 0$ beyond separation, upstream of reattachment, and in wake flows.

Again the turbulent case can be treated only by analogy. For the flat plate in the incompressible case, the nondimensional expression $\frac{\overline{m}_i}{\mu_0}$ is again a function only of the Reynolds number. If it is assumed that the $1/7^{th}$ power law holds for the velocity distribution, then two relations can be written:

$$k_i = C\left(\frac{\mu_0}{\overline{m}_i}\right)^{\frac{1}{4}} \quad ; \qquad c_{f_i} = D\left(\frac{\mu_0}{\overline{m}_i}\right)^{\frac{1}{4}} \quad ,$$

with constant values for C and D. Equations analogous to (2.23) and (2.24) could be written, where C and D could be considered as functions of $\mathcal{H}$, and $\frac{\mu_e}{\overline{m}}$ would appear to the $1/4^{th}$ power. But it is doubtful if these relations could give a correct answer, including the effects of approaching separation and of Mach number. For the present, considering that the mass flow variation seems to have but little effect on the turbulent values, and that insufficient experimental data are available on the spreading of turbulence with varying pressure, it seems justified to introduce the approximation that k is constant throughout the turbulent region. The skin friction coefficient c_f is neglected in separated flows, or is taken as a simple function of $\mathcal{H}$ in separating or reattached flows. Of course the same rough assumption could be made in the laminar case, especially when only narrow regions of flow are considered. In physical terms the approximation that k is constant amounts to the assumption that the rate of mass transport from isentropic to dissipative flows is proportional to the mass flux density of the isentropic stream. (See Equation (2.22)).

So far as the order of magnitude of k is concerned, for the boundary layer on a flat plate with zero pressure gradient, Equation (2.9)

yields the relation

$$k_0 = \frac{c_{f_0}}{2(1-\mathcal{L}_0)} ,$$

where the subscript zero here denotes conditions at zero pressure gradient. At a local Reynolds number of 10^6 and a Mach number of 2.0, one finds $k_0 = 1.6 \times 10^{-3}$ for the laminar boundary layer with $\frac{u(\delta)}{u_e} = 0.99$, while $k_0 = 1.5 \times 10^{-2}$ for the turbulent layer. In turbulent separated flows and jets somewhat larger values of k are expected. From the Schubauer and Klebanoff data[3] one finds that $k \rightarrow 0.03$ near turbulent boundary layer separation, and this value is utilized for turbulent flows in the present paper as a first approximation. The fact that the turbulent mixing coefficient k is of the order of ten times the laminar value is largely responsible for the marked difference between turbulent and laminar interaction phenomena.

The constant mixing coefficient introduced in this way should be regarded only as an average value, the introduction of which makes it possible to decide whether mixing furnishes the main mechanism for the pressure rise in interactions between dissipative and isentropic gas streams. Refinements can be introduced later when this mechanism is firmly established, and when more experimental data are obtained on the mixing process with varying pressure.

2.4 Reduction of Equations of Motion to a Single Equation for Constant Mixing Coefficient.

By introducing the relation (2.17) between mean temperature and mean velocity, and the additional Equation (2.22) for the mixing rate,

which can be also written as

$$(2.25) \quad \frac{dm}{dx} = k \frac{p}{\varphi_e} ,$$

the equations describing the flow are completely defined, provided the coefficients k and c_f are known. In what follows, the discussion is restricted to the simplest case of constant k mentioned in the preceding section, which permits a great simplification in the discussion of the important properties of the equations and, moreover, at the present time seems to be the most reasonable assumption in the case of turbulent flow. On the other hand c_f can be replaced by the quantity

$$\sigma = \frac{c_f}{2k(1-\mathcal{H})} ,$$

with the advantage that even when k and c_f are assumed to depend on m, as for instance in the laminar case [Equations (2.23) and (2.24)] the effect of m is eliminated in σ, which is therefore a function of $\mathcal{H}$ alone. For separated flows or wake flows c_f is negligible or zero and therefore $\sigma = 0$. For the flat plate $\sigma = 1$.

By utilizing Equation (2.25), Equation (2.1) is reduced to the suggestive form

$$(2.26) \quad \frac{d\delta}{dx} = \theta + k$$

The distance x along the surface is now eliminated from Equations (2.7), (2.8) and (2.9) with the help of Equation (2.25), and the momentum and continuity relations are reduced to two simultaneous equations for $\frac{d\mathcal{H}}{d\ln m}$ and $\frac{dw_e}{d\ln m}$. These equations furnish a single equation for $\frac{d\mathcal{H}}{dw_e}$, or for $\frac{dF}{dw_e}$.

First, with the aid of Equations (2.6c), (2.17) and (2.19), the mass flow equation (Equation (2.7)) is rewritten in the form

$$(2.27)\quad m\mathcal{H}\left[F+1-\frac{\gamma-1}{2}w_e^2\right]=\gamma p w_e \delta$$

By differentiating the value of δ obtained from this equation with respect to X, dividing through by $\frac{dm}{dx}$, and using Equation (2.26), the following equation is obtained:

$$(2.28)\quad \frac{d}{d\ln m}\left\{\mathcal{H}\left[F+1-\frac{\gamma-1}{2}w_e^2\right]\right\}-\mathcal{H}\left[F+1-\frac{\gamma-1}{2}w_e^2\right]\frac{d}{d\ln m}(\ln p w_e)$$
$$=\left(\frac{\theta}{k}+1\right)\left(1-\frac{\gamma-1}{2}w_e^2\right)-\mathcal{H}\left[F+1-\frac{\gamma-1}{2}w_e^2\right]$$

Similarly, the momentum equation (Equation (2.9)) becomes

$$(2.29)\quad \frac{d}{d\ln m}(\mathcal{H}w_e)-\frac{\mathcal{H}\left[F+1-\frac{\gamma-1}{2}w_e^2\right]}{\gamma\Phi_e}\frac{d\ln w_e}{d\ln m}=w_e(1-\sigma)(1-\mathcal{H}),$$

where the Bernoulli equation (Equation (2.6d)) has been employed to eliminate the pressure.

So long as the determinant of the simultaneous equations (2.28) and (2.29) for $\frac{d\mathcal{H}}{d\ln m}$ and $\frac{dw_e}{d\ln m}$ does not vanish, these equations yield a single non-linear first-order equation for $\frac{d\mathcal{H}}{dw_e}=\frac{\left(\frac{d\mathcal{H}}{d\ln m}\right)}{\left(\frac{dw_e}{d\ln m}\right)}$, or for $\frac{dF}{dw_e}$ if the relation $\frac{d\mathcal{H}}{dw_e}=\frac{d\mathcal{H}}{dF}\frac{dF}{dw_e}$ is employed:

(2.30)

$$\frac{dF}{dw_e} = \frac{\left(\frac{\gamma+1}{2}w_e^2-1\right)\left(1-\frac{\gamma-1}{2}w_e^2\right)(1-\sigma)+F\left[\gamma w_e^2(1-\sigma)-\frac{F\mathcal{H}}{1-\mathcal{H}}+\frac{\Theta}{k}\frac{1-\frac{\gamma-1}{2}w_e^2}{1-\mathcal{H}}\right]+\sigma F\left(1-\frac{\gamma-1}{2}w_e^2\right)}{w_e\left(1-\frac{\gamma-1}{2}w_e^2\right)\left\{\left[\frac{1-\frac{\gamma-1}{2}w_e^2}{\mathcal{H}(1-\mathcal{H})}\frac{\Theta}{k}-\frac{F}{\mathcal{H}(1-\mathcal{H})}\right]\frac{d\mathcal{H}}{dF}-1+\sigma\left[-\frac{F+1-\frac{\gamma-1}{2}w_e^2}{\mathcal{H}}\frac{d\mathcal{H}}{dF}+1\right]\right\}}$$

Since k, $\sigma(\mathcal{H})$ and $F = F(\mathcal{H})$ are presumed known and $\Theta(w_e)$ is given by the Prandtl-Meyer relation (or by any other procedure for non-isentropic flows), this equation is integrable by numerical methods.

When $\mathcal{H}$ = constant and $\sigma = 0$, as in separated flows or wakes, Equation (2.30) reduces to

$$(2.31)\quad w_e\frac{dF}{dw_e} = -\left(\frac{\gamma+1}{2}w_e^2-1\right)-\frac{F}{1-\frac{\gamma-1}{2}w_e^2}\left[\gamma w_e^2-\frac{\mathcal{H}}{1-\mathcal{H}}F+\frac{1-\frac{\gamma-1}{2}w_e^2}{1-\mathcal{H}}\frac{\Theta}{k}\right],$$

which is a Riccati equation. A "simplified" theory has been developed in Section 4 for this important special case.

When the determinant of the equations (2.28) and (2.29) vanishes, the numerator and denominator of the right-hand side of Equation (2.30) also vanish, and the equation for $\frac{dF}{dw_e}$ has a "critical point" which turns out to be very significant for the determination of the proper solution.

2.5 Critical Point of the Equation for $\frac{dF}{dw_e}$ and Its Significance.

Suppose, for simplicity, that only wake flows or separated flows for which $\sigma = 0$ are considered here. (Flows in which skin-friction is not negligible can be included in the analysis, and will form the subject of a later paper.) Suppose also that the external flow is isentropic. By

setting both the numerator and denominator of Equation (2.30) equal to zero and solving the resultant simultaneous equations for F_{CR} and $W_{e_{CR}}$ with the aid of the Prandtl-Meyer relation, the location of the critical point is determined as a function of $\overline{W}_e$ or $\overline{M}$, where $\overline{M}$ is the Mach number of the free stream far from the body, where $\theta = 0$. When the denominator vanishes

$$(2.32)\quad \mathcal{H}_{CR}(1-\mathcal{H}_{CR})\left(\frac{dF}{d\mathcal{H}}\right)_{CR} + F_{CR} = \left(1-\frac{\gamma-1}{2}W_e^2\right)\frac{\theta_{CR}}{k} \quad ;$$

provided $\frac{d\mathcal{H}}{dF} \neq 0$. If $\frac{d\mathcal{H}}{dF} = 0$, or $\mathcal{H}$ = const., the denominator never vanishes and no critical point exists. When the numerator also vanishes,

$$(2.33)\quad F_{CR}\left[\gamma W_{e_{CR}}^2 + F_{CR} + \mathcal{H}_{CR}\left(\frac{dF}{d\mathcal{H}}\right)_{CR}\right] = -\left(\frac{\gamma+1}{2}W_{e_{CR}}^2 - 1\right)\left(1-\frac{\gamma-1}{2}W_{e_{CR}}^2\right)$$

where Equation (2.32) has already been used to simplify the result. Equations (2.32) and (2.33) define $\frac{\theta_{CR}}{k}$ and $W_{e_{CR}}$ as functions of $\mathcal{H}_{CR}$. Since $\frac{\theta_{CR}}{k} = O(1)$, when k is very small, as in the laminar case $\theta_{CR} \approx 0$ and $W_{e_{CR}} \approx \overline{W}_e$. In the turbulent case, however, k is not small. For example, choosing k = 0.03 on the basis of the Schubauer-Klebanoff data near turbulent separation,[3] and utilizing the F-$\mathcal{H}$ curve of Figure 3a and the $\frac{d\mathcal{H}}{dF}$ curve of Figure 3b, the values of θ_{CR}, $\mathcal{H}_{CR}$ and W_e shown in Figure 5 are obtained as functions of $\overline{W}_e$. It appears that θ_{CR} is always negative.

Now, what is the significance of the critical point? Since $\theta_{CR} < 0$ it is necessary to consider only "reattaching flows", such as the flow aft

of a supersonic airfoil with a blunt trailing edge, or the re-attachment of the separated flow downstream of the reflected expansion "fan" in the laminar boundary layer-shock wave interaction.

In the first case, for example, $\mathcal{H}$ must increase, or F must decrease and w_e must decrease steadily during the recompression that occurs in the wake after the expansion around the sharp "corner" at the trailing edge. In other words, $\frac{dF}{dw_e}$ is always positive (see Figure 6). Now, in the separated or "free jet" region just aft of the base $\mathcal{H}$ is constant and $\frac{d\mathcal{H}}{dF} = 0$, so that the denominator in the expression for $\frac{dF}{dw_e}$ in Equation (2.30) is initially negative. Therefore the numerator must also be initially negative. If θ_i, or the flow inclination angle after the expansion around the corner, is <u>larger</u> than the proper value θ_b, then the denominator will vanish before the numerator during the recompression (since $\frac{d\mathcal{H}}{dF} < 0$), and the slope $\frac{dF}{dw_e}$ will become infinite at some point and negative thereafter. In that case the $F(w_e)$ integral curve can never represent the actual flow (Figure 6). On the other hand, if θ_i is <u>smaller</u> than the proper value, the numerator vanishes before the denominator, and $\frac{dF}{dw_e}$ passes through zero and becomes negative thereafter. Again, the $F(w_e)$ curve cannot be the correct representation of the flow. Only one value of θ_i, say θ_b, permits the integral curve to pass through the critical point where numerator and denominator vanish simultaneously. Thus the critical point acts somewhat like the throat of a nozzle in determining θ_b and the base pressure for the given boundary conditions at the base (Section 3).

It is an interesting fact that the location of the critical point does not in general coincide with the smallest cross-section of the mixing

region, that is, with the point at which $\frac{d\zeta}{dx} = \theta + k = 0$, or $\frac{\theta}{k} = -1$. By referring to Figure 5 one sees that in the turbulent case $\frac{\theta_{cr}}{k} > -1$ for $1 < \overline{W}_e < 1.61$, so that the critical point lies downstream of the narrowest cross-section, while $\frac{\theta_{cr}}{k} < -1$ for $\overline{W}_e > 1.61$, so that the critical point in this range lies upstream of the narrowest cross-section. In any case, most of the recompression occurs before the critical point is reached.

Evidently, the mixing plays an essential role here, because for $k = 0$, $W_e \frac{dF}{dW_e}$ is positive and equal to $\frac{F}{\partial \ell}$ and no critical point exists. An analysis of compression flows of this type that ignores the mixing process cannot possibly represent the actual conditions.

The discussion of the role of the critical point (when it exists) applies also to the reattaching flow in the boundary layer-shock wave interaction phenomenon, even when $\sigma \neq 0$, although the discussion is more complicated and will be given in a later paper. In the case of a turbulent boundary layer-shock wave interaction, the flow problem is undoubtedly modified not only by the action of skin-friction, but also by the penetration of the incident and reflected shock waves through the layer (see Section 6).

3. Application to the Base-Pressure Problem in Plane Supersonic Flow.

In order to illustrate the concepts and methods, the general theory is applied to the problem of the determination of the base pressure for a supersonic airfoil with a blunt trailing edge and a turbulent wake (Figure 7)*. Consider the simplest case in which the airfoil surface is

---

* Extension of the theory to axially-symmetric flows and application to the base-pressure problem for blunt-based bodies of revolution is now in progress at this Laboratory.

parallel to the flight direction at the trailing edge, and the Mach number just before the expansion around the "corner" is approximately equal to the free stream Mach number. If the recompression in the wake is regarded as isentropic the Mach number far downstream is again the free stream value.* The values of $\mathcal{H}$ and F at the critical point are then completely determined once the non-dimensional mixing rate, k, is known. Integration of Equation (2.30) may be started at the critical point, and proceeds both downstream in the wake and upstream toward the airfoil trailing edge. Since both numerator and denominator in Equation (2.30) vanish at the critical point, a parabola defined by the equation

$$F - F_{CR} = \left(\frac{dF}{dw_e}\right)_{CR} \left(w_e - w_{e_{CR}}\right) + \frac{1}{2!}\left(\frac{d^2F}{dw_e^2}\right)_{CR} \left(w_e - w_{e_{CR}}\right)^2$$

is utilized in the immediate vicinity of this point. [The values of $\left(\frac{dF}{dw_e}\right)_{CR}$ and $\left(\frac{d^2F}{dw_e^2}\right)_{CR}$ are calculated by substituting the parabolic representation of $F(\omega_e)$ into Equation (2.30)]. An analytical representation of the $F-\mathcal{H}$ curve of the form $\mathcal{H} = 0.92954 - 0.10382F - 0.36842F^2 + 0.44575F^3 - 0.09582F^4 - 0.09948F^5 + 0.04505F^6$ is employed near the critical point, and appropriate polynomial approximations involving fewer terms are utilized away from the critical point, where the integral curve is less sensitive to the function $\mathcal{H} = \mathcal{H}(F)$. Numerical integration is begun as soon as the slope $\frac{dF}{dw_e}$ can be calculated numerically with sufficient accuracy from Equation (2.30)**.

---

* If the oblique shocks in the wake are sufficiently strong, shock wave losses can also be taken into account in a more exact calculation.

** It would also be possible to begin the integration just after the expansion at the trailing edge, with various trial values of θ_i (or w_{e_i}),

Far downstream of the airfoil, as already discussed, $\mathcal{H} \to 1$ and $F \to 0$. The proper formulation of the boundary condition at the trailing edge, on the other hand, requires a knowledge of the process by which the boundary layer flow at the body surface just upstream of the trailing edge is transformed to the wake flow downstream of the trailing edge. No similarity parameter exists for this viscous flow, and the problem is further complicated by the interaction between the viscous flow and the "external", isentropic supersonic expansion around the "corner". In the $F - \mathcal{H}$ diagram the actual transition 1-2-3, indicated by a dotted curve in the accompanying sketch,

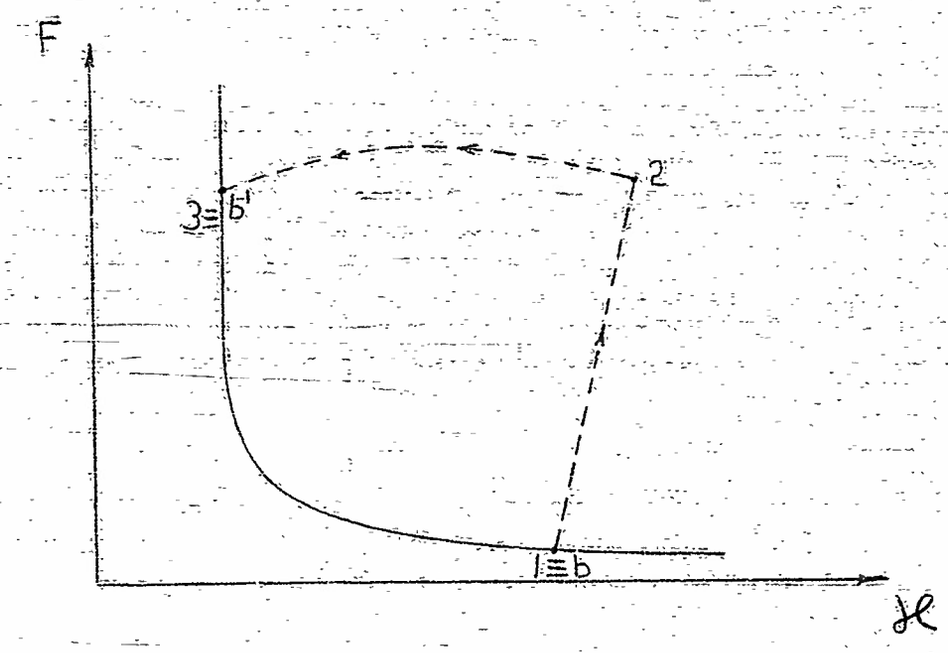

consists first of the expansion 1-2, in which $\mathcal{H}$ increases because of the uniformizing effect of the expansion, and F increases because the

---

(Footnote continued from preceding page)
and thus determine the value of θ_c for which the integral curve passes through the critical point (see Figure 6). In fact, this method is the only feasible one for the general case when k is a function of m and $\mathcal{H}$, or for axially-symmetric supersonic flows, where the relation between w_e and θ is not known a priori.

dead-water region is now included in the dissipative flow. A subsequent smooth adjustment 2-3 occurs to a condition close to that of a free jet. To be consistent with previous approximations (Section 2.2) it is assumed that point 3 lies on the vertical extension of the mean $F-\mathcal{H}$ curve (Figure 3a).

A rough calculation indicates that the "free jet" flow is established in a distance less than one boundary layer thickness, δ_b. Provided that the ratio of boundary layer thickness to airfoil thickness at the trailing edge is small, it seems justified to treat the problem approximately by assuming that the transition to the "free-jet" flow occurs over a negligible portion of the wake just behind the body, and that negligible mixing occurs between stations 2 and 3, i.e., $m_{b'} \approx m_b$. The actual transition 1-2-3 is replaced by a "jump" 1-3 to the free jet condition. In integrating Equation (2.30) from the critical point toward the airfoil, the $F-\mathcal{H}$ curve is followed until $\mathcal{H}$ equals $\mathcal{H}_j$, or the free jet value, and the value of $\mathcal{H}$ is taken to be constant thereafter and equal to $\mathcal{H}_j$. Of course, Equation (2.30) is replaced by Equation (2.31) in this region.

To this approximation the boundary condition at the trailing edge is $\delta = \frac{h}{2} + d$, or

$$\frac{\delta}{\delta_b} = \frac{h}{2\delta_b} + \frac{d}{\delta_b} \tag{3.1}$$

where h is the airfoil thickness at the trailing edge, and the value of d lies somewhere between δ_b, the boundary layer thickness at the trailing edge, and $\delta_{b'}$, the thickness of the "free-jet" mixing region (point 3) established just aft of the isentropic expansion around the trailing edge

(Figure 7). Since $\frac{d}{\delta_b}$ is generally small compared with $\frac{h}{2\delta_b}$ it does not need to be calculated with the same degree of accuracy as $\frac{\delta}{\delta_b}$. Therefore, the approximation $d = \delta_{b'}$, which seemed to be a reasonable one, was actually employed in the present calculations. The ratio $\frac{\delta_b}{\delta_{b'}}$ is obtained from the mass flow relation, as follows:

$$(3.2a)\quad \overline{m}_{b'} = (\rho_e u_e)_{b'} \cdot \delta_{b'} \left(1 - \frac{\delta^*}{\delta}\right)_{b'} = \overline{m}_b = (\rho_e u_e)_b \, \delta_b \left(1 - \frac{\delta^*}{\delta}\right)_b$$

or

$$(3.2b)\quad \frac{\delta_b}{\delta_{b'}} = \frac{\left(1 - \frac{\delta^*}{\delta}\right)_{b'}}{\left(1 - \frac{\delta^*}{\delta}\right)_b} \; \frac{G(M_{b'})}{G(M_b)}$$

where $G(M) = M\left(1 + \frac{\gamma - 1}{2} M^2\right)^{-\frac{1}{2}\frac{\gamma+1}{\gamma-1}}$ and $M_b = \overline{M}$,

the Mach number at large distances from the body. For a turbulent boundary layer with a 1/7th power velocity distribution*, zero heat transfer at the surface and constant stagnation enthalpy, the values of $\left(1 - \frac{\delta^*}{\delta}\right)_b$ are tabulated below:

M	$\left(1 - \frac{\delta^*}{\delta}\right)_b$
1.5	0.806
2.0	0.763
3.0	0.669
4.0	0.583
5.0	0.506

* The meager data available indicate that the 1/7th power velocity distribution is not too far from the truth.

The quantity $\left(1-\frac{\delta^*}{\delta}\right)_b$ is assumed to have the value corresponding to a turbulent boundary layer right up to the point where transition reaches the trailing edge.

The value of $\left(1-\frac{\delta^*}{\delta}\right)_{b'}$ calculated for a low-speed isothermal constant-pressure turbulent half-jet according to Tollmien's theory is 0.45, and this value is utilized in Equation (3.2b).

With the aid of the assumption that $m_b = m_{b'}$, the ratio $\frac{\delta}{\delta_b}$ appearing in the boundary condition [Eq. (3.1)] is obtained as a function of $W_{e_{b'}}$ from Equation (2.27), as follows:

$$(3.3) \quad \frac{\delta}{\delta_b} = \frac{\left\{\left(1+F-\frac{\gamma-1}{2}W_e^2\right)\frac{\varkappa}{pW_e}\right\}_{b'}}{\left\{\left(1+F-\frac{\gamma-1}{2}W_e^2\right)\frac{\varkappa}{pW_e}\right\}_b}$$

Here $\varkappa_{b'} = 0.720$. To be consistent with the previous assumption regarding the effect of compressibility in turbulent flow [Eq. (2.17)] the values of $\varkappa_b$ and F_b at the trailing edge must be taken as identical to the corresponding values for zero pressure gradient at low speeds. Actually, it is believed that the variation of the zero pressure gradient values of F and $\varkappa$ with Mach number is quite small.

By utilizing the results of the numerical integration of Equation (2.30) for $F(W_e)$, together with Equations (3.2b) and (3.3), both $\frac{\delta}{\delta_b}$ and $\frac{\delta_{b'}}{\delta_b}$ are determined as functions of $W_{e_{b'}}$. Therefore, to each value of $W_{e_{b'}}$, or $\theta_{b'}$, there corresponds a value of $\frac{\delta_b}{h}$ calculated from Equation (3.1), so that the base pressure ratio $\frac{p_{b'}}{p_k} = f(\theta_{b'}, \bar{W}_e)$ is determined as a function of $\frac{\delta_k}{h}$ and the mixing coefficient, k.

Chapman's correlation[17] of base-pressure data in terms of $\frac{\delta_b}{h}$ for an airfoil with a blunt trailing edge and a turbulent wake is now completely understandable. From the nature of the integral curve $F(w)$, the relation between $\frac{\delta}{\delta_b}$ and F (Equation (3.3)), and the boundary condition at the airfoil trailing edge (Equation (3.1)), one sees also that for a given mixing rate in the wake, $w_{e_{b'}}$ is larger and the base pressure ratio $\frac{p_{b'}}{\bar{p}}$ is lower the smaller the value of $\frac{\delta_b}{h}$.

For any given body shape $\frac{\delta_b}{h} = \frac{\delta_b}{c}\,\frac{c}{h} = \frac{c}{h}\, g\left(Re_c, \bar{M}, P_R, \frac{T_w}{T_1}\right)$, where the functional relationship for $\frac{\delta_b}{c}$ depends on the Reynolds number range for laminar-turbulent transition on the body. The base pressure is therefore determined as a function of Reynolds number, Mach number, Prandtl number and thermal conditions at the airfoil surface once the Reynolds number range for boundary layer transition on the body is known, and once k in the turbulent wake is known. A detailed discussion of the various flow regimes in the base-pressure problem will be given in connection with the application of the "simplified" mixing theory in Section 5.

The dependence of boundary layer thickness $\frac{\delta_b}{c}$ on Reynolds number and Mach number can be prescribed as follows:

At sufficiently high Reynolds numbers boundary layer transition occurs well forward of the trailing edge, and the turbulent boundary layer thickness is approximated by the following formula for zero heat transfer to the airfoil surface.

$$\frac{\delta_b}{c} = \frac{0.037}{(Re_c)^{1/5}}\,\frac{C_{f_M}}{C_{f_{M<<1}}}\,\frac{1}{\left(\frac{\delta^{**}}{\delta}\right)} \tag{3.4}$$

The ratio $\frac{\delta^{**}}{\delta}$ is evaluated by assuming a 1/7th power velocity distribution and isoenergetic flow,* and the "compressibility correction" $\frac{C_{f_M}}{C_{f_{M<<1}}}$ is taken from Figure 19 of van Driest's paper[18].

(The factor $0.037\ Re_c^{-\frac{1}{5}}$ is of course the low-speed value of $\frac{\delta^{**}}{c}$)

Values of $\frac{C_{f_M}}{C_{f_{M<<1}}}$ and $\frac{\delta^{**}}{\delta}$ are tabulated below:

M	$\frac{\delta^{**}}{\delta}$	$\frac{C_{f_M}}{C_{f_{M<<1}}}$
1.5	0.0842	0.870
2.0	0.0773	0.810
3.0	0.0635	0.680
4.0	0.0495	0.600
5.0	0.0395	0.510

In this so-called "fully turbulent" regime it is clear that the base pressure ratio depends only upon the parameter $Re_c^{\frac{1}{5}}\frac{h}{c}$ at a given Mach number, as found by Chapman[6,17].

At sufficiently low Reynolds numbers, on the other hand, the airfoil boundary layer is completely laminar and, for zero heat transfer at the airfoil surface, Pr = 1 and $\mu \sim T$,

$$(3.5) \quad \frac{\delta_b}{c} = \frac{5.60 + 1.20(\gamma-1)M_b^2}{\sqrt{Re_c}} \quad **$$

* Of course it is possible to compute $\frac{\delta^{**}}{\delta}$ also from van Driest's formulae[18], but as no evidence exists that permits us to decide between the van Driest velocity distribution and the 1/7th power distribution, we have used the latter until reliable data is obtained.

** The value 5.60 appearing in Equation (3.5) corresponds to $\frac{u(r)}{u_e} = 0.9975$.

(See next page)

Two different types of transition between laminar and turbulent flow in the airfoil boundary layer are assumed at intermediate Reynolds numbers: (Figure 8).

(I) Transition for a smooth body, with the transition point located at the trailing edge when $Re_c = 4 \times 10^6$, and a very gradual approach to fully turbulent flow, which is assumed to be attained at the trailing edge when $Re_c = 12 \times 10^6$. Such gradual transitions have been observed experimentally by Wilson[19], for example.

(II) Transition for a body with some small roughness or external disturbances, with the transition point located at the airfoil trailing edge at $Re_c = 3 \times 10^6$, and fully turbulent conditions approached much more rapidly than in I, at $Re_c = 6 \times 10^6$.

The transition Reynolds numbers are assumed to be independent of Mach number. Values of F_b and $\mathcal{H}_b$ for the boundary layer at the airfoil trailing edge are taken to be those corresponding to a fully turbulent boundary layer until the transition point moves aft to the trailing edge.

Since the wake is turbulent it is justified to regard k as constant in first approximation (Section 2.3). From the Schubauer-Klebanoff data[3], $k \approx 0.03$ near turbulent separation, and this value is utilized in the present computations. With this approximation, the integral curve $F(w_e)$ obtained by numerical integration of Equation (2.30) is independent of Reynolds number at a given Mach number, and this curve is utilized for the

---

(Footnote continued from preceding page)

To be consistent this value would have to be adjusted to conform to the value of $\frac{u(\delta)}{u_e}$ chosen in calculating the laminar f-$\mathcal{H}$ curve. For example, for $\frac{u(\delta)}{u_e} = 0.99$, the constant is 5.0. Calculations based on 5.60 had already been made before this point was noticed; however the resulting differences are quite small, particularly in view of the other approximations introduced in the computations.

Two different types of transition between laminar and turbulent flow in the airfoil boundary layer are assumed at intermediate Reynolds numbers: (Figure 8).

(I) Transition for a smooth body, with the transition point located at the trailing edge when $Re_c = 4 \times 10^6$, and a very gradual approach to fully turbulent flow, which is assumed to be attained at the trailing edge when $Re_c = 12 \times 10^6$. Such gradual transitions have been observed experimentally by Wilson[19], for example.

(II) Transition for a body with some small roughness or external disturbances, with the transition point located at the airfoil trailing edge at $Re_c = 3 \times 10^6$, and fully turbulent conditions approached much more rapidly than in I, at $Re_c = 6 \times 10^6$.

The transition Reynolds numbers are assumed to be independent of Mach number. Values of F_b and $\mathcal{H}_b$ for the boundary layer at the airfoil trailing edge are taken to be those corresponding to a fully turbulent boundary layer until the transition point moves aft to the trailing edge.

Since the wake is turbulent it is justified to regard k as constant in first approximation (Section 2.3). From the Schubeuer-Klebanoff data[3], $k = 0.03$ near turbulent separation, and this value is utilized in the present computations. With this approximation, the integral curve $F(w_e)$ obtained by numerical integration of Equation (2.30) is independent of Reynolds number at a given Mach number, and this curve is utilized for the

---

(Footnote continued from preceding page)

To be consistent this value would have to be adjusted to conform to the value of $\frac{u(\delta)}{u_e}$ chosen in calculating the laminar f-$\mathcal{H}$ curve. For example, for $\frac{u(\delta)}{u_e} = 0.99$, the constant is 5.0. Calculations based on 5.60 had already been made before this point was noticed; however the resulting differences are quite small, particularly in view of the other approximations introduced in the computations.

4. "Simplified" Mixing Theory for Separated and Re-attaching Flows and Wakes.

4.1 Basic Assumptions and Equations.

Certain outstanding characteristics of separated and re-attaching flows and wakes behind blunt-based bodies suggest that the treatment of these flows can be somewhat simplified with the aid of a very few physical approximations. The aim of such a "simplified" mixing theory is to furnish an approximate description of the main characteristics of separated and re-attaching flows, in such a form that some general conclusions can be drawn, and a clearer insight gained into the role of the mixing process in these flows. Of course the results of the simplified approach must be compared with those obtained by the more exact analysis in a few critical cases to test the validity of the approximations employed.

Consider first the flow in the wake behind a supersonic airfoil with a blunt trailing-edge (Figure 7). Two flow regions may be distinguished: (1), a region in which the "external" gas streams from the upper and lower airfoil surfaces are approaching one another, and the "dead-water" area just aft of the body is being obliterated by mixing. Most of the flow deflection and recompression occur in this region; (2) a region downstream of (1), in which the dead-water region has vanished and the external velocity u_e varies only slightly. Because of the "mixing", the velocity profile across the internal dissipative flow approaches a uniform distribution far behind the body, i.e., $u_1 \rightarrow u_e$, or $\mathcal{H} \rightarrow 1$, while $u_e \rightarrow \bar{u}_e$ and $\Theta \rightarrow 0$.

In region 1 $\mathcal{H}$ is nearly constant while f is varying; in region 2 both f and $\mathcal{H}$ vary in general. Suppose now that the actual $f-\mathcal{H}$ curve in Figure 2a or Figure 3a is replaced by a broken curve, consisting

of the extension of the vertical line $\mathcal{H}$ = const. down to f = 1, and the horizontal segment f = 1 up to $\mathcal{H}$ = 1. The corresponding curve in the $F-\mathcal{H}$ plane is composed of a vertical line and an arc of the curve $F = \frac{1}{\mathcal{H}^2} - 1$ as shown, for example, in Figure 3a. Especially in the turbulent case this approximation is not too far from the actual $F-\mathcal{H}$ curve.

The two flow regions will now be distinguished more sharply by the conditions $\mathcal{H}$ = const. = $\mathcal{H}_j$ in region 1, and f = 1, $\mathcal{H}_j \leq \mathcal{H} \leq 1$ in region 2. The differential equation corresponding to the first region is the Riccati equation (Equation (2.31)), the integration of which gives $F(w_e)$ in region 1. By integrating Equation (2.29) with $\mathcal{H} = \mathcal{H}_j$ and $\sigma = 0$ the mass flux m is obtained as a function of w_e. Finally, Equation (2.27) gives δ as a function of w_e and by utilizing Equation (2.26) both δ and w_e are obtained as functions of x in region 1.

In region 2 the governing equation (to be given later) is that corresponding to Equation (2.30) with f = 1.0 and $\sigma = 0$. By properly connecting the solutions for the two regions at the junction point f = 1, $\mathcal{H} = \mathcal{H}_j$, the complete (approximate) solution is obtained.

Actually, a different and somewhat more direct procedure was employed, as follows:

Region 1.

In this region, the mass flux is given approximately by

$$m = \frac{\rho\delta}{\varphi} = \frac{\rho}{\varphi_e}\left(\delta_j - \delta_j^*\right), \tag{4.1}$$

where δ_j is the thickness of the "jet" or mixing region, and δ_j^* is the displacement thickness, corresponding to the velocity and temperature

distribution across the jet. In this region $\mathcal{H} = \text{const.} = \mathcal{H}_j$, and by utilizing Equation (4.1) the momentum equation (Equation (2.9)) becomes

$$(4.2) \quad \frac{1}{\rho_e}\frac{dw_e}{dm}\left[\delta - \mathcal{H}_j(\delta_j - \delta_j^*)\right] = -\frac{w_e}{p}(1-\mathcal{H}_j)$$

where the Bernoulli equation (Equation (2.6d)) is also employed. Since $\frac{d\delta}{dx} = \theta + k$ and $\frac{dm}{dx} = k\frac{p}{\rho_e}$ it follows that

$$(4.3) \quad \frac{d\delta}{dm} = \frac{\frac{\theta}{k}+1}{\frac{p}{\rho_e}}$$

When Equation (4.3) is divided by Equation (4.2), and the Prandtl-Meyer relation $\frac{dw_e}{w_e} = -\frac{d\theta}{\sqrt{M^2-1}}$ for the external flow is introduced, one obtains the relation

$$(4.4) \quad \frac{d\delta}{d\theta} = \frac{1}{1-\mathcal{H}_j}\,\frac{\frac{\theta}{k}+1}{\sqrt{M^2-1}}\left[\delta - \mathcal{H}_j(\delta_j - \delta_j^*)\right]$$

As a first approximation, it seems justified to regard the variation in the quantity $\mathcal{H}_j(\delta_j - \delta_j^*)$ appearing in Equatinn (4.4) as of secondary importance compared to the variation in δ . Actually, $\mathcal{H}_j \approx 0.720$ and $\left(1-\frac{\delta^*}{\delta}\right)_j \approx 0.45$ for a low-speed turbulent jet, so that the quantity $\mathcal{H}_j(\delta_j - \delta_j^*)$ is never greater than about $\frac{1}{3}\delta_j$, while $\delta \geqq \delta_j$. Suppose that $\mathcal{H}_j(\delta_j - \delta_j^*)$ is regarded as a constant, which corresponds to taking a constant mean value of δ_j ; for instance, the value δ_R at the junction point with region 2, where the effect of variations in δ_j is most important. Then we may define

$$\bar{\delta} = \frac{\delta - \mathcal{H}_j(\delta_j - \delta_j^*)}{\delta_R}$$

Equation (4.4) is rewritten in the form

$$(4.5)\quad \frac{1}{\bar{\delta}}\frac{d\bar{\delta}}{d\theta} = \frac{\frac{\theta}{k}+1}{\sqrt{M^2-1}}\,\frac{1}{1-\mathcal{H}_j}$$

The solution of Equation (4.5) is simply

$$(4.6a)\quad \frac{\bar{\delta}}{\bar{\delta}_R} = e^{\frac{1}{1-\mathcal{H}_j}\,I(\theta,\theta_R)}$$

where, $$(4.6b)\quad I(\theta,\theta_R) = \int_{\theta_R}^{\theta} \frac{\frac{\theta}{k}+1}{\sqrt{M^2-1}}\,d\theta$$

and $\bar{\delta}_R = 1-\mathcal{H}_j\left(1-\frac{\delta^*}{\delta}\right)_j$

By utilizing the characteristic relation $\theta = \bar{\nu} - \nu$,

where $\nu(M) = \sqrt{\frac{\gamma+1}{\gamma-1}}\,\tan^{-1}\left[\sqrt{\frac{\gamma-1}{\gamma+1}}\sqrt{M^2-1}\right] - \tan^{-1}\sqrt{M^2-1}$

and $\bar{\nu} = \nu(\bar{M})$,

the function $I(\theta,\theta_R)$ is evaluated as follows:

$$(4.7)\quad I(\theta,\theta_R) = \frac{1}{k}\left[J(M) - J(M_R)\right] - \left(\frac{\bar{\nu}}{k}+1\right)\ln\frac{W_e}{W_{eR}}$$

where $J(M) = \int_1^M \frac{\gamma \, dM}{M\left(1 + \frac{\gamma - 1}{2} M^2\right)}$

The function J(M) is tabulated in Table I and plotted against Mach number in Figure 10.

By utilizing Equations (4.5), (4.6a) and (4.6b) and Equation (2.24) the variation of θ, or $\frac{p}{p_1}$ with axial distance x, is readily calculated. One finds that

$$(4.8) \quad \frac{d\theta}{d\bar{x}} = \frac{(1 - \gamma \ell_j) k \sqrt{M^2 - 1}}{\bar{\delta}}$$

or,

$$(4.9) \quad \frac{\bar{x} - \bar{x}_R}{\bar{\delta}_R} = \frac{1}{1 - \gamma \ell_j} \int_{\theta_R}^{\theta} \frac{1}{k} \left(\frac{\bar{\delta}}{\bar{\delta}_R}\right) \frac{d\theta}{\sqrt{M^2 - 1}}$$

where $\bar{x} = \frac{x}{\delta_R}$

When transition occurs in the wake the mixing rate parameter k is approximated by a step-function, as shown in the accompanying sketch (p. 45) (θ_{TR} denotes the value of θ at which abrupt laminar-turbulent transition is assumed to occur).

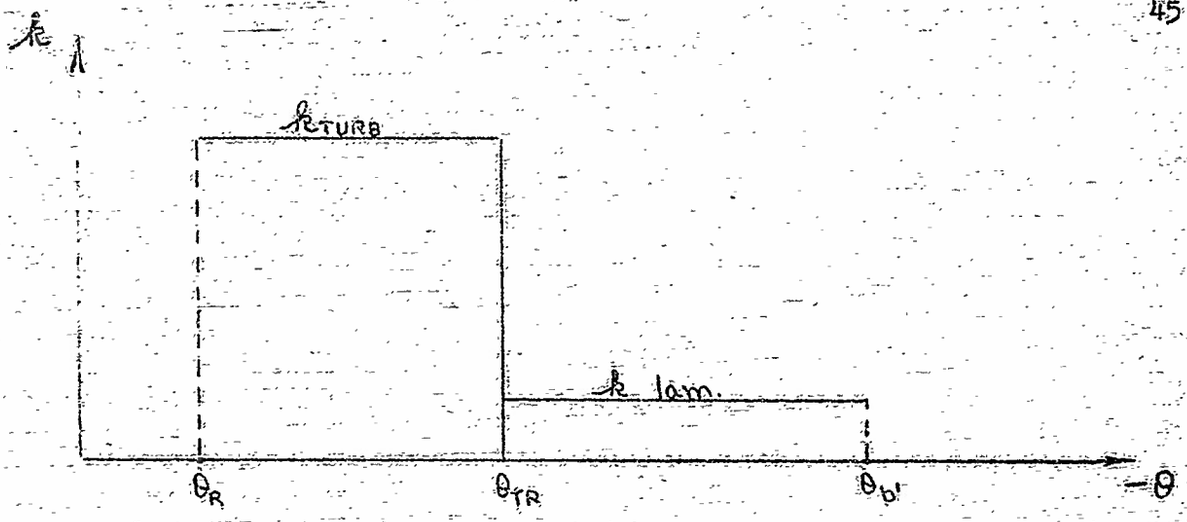

For the range $|\theta_R| \leqq |\theta| \leqq |\theta_{TR}|$ the function $I(\theta, \theta_R)$ in Equations (4.6b) and (4.7) is evaluated exactly as before, with $k = k_{turb}$. In the laminar region, $|\theta_{TR}| \leqq |\theta| \leqq |\theta_b|$ the integral in Equation (4.6b) is split into two parts, and

$$I(\theta,\theta_R) = \frac{1}{k_{lam}}\left[J(M) - J(M_{TR})\right] + \frac{1}{k_{TURB}}\left[J(M_{TR}) - J(M_R)\right]$$

(4.10) $$- \bar{\nu}\left[\frac{1}{k_{TURB}} \ln \frac{We_{TR}}{We_R} + \frac{1}{k_{lam}} \ln \frac{We}{We_{TR}}\right] - \ln \frac{We}{We_R}$$

The integral appearing in the relation between θ and x (Equation (4.9)) is also evaluated in two parts. Details of the calculation are discussed later in connection with the application of the "simplified" theory to the base pressure problem (Section 5).

Region 2.

In Section 2.5 it was pointed out that a critical point of Equation (2.30) does not exist when $\mathcal{K}$ = const., as in Region 1. The condition

determining the integral curve must therefore be associated with Region 2. In this region $\mathcal{H}_j \leq \mathcal{H} \leq 1$ and $f = 1$, or $\phi_1 = \dfrac{1 - \frac{\gamma-1}{2} w_1^2}{\gamma w_1}$, and the equation corresponding to Equation (2.30) is

$$(4.11)\quad \frac{dw_e}{dw_1} = \frac{\phi_e}{\phi_1} \frac{\left[\phi_e \sqrt{\gamma}\left(\frac{\theta}{k}+1\right) + w_e\sqrt{\gamma} - \frac{2}{w_1\sqrt{\gamma}} + \left(\frac{1-\frac{\gamma-1}{2}w_1^2}{w_1^2\sqrt{\gamma}}\right) w_e\right]}{\left[\phi_e \sqrt{\gamma}\left(\frac{\theta}{k}+1\right) + w_e\sqrt{\gamma} - \frac{1+\frac{\gamma+1}{2}w_1^2}{w_1\sqrt{\gamma}}\right]}$$

The critical point of Equation (4.11) occurs when $w_1 = \sqrt{\frac{2}{\gamma+1}}$, or $M_1 = 1.0$, and, by analogy with the exact solution (Section 3), the integral curve in region 2 is made to pass through this point, although it lies outside the region of real flows. The two regions are then joined by requiring that $\mathcal{H}_2$ equal $\mathcal{H}_j$ at the junction point. Also the dead-water region is assumed to vanish at this point, and therefore δ coincides with δ_j.

Equation (4.11) is integrated by two different methods:

(1) When $\bar{M} < 2.0$ (approx.) $\frac{dw_e}{dw_1}$ is so small that the equation can be integrated by an iteration scheme in which $\frac{dw_e}{dw_1} = 0$ in first approximation. By solving the equation obtained by setting the numerator of the term on the right-hand side of Equation (4.11) equal to zero, one finds w_e and therefore $\frac{dw_e}{dw_1}$ as functions of w_1. The value of $\frac{dw_e}{dw_1}$ so derived is then introduced on the left-hand side of Equation (4.11) and the resulting equation is again solved for $w_e = f(w_1)$, etc.

(2) When $\bar{M} > 2.0$ (approx.) the first scheme did not converge sufficiently fast. The integral curve is then obtained by passing a parabola with the correct slope and curvature through the cirtical point at $w_1 = \sqrt{\frac{2}{\gamma+1}}$

and utilizing numerical integration thereafter. This method is similar to the scheme utilized for the "exact" equation (Equation (2.30)).

The result of a typical integration for the flow in regions 1 and 2 is shown in the $W_e - W_1$ plane in Figure 11 for $\bar{M} = 3.0$ and a turbulent wake ($k = 0.03$). The dashed curve represents the more exact solution obtained by the methods described in Section 3. (Clearly for the curve passing through the point $W_1 = \sqrt{\frac{2}{\gamma+1}}$ only the segment on which $\mathcal{H}_j \leq \mathcal{H} \leq 1.0$ has any reality).

Values obtained for θ_R at $\mathcal{H}_2 = \mathcal{H}_j = 0.720$ are tabulated below:

M	$\theta_R{}^\circ$
1.5	-0.38
2.0	-0.54
3.0	~~[illegible]~~ -1.34
4.0	-3.38

The value of w_e at the junction point does not differ appreciably from $\bar{w}_e$, so that the character of the solution in region 1 is not very sensitive to small errors in the value of w_e as determined by this approximate method.

4.2 Characteristics of Separated and Re-attaching Flows and Recompression in Wakes ("Simplified" Theory).

Re-attaching Flows. Once it is known that θ_R and the recompression in Region 2 are small, the main characteristics of the recompression in wakes, or of re-attaching flows in general, can be predicted from the form of the

momentum equation and the flow solution in Region 1 (Equations (2.9) or (4.2), and Equations (4.6) and (4.8)). By referring to the momentum equation (Equation (2.9)) in a jet-like flow $(\tau_w = 0,\ \mathcal{H} = \mathcal{H}_j)$, one sees that the value of the pressure rise Δp times a mean δ is equal to the momentum transported to the dissipative flow, $\int u_e \, d\bar{m}$, which is of the order of magnitude of $\bar{u}_e \Delta\bar{m}$, minus the net change in momentum of the dissipative flow, which is of the order of magnitude $\mathcal{H}_j \bar{u}_e \Delta\bar{m} + \bar{m}\mathcal{H}_j \Delta u_e$. Now $\Delta u_e \approx \frac{\Delta p}{\rho_e \bar{u}_e}$, and $\Delta\bar{m}$ is not much larger in order of magnitude than $\bar{m}$ itself, or, $\Delta m \approx \bar{\rho}_e \bar{u}_e \delta_j (1 - \frac{\delta^*}{\delta})_j$. By making use of these approximate relations one finds that, (roughly)

$\frac{\Delta p}{\rho_e u_e^2} \approx \frac{\delta_j}{\delta}$. When $\delta >> \delta_j$, as in the more familiar case of a "half-jet", then the pressure is practically constant at the ambient value. But when two gas streams converge, or when a gas stream is directed toward a surface, then $\delta \to \delta_j$, and large increases in static pressure are made possible by the transport of mass (and momentum) to the internal dissipative flow. This mechanism is not confined to supersonic flows; it is undoubtedly the main factor in the rapid pressure rise observed on an airfoil in low-speed flow when the separated laminar flow re-attaches itself as a turbulent region downstream of the "separation bubble" (see, for example, Reference 21). Incidentally, for a given mixing rate one would expect a much larger increase in pressure ratio at high velocities than at low velocities, because $\frac{\Delta p}{p_1} = \left(\frac{\Delta p}{\rho_e u_e^2}\right) \frac{\rho_e u_e^2}{p_1} \approx M_e^2$

This conjecture is borne out by the numerical calculations to be discussed later and by experimental evidence.

Qualitatively the form of the pressure distribution in re-attaching flows or wake flows can be predicted from the relations (4.6) - (4.8). It is clear that $\frac{d\theta}{dX}$, and therefore $\frac{1}{p}\frac{dp}{dX}$, is small when $\delta >> \delta_j$ and reaches its maximum value very rapidly when $\delta \rightarrow \delta_R$ because of the exponential character of the δ-θ relation. The variation of $\frac{\bar{\delta}}{\delta_R}$ with θ for Mach numbers of 1.5, 2.0 and 3.0 is illustrated for a turbulent wake (k = 0.03) in Figure 12a, while Figure 12b shows the corresponding axial static pressure distribution for these cases. A typical case with transition in the wake is shown in Figure 13a, and the corresponding pressure distribution is plotted in Figure 13b. Here $\bar{M} = 3.0$, $k_{turb} = 0.03$ and $Re_c = 2 \times 10^6$. For simplicity k_{lam} has been taken constant (see discussion in Section 2.3), and equal to the flat plate value 0.00124 at $Re_c = 2 \times 10^6$. (These numerical examples are taken from the base-pressure calculations to be discussed later.)

From Equations (4.6a) and (4.6b) and Figures 12 and 13 it is clear that $\frac{\bar{\delta}}{\delta_R}$ increases very rapidly with $|\theta|$. As predicted from the qualitative discussion of re-attaching flows (page 48), most of the compression occurs near re-attachment, in the range $1 \leq \frac{\bar{\delta}}{\delta_R} \leq 5$ say. In fact, by Equations (4.6a) and (4.6b), (4.6c) $\frac{\bar{\delta}}{\delta_R} \approx e^{\frac{\theta^2}{\lambda}}$, roughly, where $\lambda = 2k\sqrt{M^2-1}\,(1-\mathcal{H}_j)$, and M is some average Mach number. In the base pressure problem, for example, when k is constant the base pressure ratio drops as $\frac{h}{\delta_b}$ or $\frac{\bar{\delta}}{\delta_R}$ increases, but at a decreasing rate (high Reynolds number regime).

Several important conclusions can be drawn from the approximate relation above (Equation (4.6c)):

(1) For a specified value of $\frac{\bar{\delta}}{\delta_R}$ one finds that $\theta \sim \sqrt{\xi}$, or the compression, as measured by the isentropic flow deflection, increases with increase in mixing rate. Since the pressure ratio is a rather sensitive function of θ, the marked difference between laminar and turbulent re-attaching flows is now placed on a quantitative basis. Figures 13a and 13b bear out the conclusion that the laminar portion of a flow with transition generally contributes very little to the recompression.

(2) Since $\theta \sim (M^2-1)^{1/4}$ the pressure ratio $\frac{\bar{p}}{p}$ in a re-attaching flow increases quite rapidly with Mach number (Figure 12b; see also Section 5.2).

(3) θ is sensitive to the value of $\mathcal{H}_j$ assumed in the "jet". The factor $(1 - \mathcal{H}_j)$ is a measure of the rate at which the internal dissipative flow "destroys" momentum received from the external flow. Experimental data is required to determine this parameter, which in this paper is taken to be 0.720, i.e., the value for a "free" jet at constant pressure.

<u>Separated Flows</u>: The approximations introduced in Region 1 of the wake behind a supersonic airfoil with a blunt trailing edge (Section 4.1) are also applicable to separated flows with a supersonic external stream, where the influence of the viscous stress at the surface is negligibly small. An important example of such a flow occurs in the laminar boundary layer-shock wave interaction, where the laminar layer separates upstream of the incident shock.

In the separated flow region,

$$(4.12) \qquad \frac{\bar{\delta}}{\bar{\delta}_s} = e^{\frac{1}{1-\mathcal{H}_j} I(\theta,\theta_s)} \qquad \text{where} \qquad \bar{\delta} = \frac{\delta - \mathcal{H}_j(\delta_j - \delta_j^*)}{\delta_s}$$

where δ_s is the thickness of the dissipative flow and θ_s is the flow inclination "at separation". [Of course the value of θ_s cannot be predicted by the simplified mixing theory; it must be obtained by an extension of the usual boundary layer theory[4], or by integration of Equations (2.28) and (2.29) with $\sigma \neq 0$, k variable, and suitable boundary conditions. This problem will be discussed in a later paper.] By referring to the expression for $\frac{d\theta}{dx}$ (Equation (4.8)) one sees that $\frac{1}{p}\frac{dp}{dx}$ has its maximum value in this case at the separation point, and drops off very rapidly downstream, because of the exponential character of the $\delta - \theta$ relation (Equation (4.12)). An example of such a laminar separated flow is illustrated in Figures 14a and 14b.

Here $Re_{x_s} = 1.10 \times 10^5$, $\theta_s = 1.23^\circ$ *, $\bar{M} = 2.0$, $k_{lam} = 0.0055$.*

A pressure distribution of this form is quite typical of laminar separated or "detached" flows, and also of turbulent separated flows, although, in the latter case, because of the much larger mixing rate, the pressure increase is correspondingly larger. A pressure distribution similar to that shown in Figure 14b is found downstream of flow detachment in an overexpanded supersonic rocket nozzle.[7,8]

In the case of the laminar boundary layer shock wave interaction the region upstream of the incident shock is a separated flow, while the flow downstream of the reflected expansion fan is a re-attaching flow. Thus the S-shaped pressure distribution on the surface observed experimentally

---

* The flow conditions at separation were computed by the approximate method of Reference 4. The value of k_{lam} is taken to be constant at the flat-plate value for a Reynolds number equal to Re_{x_s}.

is understandable. Provided that friction is neglected, which is strictly correct only if the plate is cut off at the beginning of Region 2, the re-attaching flow can be treated exactly as in the base pressure problem. Therefore, the laminar boundary layer-shock wave interaction problem can be solved, at least approximately, by means of the simplified mixing theory, provided a suitable reflection condition for the incident shock wave is introduced. If the incident shock wave is reflected from the "jet" as from a free boundary, then the pressure drop across the reflected expansion fan exactly cancels the pressure rise across the incident wave. In that case $\theta_2 = \theta_3 - 2\theta_W$, where θ_3 is the flow inclination angle in the separated region just upstream of the incident shock, θ_2 is the flow inclination angle in the re-attaching flow just downstream of the reflected expansion fan, and θ_W is the flow deflection across the incident shock. The other boundary condition at the junction of the separated and re-attaching flow regions is of course $\delta_3 = \delta_2$. [θ_R for the re-attaching flow is determined from $M_{+\infty}$ (see Section 4.1)] In Figure 15 the calculated static pressure distribution on the wall is shown for $\bar{M} = M_{-\infty} = 2.0$, $\theta_W = 4^\circ$, $Re_{x_s} = 2.5 \times 10^5$, $k_{lam} = 0.0037$. For this case the pressure increase on both sides of the shock is about equal, and the flow pattern is nearly symmetrical. The asymetric flow pattern and pressure distribution found at higher Reynolds numbers, or for stronger incident shocks, appears to be associated with transition in the reattaching flow, which greatly increases the mixing rate and pressure rise in this region. This flow regime can be treated by methods similar to those employed in the base pressure problem for the case when transition occurs in the wake

(Section 5). A detailed treatment is reserved for a later paper.

For the turbulent boundary layer the situation is more complicated. In this case, the deep penetration of the shock makes it necessary to modify some of the basic assumptions of the present paper, at least locally, particularly the assumption of constant pressure across the internal dissipative flow (See Section 6).

5. Application of Simplified Mixing Theory to the Base Pressure Problem in Plane Supersonic Flow.

5.1 Method and Assumptions.

This problem has already been formulated in Section 3 as an application of the more exact theory. When the wake is fully turbulent the procedure for the simplified theory is quite similar to that previously described in Section 3, but when transition occurs in the wake the scheme is somewhat modified.

(a) Turbulent Wake - Transition in Airfoil Boundary Layer.

When the wake is fully turbulent it is again assumed that k = const., and $\frac{\bar{\delta}}{\bar{\delta}_R}$ is then completely determined as a function of θ for every Mach number $\bar{M}$ by Equations (4.6) and (4.7). At the airfoil trailing edge the boundary condition $\delta = \frac{h}{2} + \delta_{b'}$ must be satisfied, or

$$(5.1) \qquad \frac{\bar{\delta}}{\bar{\delta}_R} = \frac{\frac{h}{2} + \delta_{b'}}{\delta_R\left[1 - \mathcal{H}_j\left(1 - \frac{\delta^*}{\delta}\right)_j\right]} - \frac{\mathcal{H}_j\left(1 - \frac{\delta^*}{\delta}\right)_j}{1 - \mathcal{H}_j\left(1 - \frac{\delta^*}{\delta}\right)_j}$$

(Approximately, $\mathcal{K}_j = 0.720$ and $(1 - \frac{\delta^*}{\delta})_j = 0.45$ for a turbulent low-speed isothermal jet) To every value of $\frac{(\frac{h}{2} + \delta_{b'})}{\delta_R} = \frac{\delta_{b'}}{\delta_R}\left[1 + \frac{h}{2\delta_b}\frac{\delta_b}{\delta_{b'}}\right]$ there corresponds a value of $\frac{\bar{\delta}}{\delta_R}$ and therefore a value of $\theta_{b'}$ by Equation (5.1), and finally a value of base pressure ratio $\frac{p_{b'}}{\bar{p}} = f(\theta_{b'}, \bar{M})$. In order to relate this value of the base pressure ratio to $\frac{\delta_b}{h}$ it is necessary to calculate $\frac{\delta_{b'}}{\delta_R}$ and $\frac{\delta_{b'}}{\delta_b}$. The ratio $\frac{\delta_R}{\delta_{b'}}$ is obtained as follows:

By definition,

$$\bar{m}_R = \frac{p_R}{q_{e_R}}\,\delta_R\left(1 - \frac{\delta^*}{\delta}\right)_R \quad \text{and} \quad \bar{m}_{b'} = \frac{p_{b'}}{q_{e_{b'}}}\,\delta_{b'}\left(1 - \frac{\delta^*}{\delta}\right)_{b'},$$

so that

$$(5.2) \qquad \frac{m_R}{m_{b'}} = \frac{\left(\frac{p_R}{q_{e_R}}\right)}{\left(\frac{p_{b'}}{q_{e_{b'}}}\right)}\,\frac{\delta_R}{\delta_{b'}},$$

where it is assumed, as in Section 3, that $\left(1 - \frac{\delta^*}{\delta}\right)_{b'} = \left(1 - \frac{\delta^*}{\delta}\right)_R = \left(1 - \frac{\delta^*}{\delta}\right)_j = \text{const.}$

By integrating Equation (2.25) for the mixing rate, and dividing through by $m_{b'}$ one obtains

$$\frac{m_R}{m_{b'}} = 1 + \frac{k}{m_{b'}}\int_{x_{b'}}^{x_R} \frac{p}{q_e}\,dx = 1 + \frac{k}{m_{b'}}\int_{\theta_{b'}}^{\theta_R} \frac{p}{q_e}\,\frac{\left(\frac{d\delta}{d\theta}\right)}{\left(\frac{d\delta}{dx}\right)}\,d\theta, \text{ OR}$$

$$(5.3) \qquad \frac{m_R}{m_{b'}} = 1 + \frac{\frac{p_R}{q_{e_R}}}{\frac{p_{b'}}{q_{e_{b'}}}}\,\frac{\delta_R}{\delta_{b'}}\left[\frac{1}{\left(1 - \frac{\delta^*}{\delta}\right)_j} - \mathcal{K}_j\right]\frac{1}{1 - \mathcal{K}_j}\,D,$$

where
$$D = \int_{\theta_{b'}}^{\theta_R} \left(\frac{\delta}{\delta_R}\right) \frac{\left(\frac{p}{q_e}\right)}{\left(\frac{p_R}{q_{eR}}\right)} \frac{d\theta}{\sqrt{M^2-1}}$$

Finally, by Equations (5.2) and (5.3),

$$(5.4) \qquad \frac{\delta_R}{\delta_{b'}}\left[1 - \left\{\frac{1}{\left(1-\frac{\delta^*}{\delta}\right)_j} - \mathcal{H}_j\right\}\frac{D}{1-\mathcal{H}_j}\right] = \frac{\left(\frac{p_{b'}}{q_{eb'}}\right)}{\left(\frac{p_R}{q_{eR}}\right)}$$

For the completely turbulent wake the integral D is a unique function of $\theta_{b'}$ for every Mach number M, according to Equations (4.6) and (4.7).

As explained in Section 3 the ratio $\frac{\delta_b}{\delta_{b'}}$ as given by Equation (3.2b) is obtained by applying the condition of conservation of mass across the expansion around the "corner" at the airfoil trailing edge.

By utilizing Equations (5.1), (5.4), and (3.2b) the base pressure ratio is related to $\frac{\delta_b}{h} = \frac{\delta_b}{c}\frac{c}{h}$. The variation of base pressure with Reynolds number at a given Mach number is obtained by introducing the same postulated variation of $\frac{\delta_b}{c}$ with Reynolds number and Mach number that is described in Section 3, and illustrated in Figure 8 for $M = 3.0$.

(b) Transition in Wake - Airfoil Boundary Layer Laminar.

When transition in the airfoil boundary layer is described in terms of curve I of Figure 8, for example, then for $Re_c < 4 \times 10^6$ the boundary layer is completely laminar, and the transition "point" moves off the body and into the wake. Since the mixing coefficient k in the

laminar portion of the wake is a function of Reynolds number, the relation between $\frac{\delta}{\delta_R}$ and θ is no longer independent of Reynolds number, and the procedure outlined in (2a) above must be modified.

In the first place a statement must be made regarding the transition Reynolds number in the wake, about which little is known at present. Transition in the wake must depend to a large extent on the previous history of the laminar oscillations in the airfoil boundary layer, as well as on the growth of disturbances along the laminar portion of the wake itself. Based on the meager data available, it is assumed that a "free", high-velocity laminar half-jet, undisturbed by oscillations fed into the jet from an upstream boundary layer, would have a transition Reynolds number of 4×10^5. Therefore when $Re_c < 4 \times 10^6$ the transition Reynolds number in the wake must approach a value of 4×10^5, while $Re_{TR_{WAKE}} = 0$ when $Re_c = 4 \times 10^6$ and transition just reaches the airfoil trailing edge. Taking a linear variation of $Re_{TR_{wake}}$ with Re_c between these two conditions, roughly,

$$(5.5) \qquad Re_{TR_{WAKE}} = 4 \times 10^5 - \frac{Re_c}{10} \quad \text{at high velocities.}$$

(For transition curve II, $Re_{TR_{wake}} = 3 \times 10^5 - \frac{Re_c}{10}$). A smooth movement of transition from airfoil to wake is presumed. All that can be claimed for this approximation is that it gives the correct form of the dependence of transition on Re_c, and provides for an accelerated forward movement of transition in the wake with increasing Reynolds number.

On the basis of this assumption regarding transition in the wake the variation of base pressure with Reynolds number at a given Mach number

in this flow regime is calculated by an iteration method. Suppose that c/h is given. For some value of $Re_c < 4 \times 10^6$ a series of trial values of θ_{tr}, or the flow deflection angle at the transition point, are selected. The corresponding locations of the transition "point" and values of $Re_{tr_{wake}}$ are calculated by an iteration scheme, in which the value of θ_{tr}, and the base pressure are also calculated. Now the correct value of $Re_{tr_{wake}}$ at the prescribed value of Re_c is given by Equation (5.5), so the proper value of θ_{tr} can be determined from a plot of $Re_{tr_{wake}}$ vs. θ_{tr}, and the corresponding base pressure calculated by interpolation.

The details of the method are as follows:

Once a trial value of θ_{tr} is selected the relation between $\frac{\bar{\delta}}{\delta_R}$ and θ required in the statement of the boundary condition (Equation (5.1)) is obtained from Equations (4.6) and (4.10). However the value of the mixing coefficient in the laminar portion of the wake must be known, or chosen. For our present purposes, it is sufficient to take k_{lam} equal to the mixing coefficient in the laminar boundary layer just at the airfoil trailing edge, i.e.,

$$k_{lam} = \frac{c_f/2}{1-\mathcal{H}_0} = \frac{g(M)}{\sqrt{Re_c}} \frac{0.332}{1-\mathcal{H}_0} \; *$$

The Mach number factor g(M) is obtained from Figure 19 of van Driest's paper[18] and is tabulated below:

M	g(M)
1.55	0.98
2.0	0.95
3.0	0.91
4.0	0.87
5.0	0.81

* If $\mu \sim T$, g(M) = 1.0.

The value of $\mathcal{H}_\delta$ utilized in calculating k_{lam} is 0.827, corresponding to $\frac{u(\delta)}{u_e} = 0.9975$, and the corresponding value of $\mathcal{H}_j$ employed is 0.720.* A typical plot of $\frac{\bar{\delta}}{\delta_R}$ vs. θ with transition in the wake is illustrated in Figure 13a.

The right hand side of Equation (5.1) is also determined as a function of θ by utilizing Equations (5.4) and (3.2b), where the value of $\left(1-\frac{\delta^*}{\delta}\right)_b$ for the laminar boundary layer with zero heat transfer at the airfoil surface is given by $\frac{3.87}{5.60 + 1.20(\gamma-1)\ M_b^2}$.*

The value of $\left(1-\frac{\delta^*}{\delta}\right)_{b'}$ is taken to be 0.45, exactly as in the case of the fully turbulent jet. The value of $\frac{\delta_b}{h} = \frac{\delta_b}{c}\frac{c}{h}$ is already known once c/h and Re_c are prescribed, since $\frac{\delta_b}{c}$ is given by Equation (3.5). The correct value of $\theta_{b'}$ for the particuaar trial value of θ_{TR} is then found from the intersection of the curves of $\frac{\bar{\delta}}{\delta_R}$ and the R.H.S. of Equation (5.1) plotted as functions of θ. The location of the transition point in the wake aft of the trailing edge is then calculated from the relation

$$(5.6)\quad \frac{\ell}{\bar{\delta}_R} = \frac{\bar{X}_{b'} - \bar{X}_{TR}}{\bar{\delta}_R} = \int_{\left(\frac{\bar{\delta}}{\bar{\delta}_R}\right)_{TR}}^{\frac{\bar{\delta}_{b'}}{\bar{\delta}_R}} \frac{1}{\theta + k_{lam}}\, d\left(\frac{\bar{\delta}}{\bar{\delta}_R}\right),$$

and the corresponding value of $Re_{TR_{wake}}$ is given by the relation

$$(5.7)\quad Re_{TR_{WAKE}} = \frac{\ell}{c}\, Re_c \left(\frac{p_{TR}}{\bar{p}}\right)^n \frac{M_{TR}}{\bar{M}},$$

---

* See footnote on pages 37 and 38.

where $n = \frac{\gamma-1}{\gamma}\left[\frac{1}{2}\frac{\gamma+1}{\gamma-1} - m\right]$, if $\mu \sim T^{m}$,

and $$\ell/c = \frac{\bar{\ell}}{\bar{\delta}_R}\left[1 - \mu_j\left(1 - \delta^*/\delta_j\right)\right]\frac{\delta_R}{\delta_{R'}}\frac{\delta_{R'}}{\delta_{R}}\frac{\delta_R}{c} .$$

For air $\gamma = 1.40$ and $m = 0.76$, so $n = 0.64$.

Since the value of $Re_{tr_{wake}}$ obtained from Equation (5.7) does not in general coincide with the assumed value given by Equation (5.5), the whole procedure must be repeated for three or four trial values of θ_{tr} in order to determine the correct $Re_{tr_{wake}}$ and base pressure by interpolation with sufficient accuracy. The scheme is repeated for several representative values of Reynolds number, Re_c. Fortunately after some experience only a few trials are necessary.

Evidently, for sufficiently low Reynolds numbers $\theta_{tr} \rightarrow \theta_R$ and the flow in Region 1 becomes completely laminar. For Reynolds numbers below the value at which θ_{tr} is calculated to be approximately equal to θ_R , the conditions are determined by analogy with the more exact theory. In this theory conditions upstream of the critical point are unaffected by conditions downstream of this point, and are therefore independent of the movement of transition once transition passes the critical point. By analogy, it is assumed now that once transition passes into Region 2, conditions in Region 1 remain independent of Region 2. The value of θ_R at a given Mach number $\bar{M}$ is regarded as a constant and the character of the flow solution in Region 1 is determined completely by the variation of laminar mixing rate with Reynolds number (see Section 5.2). At very low Reynolds numbers, the present mixing theory must be modified because δ_R/ℓ is no longer small.

5.2 Effect of Reynolds Number on Base Pressure: The Various Flow Regimes.

A sufficient number of numerical examples have been calculated for all flow regimes to indicate the important trends in the variation of base pressure with Reynolds number, Mach number, c/h and type of transition in the airfoil boundary layer. Figure 16 shows the variation at $\bar{M} = 3.0$ of $\frac{p_e}{p}$ with Reynolds number for c/h = 10.0, with the two types of assumed boundary layer transition. (In all the other figures only the calculated base pressure for curve I is shown). In Figure 9 the curve computed from the simplified theory for $\bar{M} = 3.0$ and c/h = 3.0 is shown in comparison with the curve obtained by the "exact" theory (Section 3). These curves show a similar qualitative behavior. In view of the assumptions made in the simplified theory, and the probable sensitivity of the results of the "exact" theory to the assumed F-μ curve (Sections 2 and 3), the differences in the numerical values of base pressure should not be taken too seriously at present. The numerical results are properly regarded as preliminary.

The effect of Reynolds number and c/h on base pressure at $\bar{M} = 2.0$ is illustrated in Figure 17 for values of c/h of 3.0 and 10.0. The low Reynolds number region at $\bar{M} = 2.0$ is emphasized in Figure 18 for c/h = 10.0, and in Figure 20 the base pressure with airfoil boundary layer laminar to the trailing edge is plotted against the parameter $Re_c^{\frac{1}{2}}\, h/c$ employed by Chapman.[17] Data for two of the airfoils with blunt trailing edges tested by Chapman in this flow regime are also shown for comparison.

In the "fully turbulent" regimes at high Reynolds numbers the base pressure ratio is plotted against the parameter $Re_c^{1/5}\, h/c$ for

$\bar{M}$ = 1.5, 2.0 and 3.0 in Figure 19. Again Chapman's data in this flow regime is shown for comparison; the curves are reproduced from Figure 28 of Reference 17, in which the "mean" curves for the entire "thickness group" of airfoils are presented. The thickness ratios for the group are 0.05, 0.075 and 0.10, and the ratio of airfoil trailing edge thickness to maximum thickness has the discrete values 0.25, 0.50, 0.75 and 1.0, so that c/h ranges from 10.0 to 80.0 in these tests.

It is remarkable that in spite of the approximate character of the present mixing theory it appears to give the correct fluid-mechanical explanation of the observed phenomena and flow regimes in the base pressure problem. Unfortunately, Chapman's data for the blunt trailing edge airfoils does not include the important intermediate regime in which transition moves upstream in the airfoil boundary layer, but base pressure data on bodies of revolution,[6,20] which should be at least qualitatively similar to the two-dimensional case, illustrate perfectly the regimes determined by our calculations. Four such flow regimes can be distinguished, in which the contrasting effects of mixing rate variations and variations of δ_b determine the quite different dependence of the base pressure on Reynolds number in the different flow regimes. In preceding discussions, it has been shown that an increase in k increases the pressure ratio across a compression, and therefore decreases the base pressure (Section 4.2), while an increase in δ_b increases the base pressure (Sections 3 and 4.2). These qualitative considerations are borne out by the results of the computations.

In order of increasing Reynolds number the four flow regimes are as follows:

(1) At sufficiently low Reynolds numbers not only the body boundary layer is laminar but also that region of the wake in which the major portion of the recompression occurs (Region 1). Within this regime, as Re_c increases, the laminar mixing rate decreases and the base pressure increases slowly with Reynolds number (Figure 18). The decrease in k_{lam} with increasing Re_c is apparently more than enough to offset the decrease in thickness of the boundary layer at the airfoil trailing edge, or the decrease in thickness of the mixing region in the wake. Because of the low laminar mixing rate the base pressure ratio is relatively high.

(2) As the Reynolds number is increased, eventually transition begins to move upstream in the wake, and the accompanying large increase in local mixing rate ($k_{turb} \approx 5\text{-}10\ k_{lam}$) counteracts the effects discussed in (1). After reaching a local maximum (Figure 18), the base pressure drops precipitously with increase in Re_c. (Figures 8, 16, 17, and 20). The large increase in local mixing rate is a much more important factor than the accompanying increase in the thickness of the mixing region, which, by itself, would have just the opposite effect on base pressure.

After transition in the wake has moved quite close to the airfoil trailing edge, the base pressure ratio continues to drop with increasing Reynolds number so long as the airfoil boundary layer remains laminar, because of the decrease in boundary layer thickness at the trailing edge

with increasing Reynolds number. This decrease is expected to be much less rapid than the first steep drop which occurs when transition moves forward in the wake. If the boundary layer transition Reynolds number is sufficiently high, and if the ratio of chord to airfoil trailing edge thickness is low, but not otherwise, the base pressure ratio depends only on the ratio δ_t/h, or on the parameter $Re_c^{\frac{1}{2}} h/c$, over an appreciable Reynolds number range in this flow regime (see pp. 65-67).

(3) At a sufficiently high Reynolds number, transition will occur in the airfoil boundary layer just at the trailing edge. When the Reynolds number is increased still further, presumably the mixing rate in the wake is little affected, but transition moves forward on the airfoil, and the boundary layer at the trailing edge thickens accordingly. Thus the base pressure ratio at first increases with increasing Reynolds number in this flow regime. However, when transition has moved upstream sufficiently far from the trailing edge, the normal decrease in local turbulent boundary layer thickness with increasing Reynolds number begins to offset the thickening effect of the forward movement of transition. The base pressure curve reaches a local maximum and then decreases again with increasing Reynolds number (Figures 8, 16, and 17).

(4) Finally, a high Reynolds number regime is reached in which transition in the airfoil boundary layer is essentially "fixed" and the base pressure ratio drops slowly but noticeably with increasing Reynolds number, because of the decrease in turbulent boundary layer thickness at the trailing edge. In this regime, the base pressure ratio is a function solely of the parameter $Re_c^{1/5} h/c$ (Figure 19), or of some similar parameter involving the product of h/c and a logarithmic function of Reynolds number.

Briefly, the effects of Mach number, c/h - ratio and transition in the airfoil boundary layer on base pressure are as follows:

(i) Transition and Mach number.

Whatever affects transition in the airfoil boundary layer also determines the location, shape and depth of the "valley" in the curve of base pressure ratio versus Reynolds number at a given Mach number. Thus the base pressure is affected by the heat transfer rate at the airfoil surface, by surface pressure gradient, surface roughness, surface irregularities such as sharp corners, free stream turbulence, etc Since transition in the airfoil boundary layer is expected to depend also on Mach number, the Reynolds number range defining the "valley" in the base pressure curve is a function of Mach number. The effect of each of these factors on base pressure can now be predicted, at least qualitatively, when its effect on the thickness and character of the boundary layer at the airfoil trailing edge is known.

On the basis of the discussion in Section 4.2, it was expected that for a given mixing rate the pressure ratio supported by the wake flow increases rapidly with Mach number, i.e., the base pressure ratio decreases rapidly with increasing Mach number (see Figure 19) This result is probably significant also for other flow phenomena in which mixing is important, such as boundary layer separation, for example. Of course the actual numerical values of base pressure depend critically upon the mixing coefficient k. By selecting k as a suitable function of Mach number coincidence between the theoretical computations and experimental data could be obtained. By referring to Figure 19 one may conclude tentatively that

the mixing rate at low supersonic Mach numbers is probably of the order of 0.05 (somewhat larger than the constant value of 0.03 assumed in this paper), and that k apparently decreases with increasing Mach number. Some support for this tentative conclusion comes from recent experimental work on the rate of spreading of a supersonic turbulent stream into quiescent air.

(ii) Chord-Trailing Edge Thickness Ratio. (Transition in Wake).

In general the higher the ratio of chord to trailing edge thickness the larger is δ_t/h and the higher the base pressure ratio at a given Reynolds number and a fixed Mach number*. The effect of c/h ratio is particularly interesting in the intermediate wake transition region, because the rate of upstream movement of transition in the wake with increasing Reynolds number is governed largely by the parameter c/h. The transition Reynolds number $Re_{tr\,wake}$ is determined by Re_c (Eq. (5.5)), and therefore so is the ratio $\ell/c = \frac{Re_{tr\,wake}}{Re_c}$, where ℓ is the distance from airfoil trailing edge to wake transition "point". But the important parameter governing the character of the wake flow is the ratio ℓ/h. When the transition "point" just enters the significant recompression region,

$$(5.8) \qquad \frac{\ell}{h} = \frac{\ell}{c}\,\frac{c}{h} \approx 2/\theta_t ,$$

roughly. Two important conclusions can now be drawn:

---

* Thus the effect of increasing body length to obtain higher Reynolds numbers in a series of experiments is certainly much different than the effect obtained when c/h is fixed and ambient density is increased. This fact was pointed out by Bogdonoff[20].

(a) At a given Reynolds number Re_c the laminar flow region occupies a larger portion of the wake the larger the c/h ratio. In other words the forward movement of transition into the major recompression region, and the accompany drop in base pressure, begins at higher Reynolds numbers the higher the c/h ratio. For every large c/h the base pressure ratio is nearly unity, and θ_b is small and varies nearly linearly with h/c. Therefore, by Equation (5.8), ℓ/c approaches a limit and the Reynolds number marking the transition between the two flow regimes also approaches an upper limit as c/h increases. These conclusions seem to be borne out by the data presented in Figures 14 and 15 of Reference 17.

(b) For large c/h a significant variation in $\frac{\ell}{h}$ occurs with only a small variation in ℓ/c, and therefore in Re_c. Once the transition point does begin to move forward into the major recompression region the base pressure drops steeply in a narrow Reynolds number range. On the other hand for small c/h the upstream movement of transition in the wake extends over a wider Reynolds number range, and the curve of base pressure vs. Re_c is much "flatter" in this flow regime (Figures 17 and 20). Since this effect of c/h ratio is greatly accentuated at very large values of c/h it may be responsible for the almost-discontinuous change in base pressure observed by Chapman[17] under certain conditions for airfoils with very thin trailing edges (c/h = 80).

In the flow regime characterized by the forward movement of transition in the wake with increasing Reynolds number, the base pressure evidently depends not only upon δ_t/h but also upon the location of transition. In general therefore, one would not expect the base pressure to be correlated

solely against the parameter δ_t/h, or $Re_c^{\frac{1}{2}}$ h/c in this regime, but to depend also on c/h. Such a correlation exists only when transition in the wake is located quite close to the airfoil trailing edge over a significant range of Reynolds numbers below the airfoil boundary layer transition Reynolds number. By referring to Equation (5.8), one sees that this condition is fulfilled only when (a) the boundary layer transition Reynolds number is high and the value of $Re_{tr_{wake}}$ varies only slowly with Re_c (ℓ/c varies slowly with Re_c); (b) c/h is small. In Figure 20 neither the theoretically calculated base pressure nor Chapman's data are correlated by the parameter $Re_c^{\frac{1}{2}}$ h/c, largely because Re_{tr} in the airfoil boundary layer is certainly not greater than 4×10^6 (probably $Re_{tr} \approx 2 \times 10^6$ in these experiments), and the values of c/h are already too large. At low Reynolds numbers the curves of base pressure ratio vs. $Re_c^{\frac{1}{2}}$ h/c for various c/h values tend to converge and cross as shown in Figure 20 and in Figures 14 and 15 of Reference 17, because the base pressure is approaching a local maximum of the type illustrated in Figure 18. However at high Reynolds numbers these curves diverge considerably. For example, any attempt to construct a "universal" curve of base pressure ratio vs. $Re_c^{\frac{1}{2}}$ h/c by utilizing data obtained at one Reynolds number over a range of c/h values could lead to appreciable errors.

In the case of blunt-based bodies of revolution[6] transition in the body boundary layer apparently occurs at quite high Reynolds numbers ($Re_{tr} > 6 \times 10^6$), and the base pressure ratio may be correlated against the parameter $Re_L^{\frac{1}{2}}$ D/L over a definite range of L/D values*.

---

* L is body length and D is base diameter.

The ability of the present theory to predict even such details of the base pressure phenomena is another confirmation of the correctness of the basic mechanism assumed.

6. Future Investigations.

The success of the mixing theory in furnishing a qualitative fluid-mechanical explanation of the phenomena occurring in the base pressure problem encourages us to attempt to apply this theory to other problems involving the interaction between a dissipative flow region and an adjacent nearly-isentropic stream. However, in certain cases either some of the basic assumptions of the present paper must be modified, or the outer boundary of the dissipative flow region must be carefully redefined. In some cases perhaps the most serious assumption is that the static pressure is constant across the dissipative flow and equal to the local value p_e in the external stream, at $y = \delta$. In a turbulent boundary layer-shock wave interaction, for example, the incident oblique shock is reflected and refracted as it enters the layer, but apparently penetrates to the sonic velocity line close to the surface. The main reflected shock wave appears to emerge from this same region[16,22]. In the important interaction region the static pressure is certainly not uniform across a plane transverse to the flow in the supersonic portion of the boundary layer, but the pressure is probably nearly constant across the subsonic and transonic zones close to the wall. Presumably it is also this region that is most strongly affected by an increasing static pressure along the surface. It might be correct physically to define this region as the new dissipative

flow, and to treat the supersonic portion of the boundary layer as an "external", inviscid, rotational flow. Experimental and theoretical studies are required to settle this point.

The mixing theory including friction (Eq. (2.30)) is expected to furnish information about the turbulent boundary layer in an adverse pressure gradient away from shock waves. It is important to determine whether the maximum pressure increase that can be supported by a turbulent layer without separation increases rapidly with Mach number, as we have found for the recompression in the wake flow.

In many respects laminar boundary layer-shock wave interaction appears to be simpler than the turbulent case, because upstream separation occurs even for very weak incident shocks, and the incident shock wave is reflected from the separated flow very nearly as if this flow were a free boundary. The static pressure is probably nearly constant across the low-velocity region between the jet-like outer boundary and the surface. The approximate solution indicated in the present paper (Section 4.2) must be regarded as a first step; in a later paper, the important influence of surface friction on the reattaching flow and the surface pressure distribution downstream of the reflected expansion "fan" will be discussed.

Another important basic assumption of the present mixing theory is that the stagnation enthalpy is constant across the flow. For separated flows and wakes there is some question whether the mixing process may not create regions of low stagnation enthalpy near a surface, or just aft of a body. This question is best settled by experiment. For flows attached to a surface the present theory can probably be extended to cases where the surface heat transfer rate is not zero.

The present theory is capable not only of giving a qualitative explanation of all these interaction phenomena, but should furnish realistic quantitative predictions once the $F-\mathcal{H}$ curve is known and the dependence of mixing coefficient k on the parameters m, w_e and $\mathcal{H}$ is determined. This information is required particularly in the turbulent case. By specifying the quantities that must be known the theory also serves as a useful guide to experimental investigations.

CONCLUSIONS

1. An important property of supersonic wake flows, or of reattaching supersonic flows directed toward a solid surface, is the existence of a singularity in the basic differential equation, or "critical point" in the flow, which acts very much like the throat of a nozzle in determining the base pressure, for example. One important reason for the marked difference between laminar and turbulent interactions is the fact that the turbulent mixing rate is 5 to 10 times larger than the laminar mixing rate.

2. According to the present mixing theory, separated flows as well as reattaching flows are capable of supporting considerable pressure increases at high velocities. The maximum compression, as measured by the isentropic flow deflection, is roughly proportional to the square root of the mixing rate parameter, and also to $(M^2-1)^{\frac{1}{4}}$, where M is some average Mach number. Thus the pressure ratio increases rapidly with Mach number, or the base pressure ratio, for example, decreases rapidly with Mach number. In separated flows the pressure gradient along the surface is a maximum at separation, and drops off steeply downstream; in reattaching flows, or wake flows, the pressure gradient is negligible some distance upstream of

the "reattachment point", and increases very rapidly toward a maximum as this point is approached. The inflected surface pressure distribution observed in laminar boundary layer-shock wave interactions is now understandable, and the distribution itself can be calculated approximately.

3. When the present mixing theory is applied to the problem of determining the base pressure for a supersonic airfoil with a blunt trailing edge, it gives the correct fluid-mechanical explanation of the observed phenomena. Four different flow regimes can be distinguished. In order of increasing Reynolds number they are as follows:

(i) A low Reynolds number region in which not only the airfoil boundary layer is laminar but also the region of the wake in which the major portion of the recompression occurs. In this regime the base pressure ratio $\frac{p_b'}{p}$ increases slowly with Reynolds number Re_c because of the decreasing laminar mixing rate.

(ii) A regime in which transition to turbulent flow moves upstream in the wake and the base pressure curve reaches a local maximum and then drops precipitously with increasing Reynolds number, because of the large increase in mixing rate. If the ratio of chord to airfoil trailing edge thickness (c/h) is low, or if the boundary layer transition Reynolds number is high (but not otherwise), an appreciable range of Reynolds numbers exists for which transition in the wake is located quite near the base, but the airfoil boundary layer remains laminar. In this range p_b/p continues to decrease with increasing Reynolds number because of the decreasing boundary layer thickness at the airfoil trailing edge, and the governing parameter is $Re_c^{\frac{1}{2}}\, h/c$.

(iii) A regime in which transition, having "jumped" from the wake to the airfoil boundary layer, moves forward on the airfoil with increasing Reynolds number. In this regime p_B/q_∞ at first increases with increasing Reynolds number, because of the increase in boundary layer thickness at the airfoil trailing edge as the transition point moves forward. Eventually the normal decrease in local turbulent boundary layer thickness with increasing Reynolds number begins to offset the thickening effect of the forward movement of transition, and the base pressure curve reaches a local maximum and then begins to drop with increasing Reynolds number.

(iv) A high Reynolds number regime in which transition on the airfoil is practically "fixed" far from the trailing edge, and the base pressure drops slowly with increasing Reynolds number, because of the decreasing turbulent boundary layer thickness at the airfoil trailing edge. The governing parameter here is $Re_c^{1/5}\ h/c$.

Clearly, anything that affects transition in the airfoil boundary layer or in the wake will affect the "valley" in the curve of base pressure versus Reynolds number. The effect of a given parameter can be predicted, at least qualitatively, once its influence on the character and thickness of the airfoil boundary layer at the trailing edge is known.

Qualitative agreement is found between these theoretical predictions and calculations and the base pressure data of Bogdonoff and Chapman on blunt-based bodies of revolution and Chapman's data on supersonic airfoils with blunt trailing edges.

4. Considerable theoretical and experimental work remains to be done in extending this mixing theory to axially-symmetric flows, to boundary layer-shock wave interactions and other flows, and in carefully determining the dependence of the mixing rate and the mean temperature-mean velocity relation on the flow parameters.

REFERENCES

1. Tsien, H. S. and Finston, M.: Interaction Between Parallel Streams of Subsonic and Supersonic Velocities. J. Aero. Sci., vol. 16, no. 9 (Sept., 1949), pp. 515-528.

2. Lighthill, M. G.: Reflection at a Laminar Boundary Layer of a Weak, Steady Disturbance to a Supersonic Stream, Neglecting Viscosity and and Heat Conduction. Quart. Journ. Mech. and Applied Math., vol. III (1950), pp. 303-325.

3. Schubauer, G. B. and Klebanoff, P. S.: Investigation of Separation of the Turbulent Boundary Layer. NACA Technical Note No. 2133 (August, 1950).

4. Lees, L.: Interaction Between the Laminar Boundary Layer over a Plane Surface and an Incident Oblique Shock Wave. Princeton University Aeronautical Engineering Laboratory. Report No. 143, January 24, 1949.

5. Ritter, A.: On Reflection of a Weak Shock Wave from a Laminar Boundary Layer. Paper presented at meeting of Fluid Dynamics Div., Amer. Phys. Soc., Cornell Univ., Ithaca, N. Y., September 11 and 12, 1951.

6. Chapman, D. R.: An Analysis of Base Pressure at Supersonic Velocities and Comparison with Experiment. NACA Technical Note No. 2137 (July, 1950).

7. Summerfield, M., Foster, C. R., and Swan, W. C.: Flow Separation in Overexpanded Supersonic Nozzles. Presented at meeting of Institute of Heat Transfer and Fluid Mechanics, Los Angeles, Cal., June, 1948.

8. Summerfield, M.: Fundamental Problems in Rocket Research. Journal of the American Rocket Society, June, 1950, pp. 78-98, esp. pp. 94-95.

9. Stewartson, K.: Correlated Incompressible and Compressible Boundary Layers. Proc. Roy. Soc. (A), vol. 200, no. 1060 (Dec. 22, 1949), pp. 84-100.

10. Falkner, V. M. and Skan, S. W.: Some Approximate Solutions of the Boundary Layer Equations. British A.R.C., R. & M. No. 1314 (1930).

11. Hartree, D. R.: On an Equation Occurring in Falkner and Skan's Approximate Treatment of the Equations of the Boundary Layer. Proc. Cambridge Phil. Soc., vol. 33 (1937), p. 237.

12. Howarth, L.: On the Solution of the Laminar Boundary Layer Equations. Proc. Roy. Soc. (A), vol. 164A (1938), pp. 547-579.

13. Chapman, D. R.: Laminar Mixing in a Compressible Fluid. NACA Technical Report No. 958 (1950).

14. Thwaites, B.: Approximate Calculation of the Laminar Boundary Layer. Aeronautical Quarterly, vol. 1, part 3, pp. 245-280 (November, 1949).

15. von Doenhoff, A. E. and Tetervin, N.: Determination of General Relations for the Behavior of Turbulent Boundary Layers. NACA Technical Report No. 772 (1943).

16. Bogdonoff, S. M. and Solarski, A.: A Preliminary Study of a Turbulent Boundary Layer-Shock Wave Interaction. Princeton University Aeronautical Engineering Laboratory Report No. 184, November 30, 1951.

17. Chapman, D. R., Wimbrow, W. R., and Kester, R. H.: Experimental Investigation of Base Pressure on Blunt-Trailing-Edge Wings at Supersonic Velocities. NACA Technical Note No. 2611, (January, 1952).

18. van Driest, E. R.: Turbulent Boundary Layer in Compressible Fluids. J. Aero. Sci., vol. 18, no. 3 (March, 1951), pp. 145-160 and p. 216.

19. Wilson, R. E.: Turbulent Boundary Layer Characteristics at Supersonic Speeds - Theory and Experiment. J. Aero. Sci., vol. 17, No. 9 (September, 1950), pp. 585-593.

20. Bogdonoff, S. M.: A Preliminary Study of Reynolds Number Effects on Base Pressure at M = 2.95. Princeton University Aeronautical Engineering Laboratory Report No. 182, June 12, 1951.

21. Bursnall, W. J. and Loftin, L. K.: Experimental Investigation of Localized Regions of Laminar-Boundary Layer Separation. NACA Technical Note No. 2338 (April, 1951).

22. Bardsley, O. and Mair, W. A.: The Interaction between an Oblique Shock-Wave and a Turbulent Boundary Layer. Phil. Mag., ser. 7, vol. 42, pp. 29-36, January, 1951.

TABLE I. The Function J(M) in Radian Measure.

M	J(M)
1.0	0
1.40	.01587
1.50	.02461
1.60	.03486
1.70	.04604
1.80	.05795
1.90	.07035
2.00	.08305
2.10	.09588
2.20	.10872
2.30	.12144
2.40	.13397
2.50	.14626
2.60	.15824
2.70	.16989
2.80	.18118
2.90	.19209
3.00	.20262
3.10	.21277
3.20	.22253
3.30	.23191
3.40	.24091
3.50	.24955
3.60	.25783
3.70	.26577
3.80	.27338
3.90	.28067
4.00	.28766

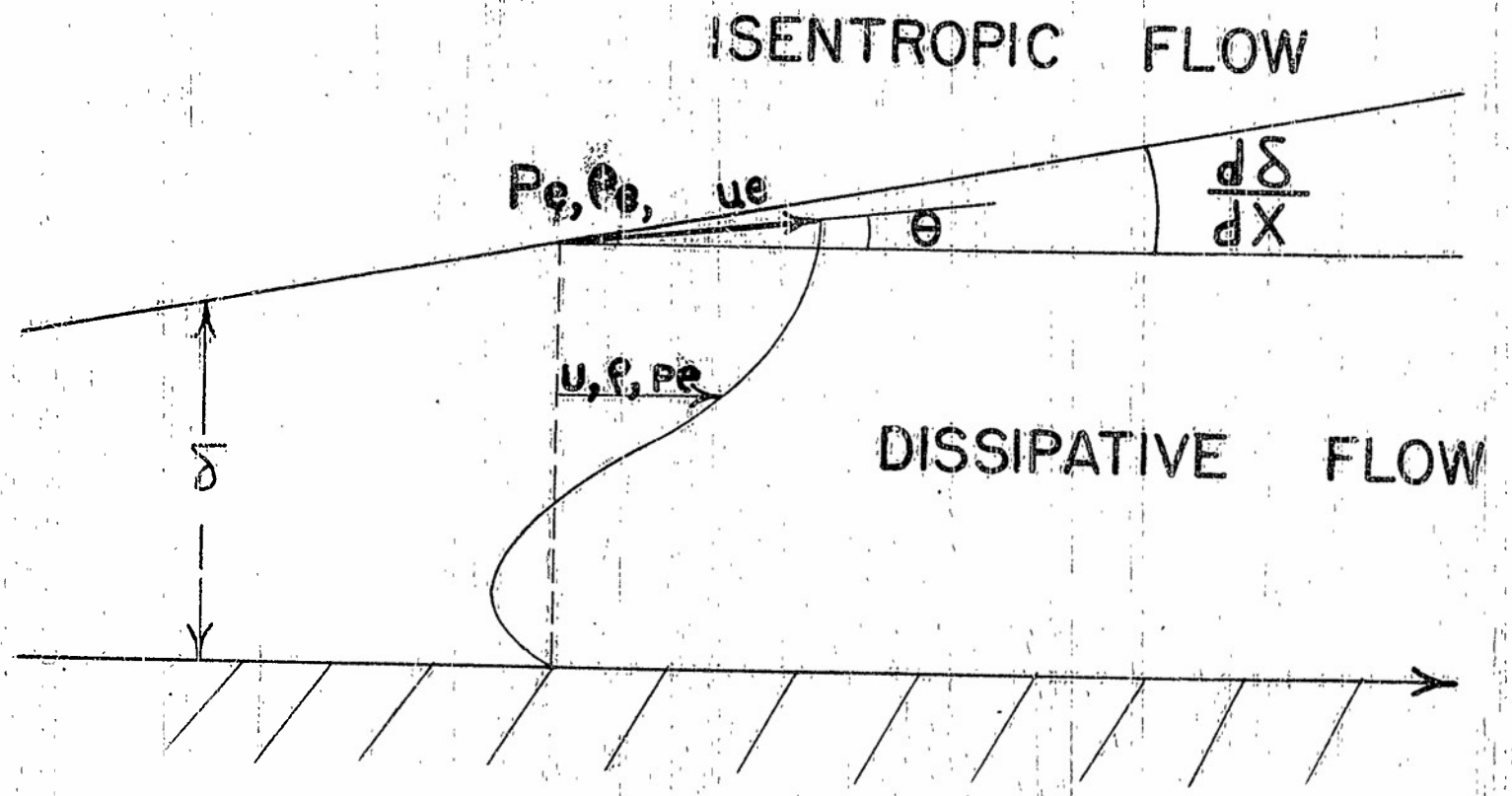

FIGURE 1. THE TWO DISTINCT FLOW REGIONS.

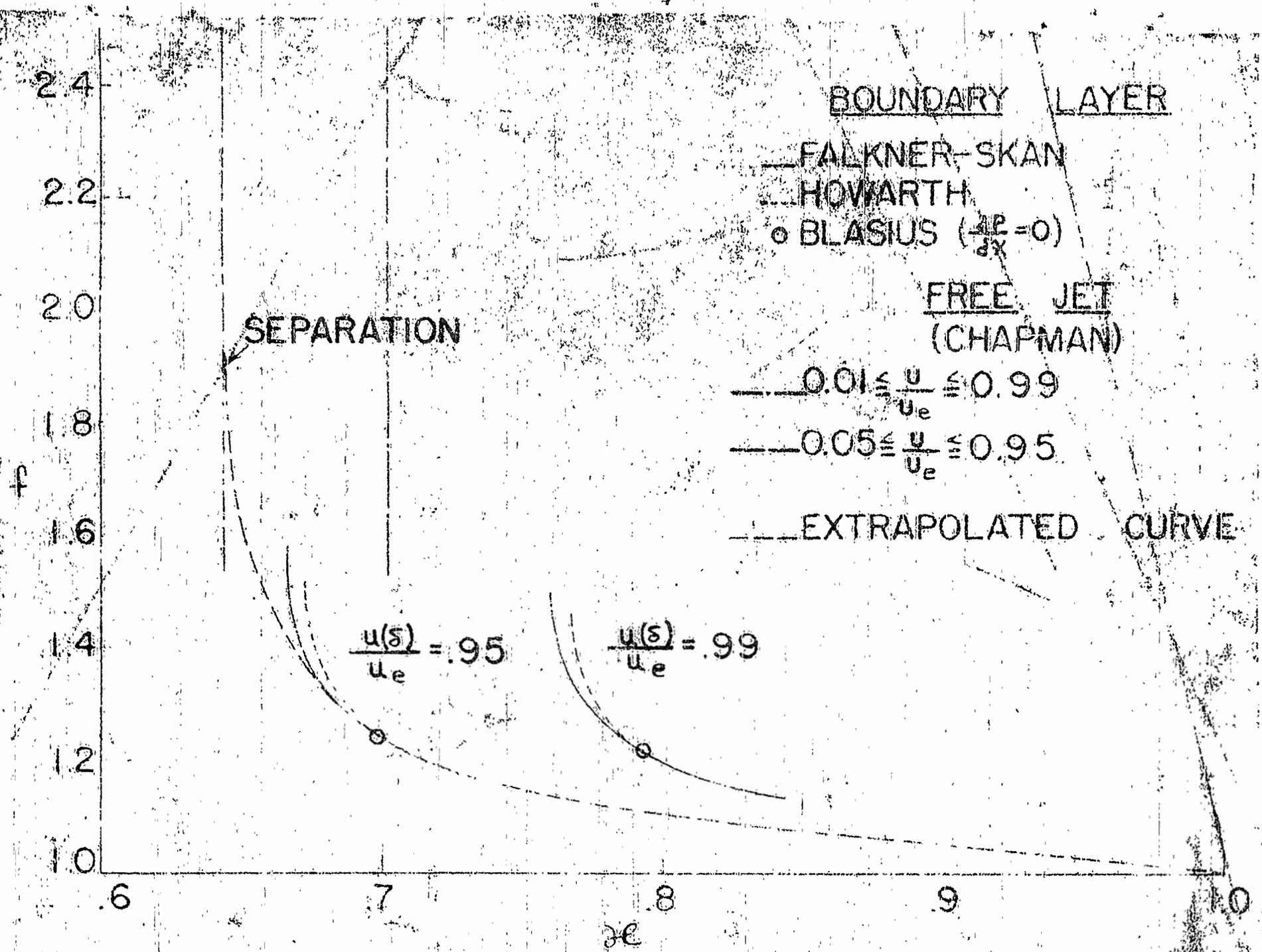

FIGURE 2a. LAMINAR FLOWS.

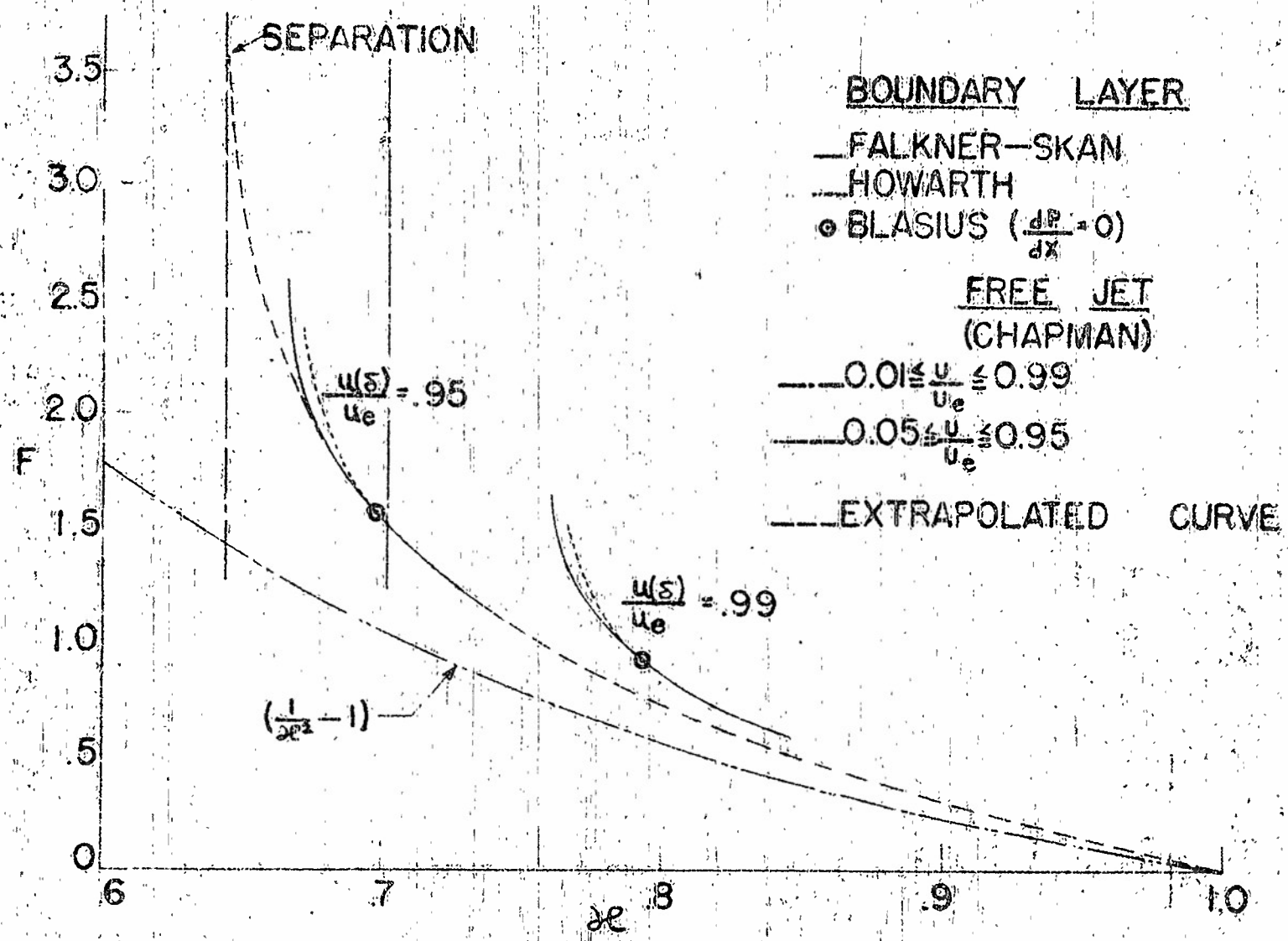

FIGURE 2b. LAMINAR FLOWS.

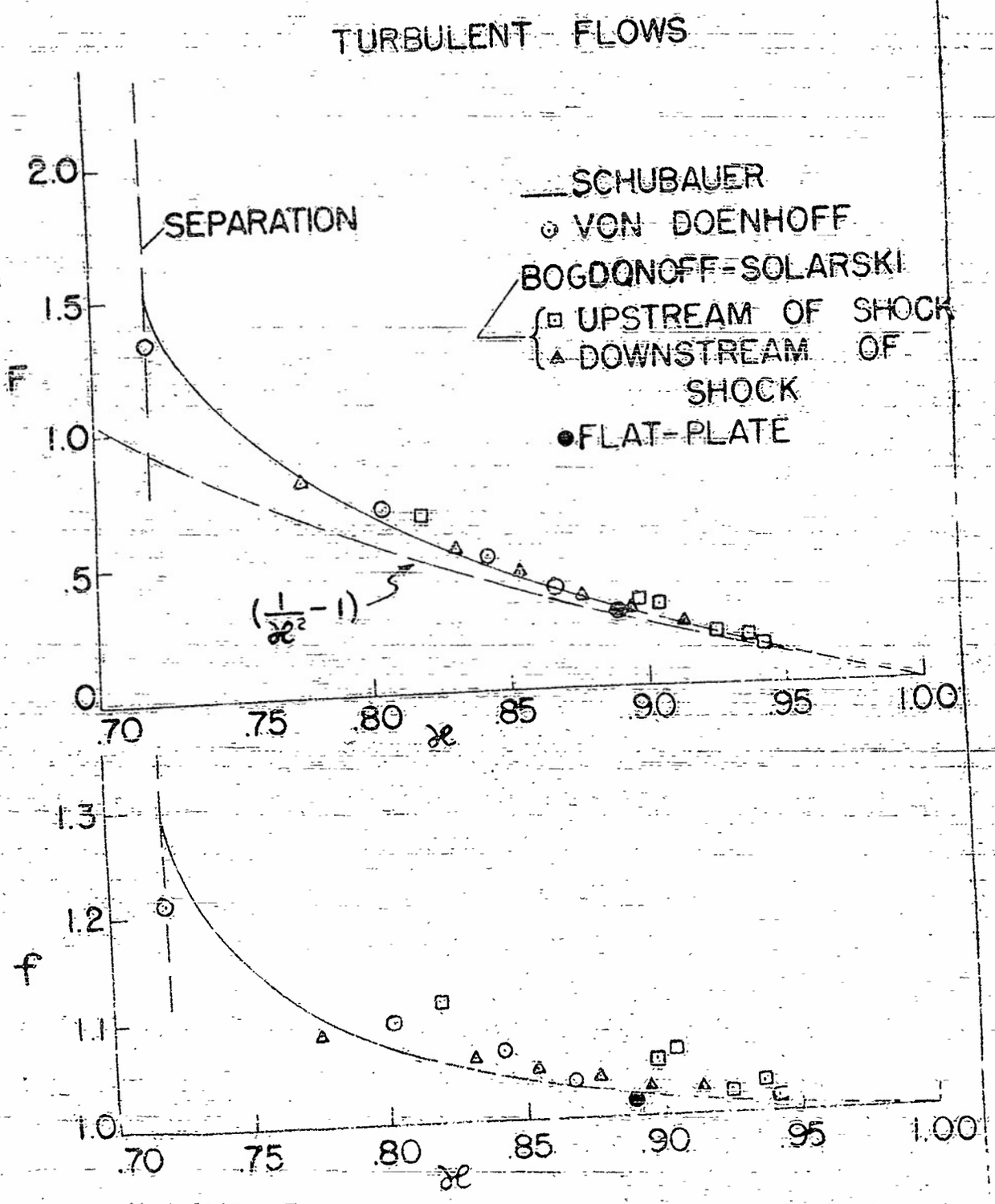
TURBULENT FLOWS
SEPARATION
SCHUBAUER
VON DOENHOFF
BOGDONOFF-SOLARSKI
UPSTREAM OF SHOCK
DOWNSTREAM OF SHOCK
FLAT-PLATE
F
f
$(\frac{1}{\varkappa^2}-1)$
$\varkappa$
2.0
1.5
1.0
.5
0
1.3
1.2
1.1
1.0
.70
.75
.80
.85
.90
.95
1.00

FIGURE 3a.

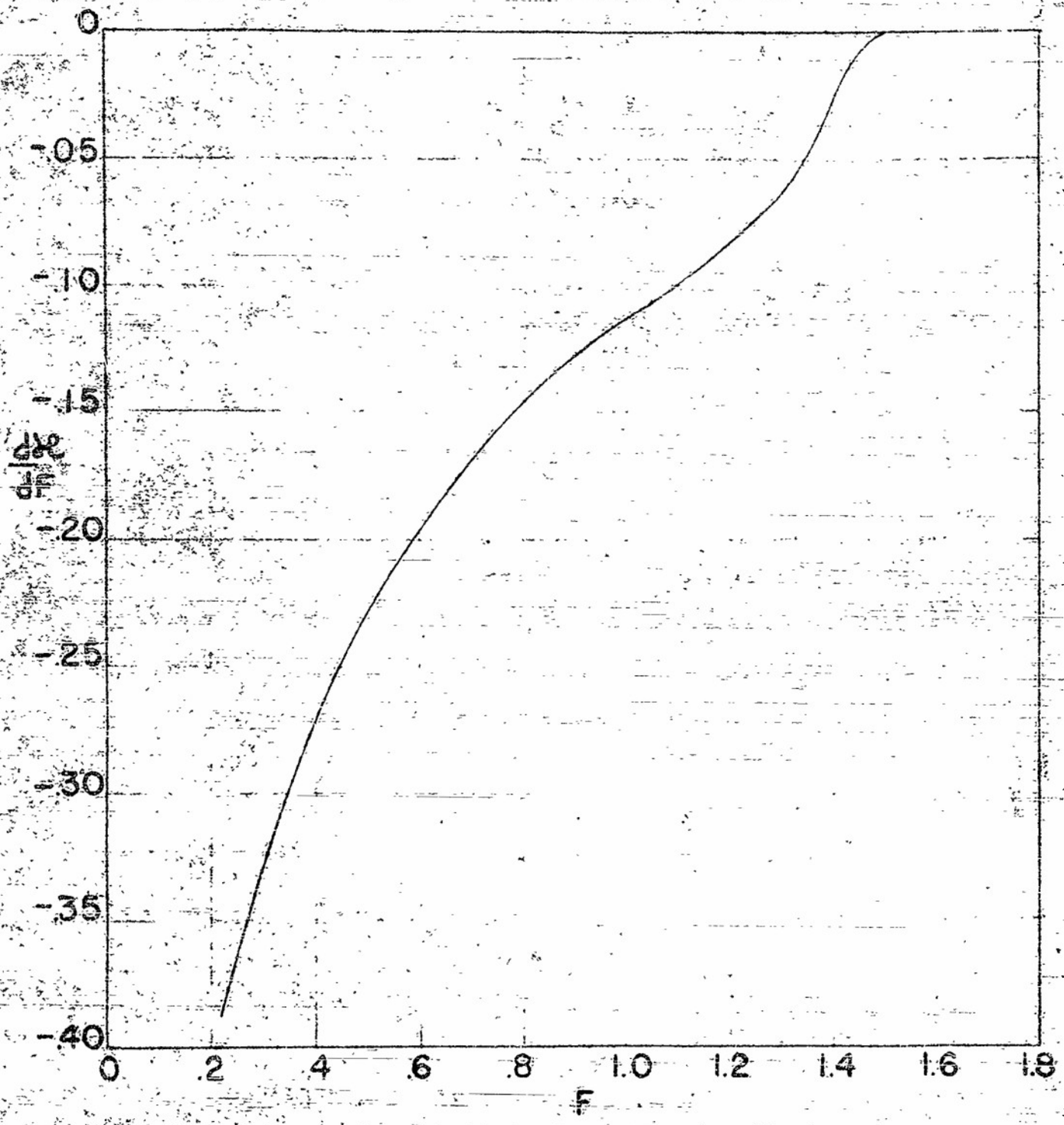

FIGURE 3b. $\frac{d\mathcal{R}}{dF}$ VS. F FOR TURBULENT FLOWS

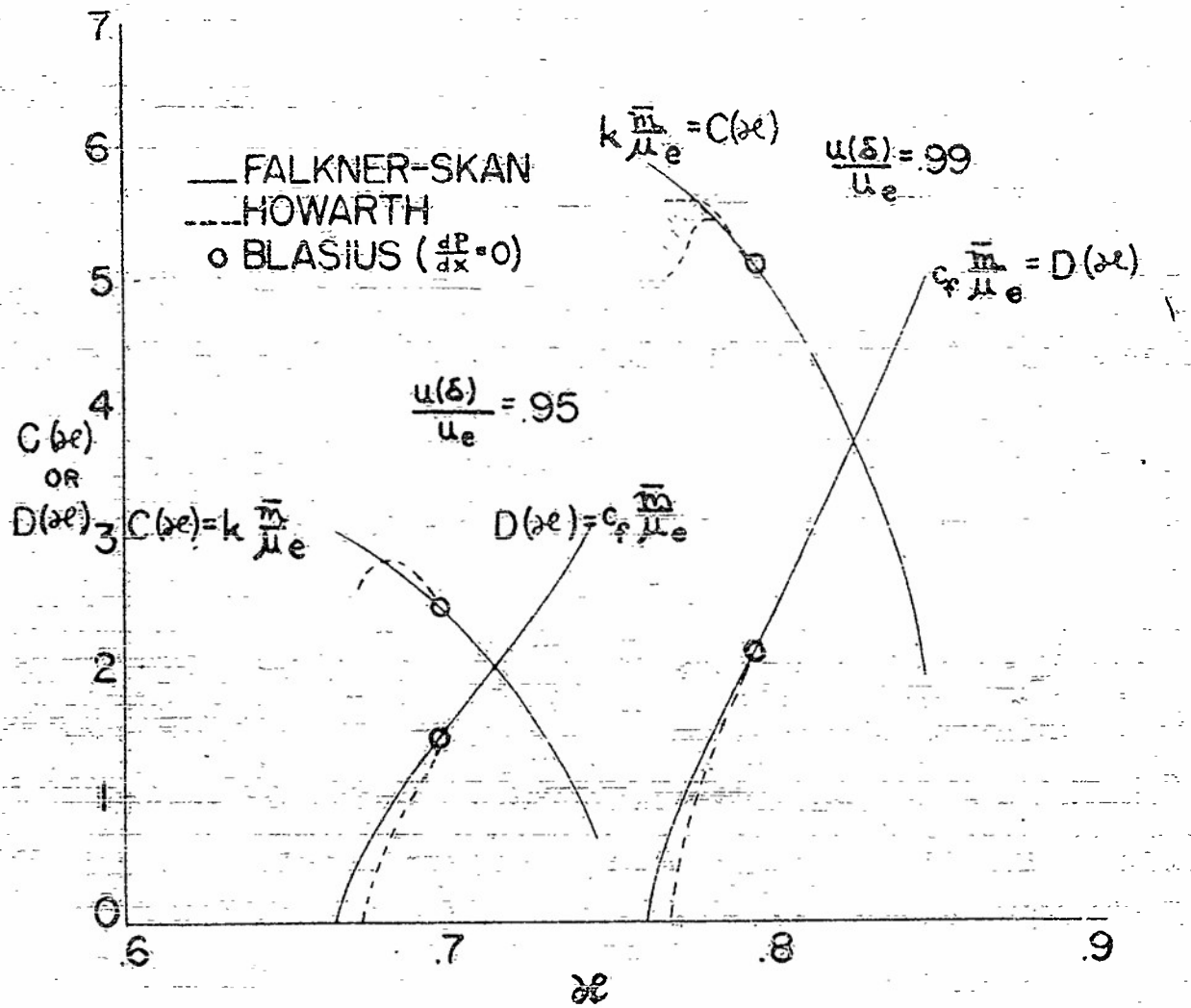

FIGURE 4. MIXING AND SKIN FRICTION COEFFICIENTS FOR LAMINAR FLOWS.

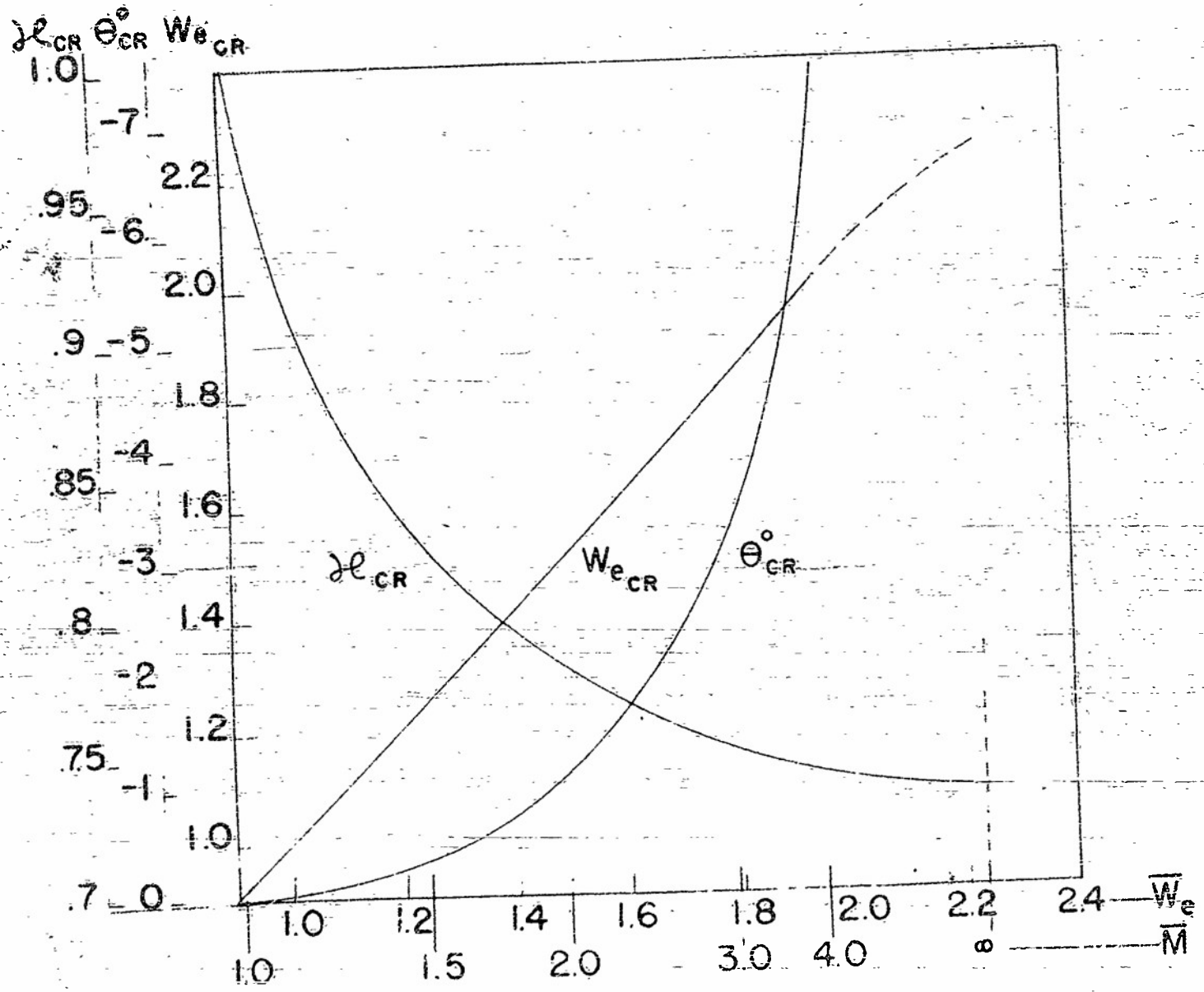

FIGURE 5. VALUES OF $\mathcal{H}$, Θ, W_e AT CRITICAL POINT FOR TURBULENT FLOW. $k=0.03$

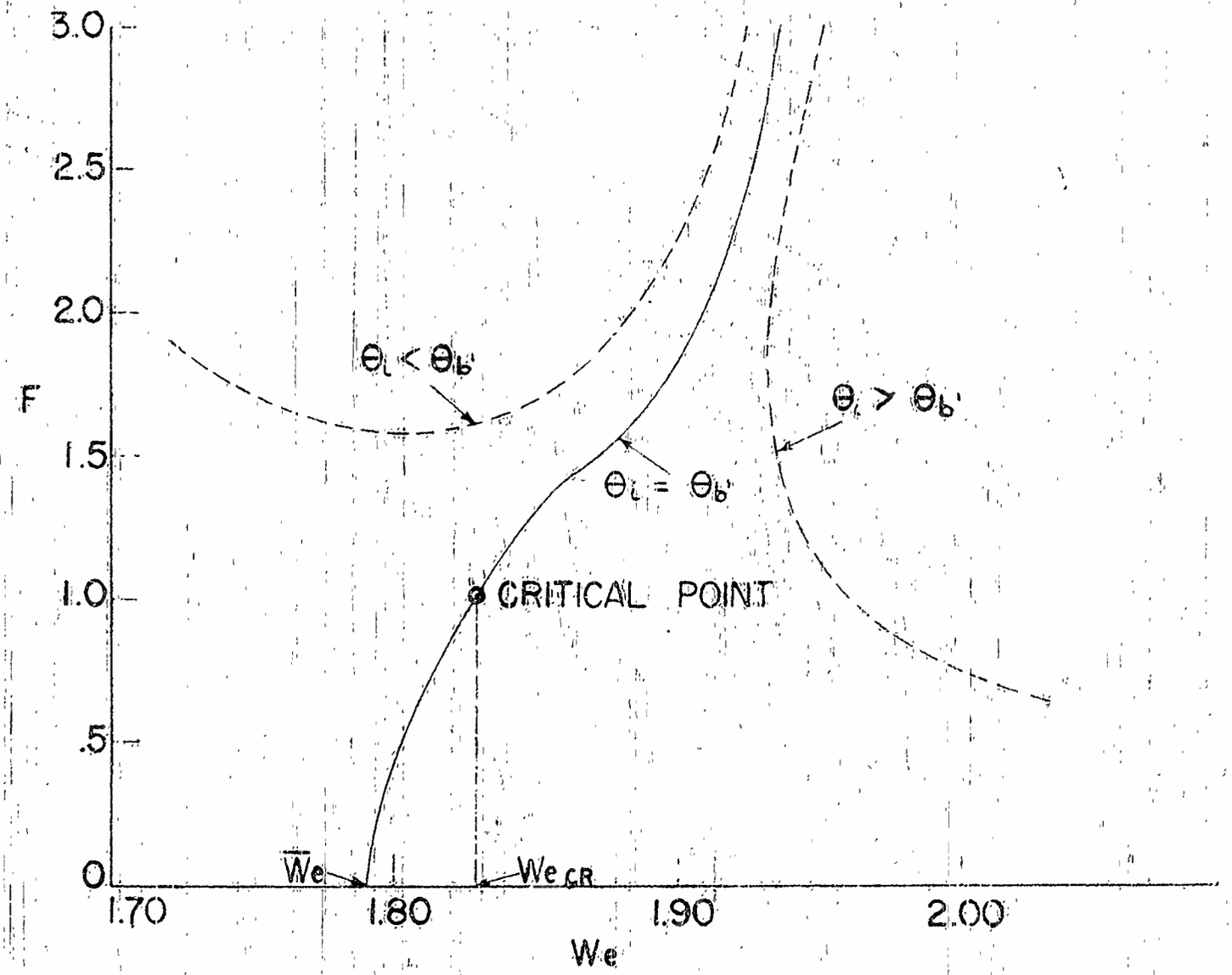

FIGURE 6. SIGNIFICANCE OF CRITICAL POINT, SHOWING INTEGRAL CURVE FOR $\overline{M}$=3.0 k=0.03, TURBULENT FLOW.

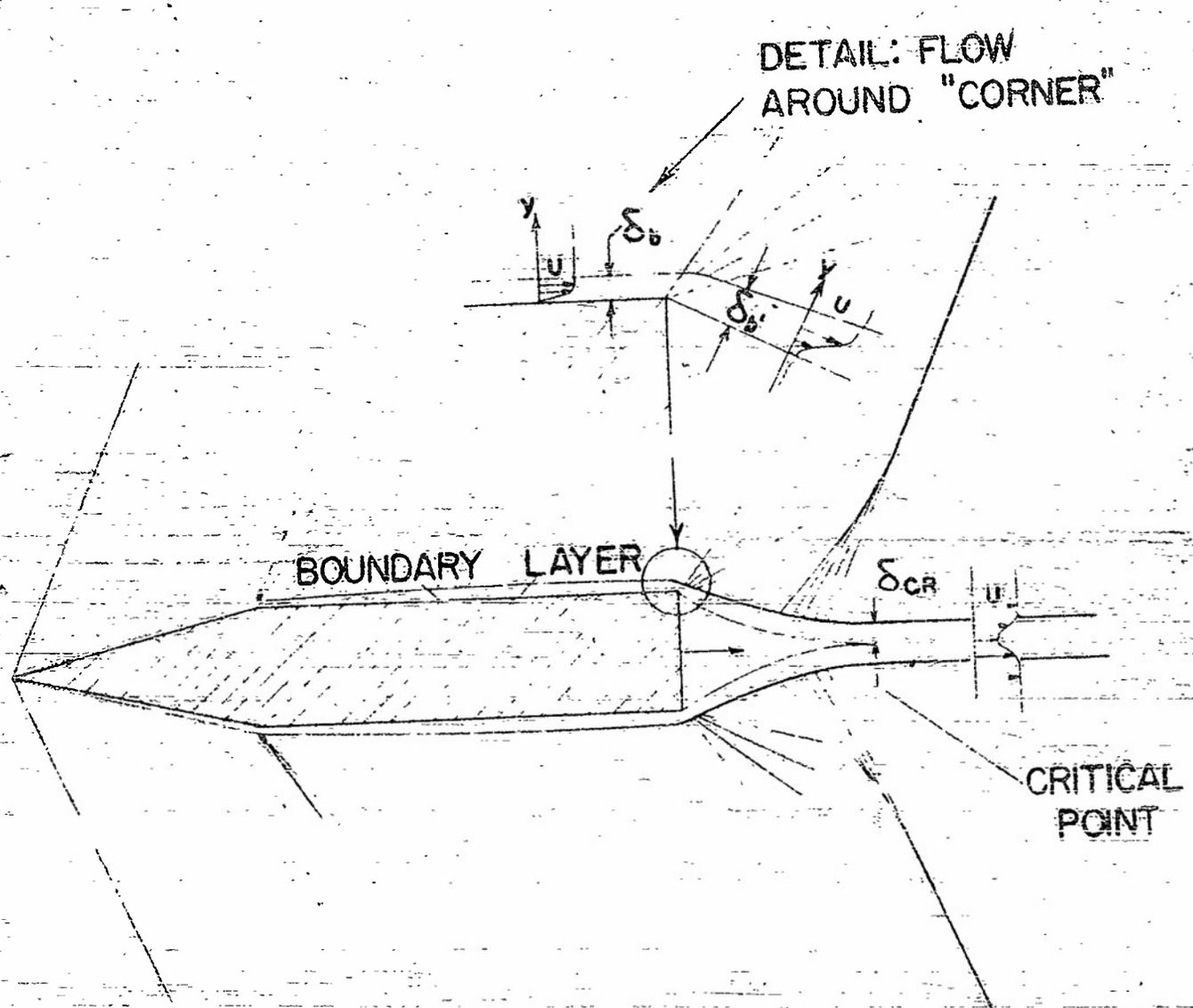

FIGURE 7. SCHEMATIC REPRESENTION OF FLOW OVER SUPERSONIC AIRFOIL WITH BLUNT TRAILING-EDGE.

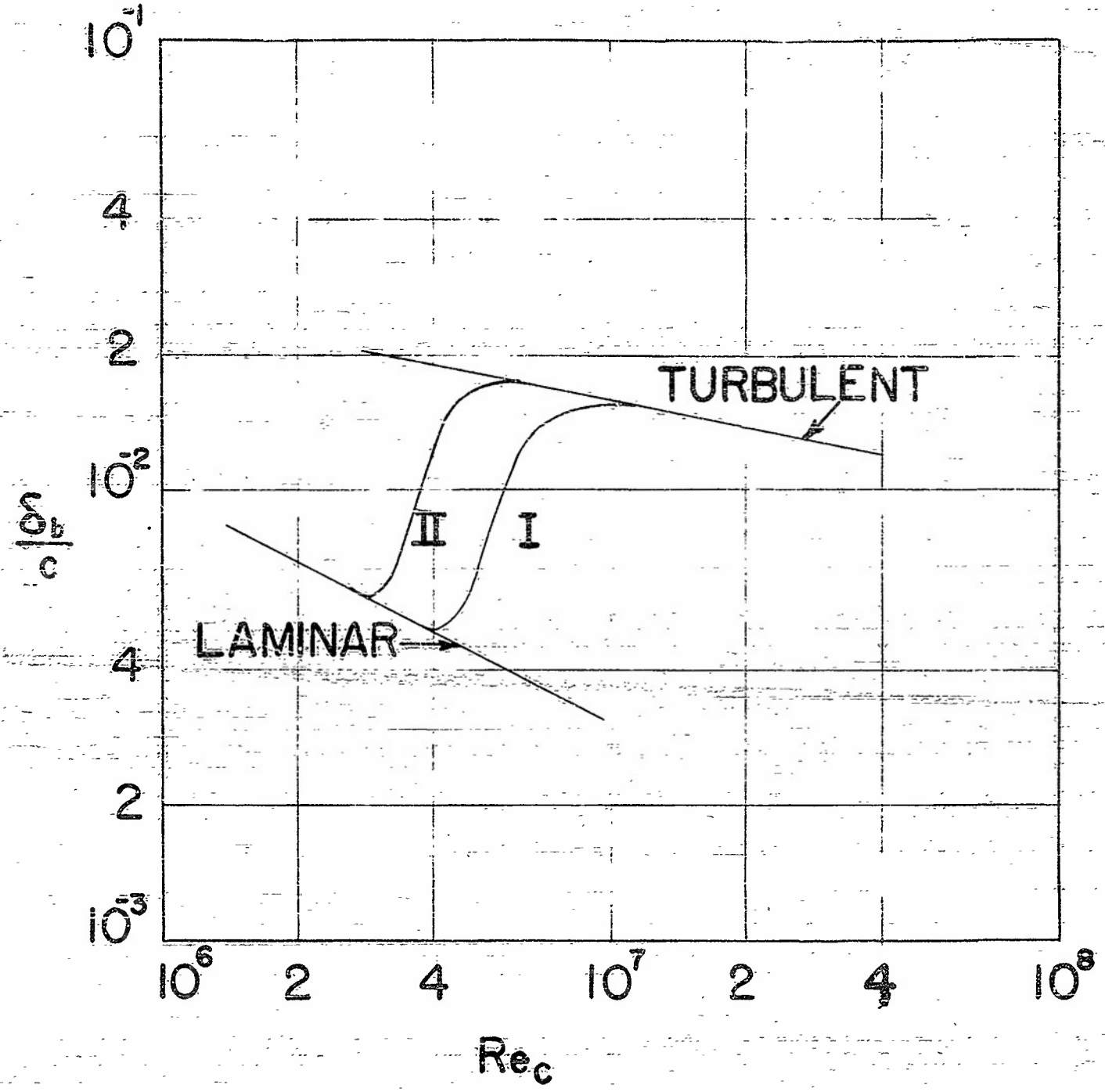

FIGURE 8. BOUNDARY LAYER THICKNESS VS. REYNOLDS NUMBER, SHOWING THE TWO ASSUMED TRANSITION CURVES. M=3.0

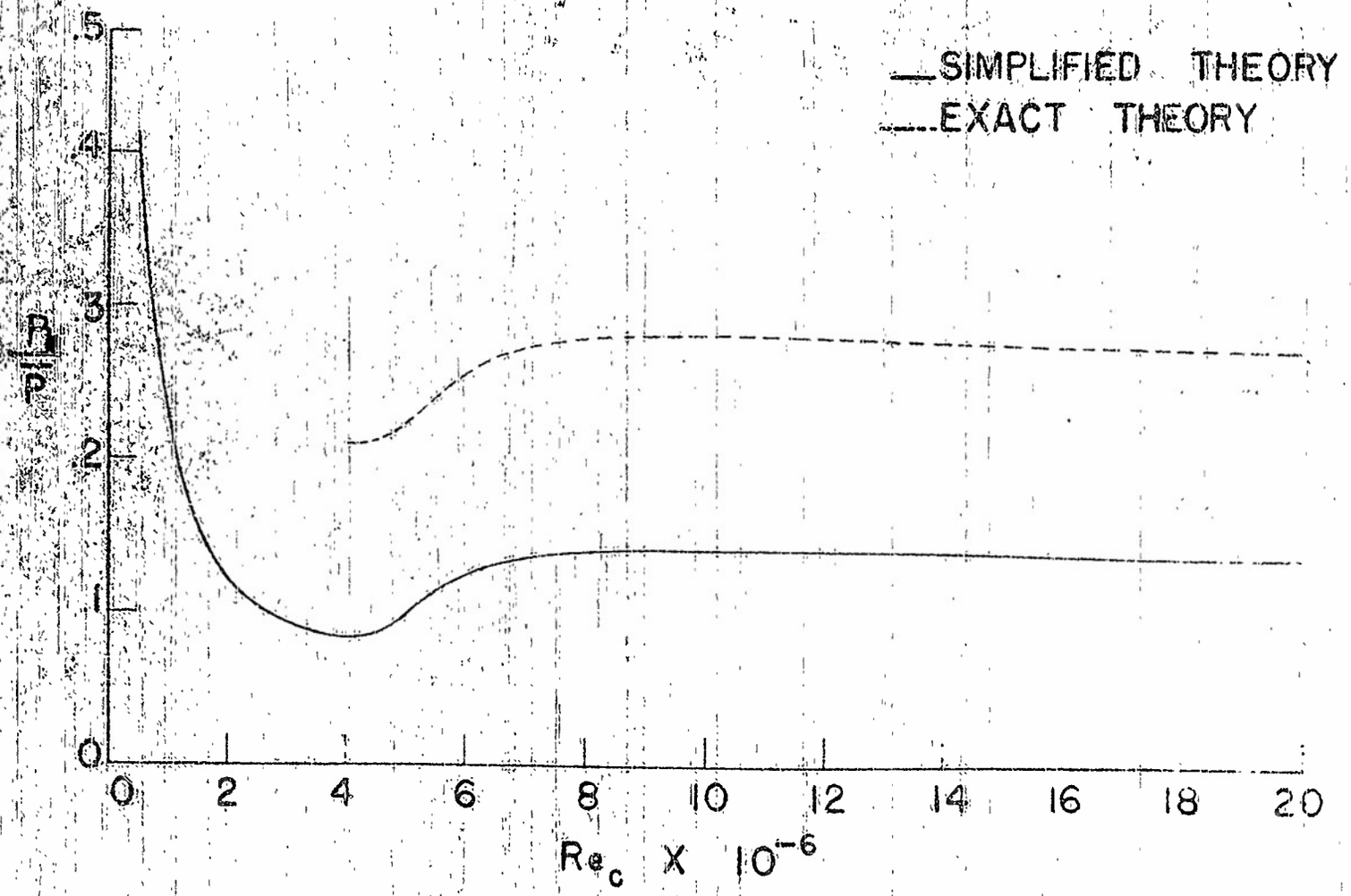

FIGURE 9. BASE PRESSURE RATIO VS. REYNOLDS NUMBER. $M = 3.0$, $k_{TURB} = 0.03$, $c/h = 3.0$ TRANSITION CURVE I.

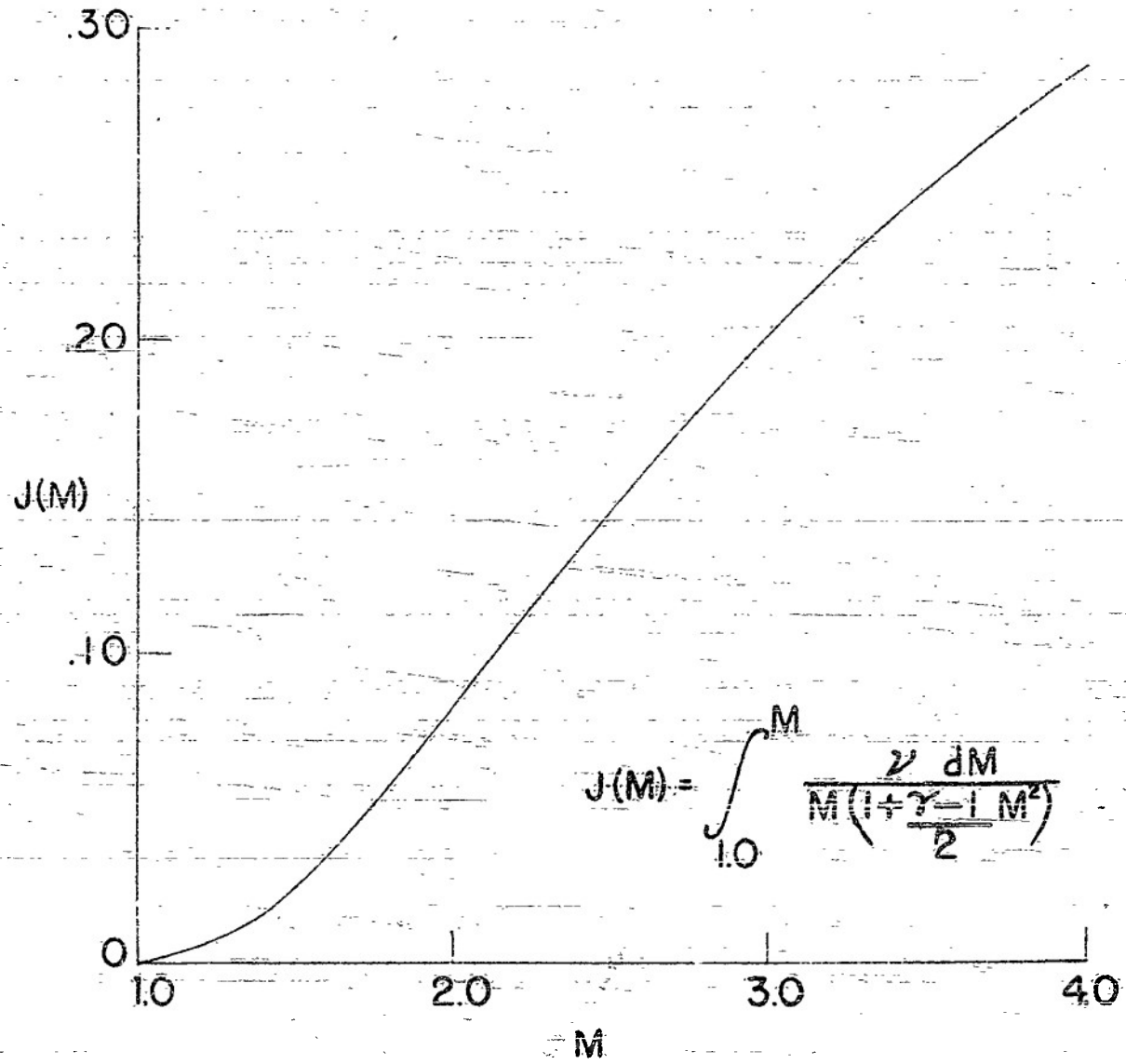

FIGURE 10. THE FUNCTION J(M)

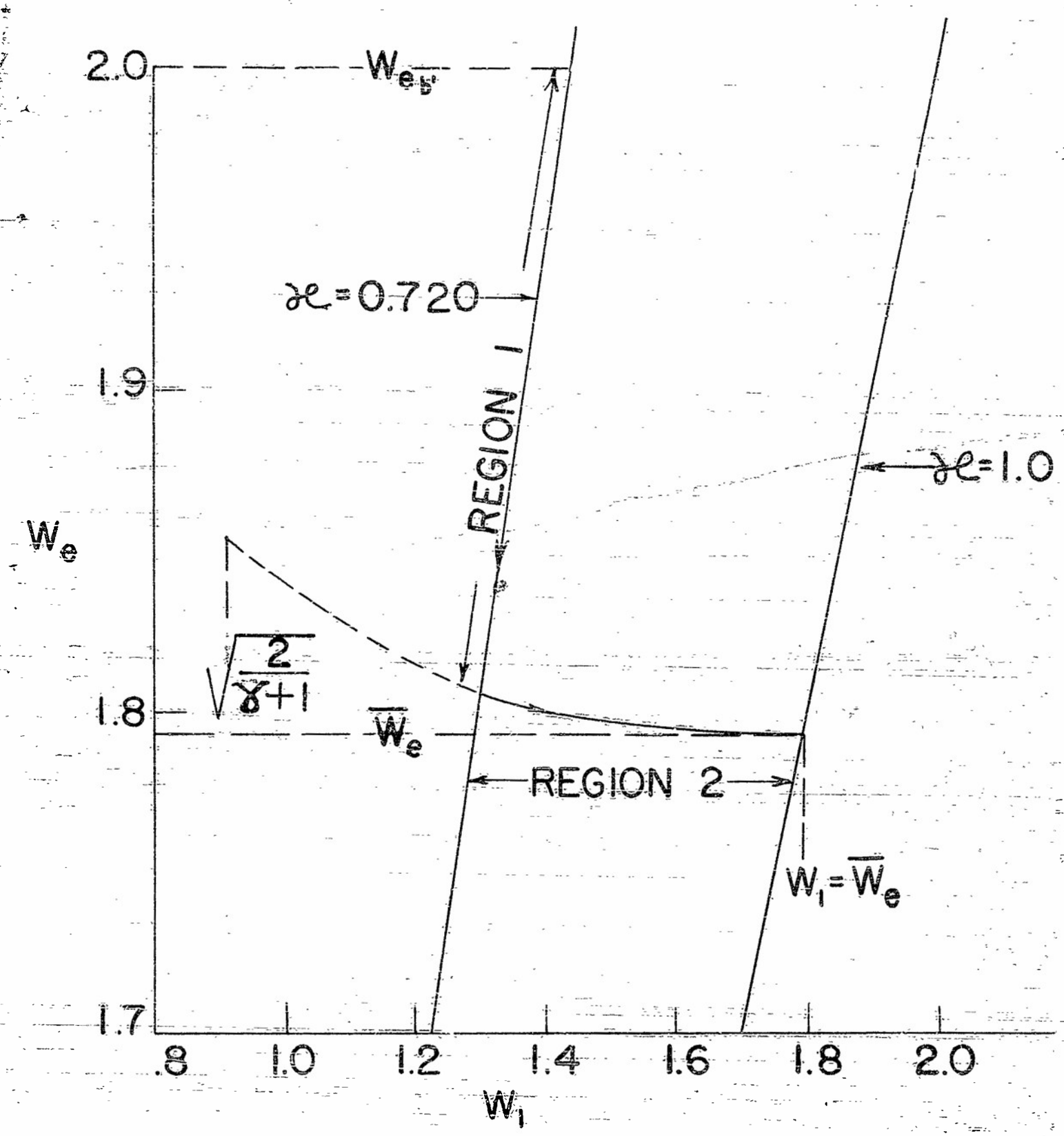

FIGURE 11. RECOMPRESSION IN TURBULENT WAKE. M=3.0, k=.03

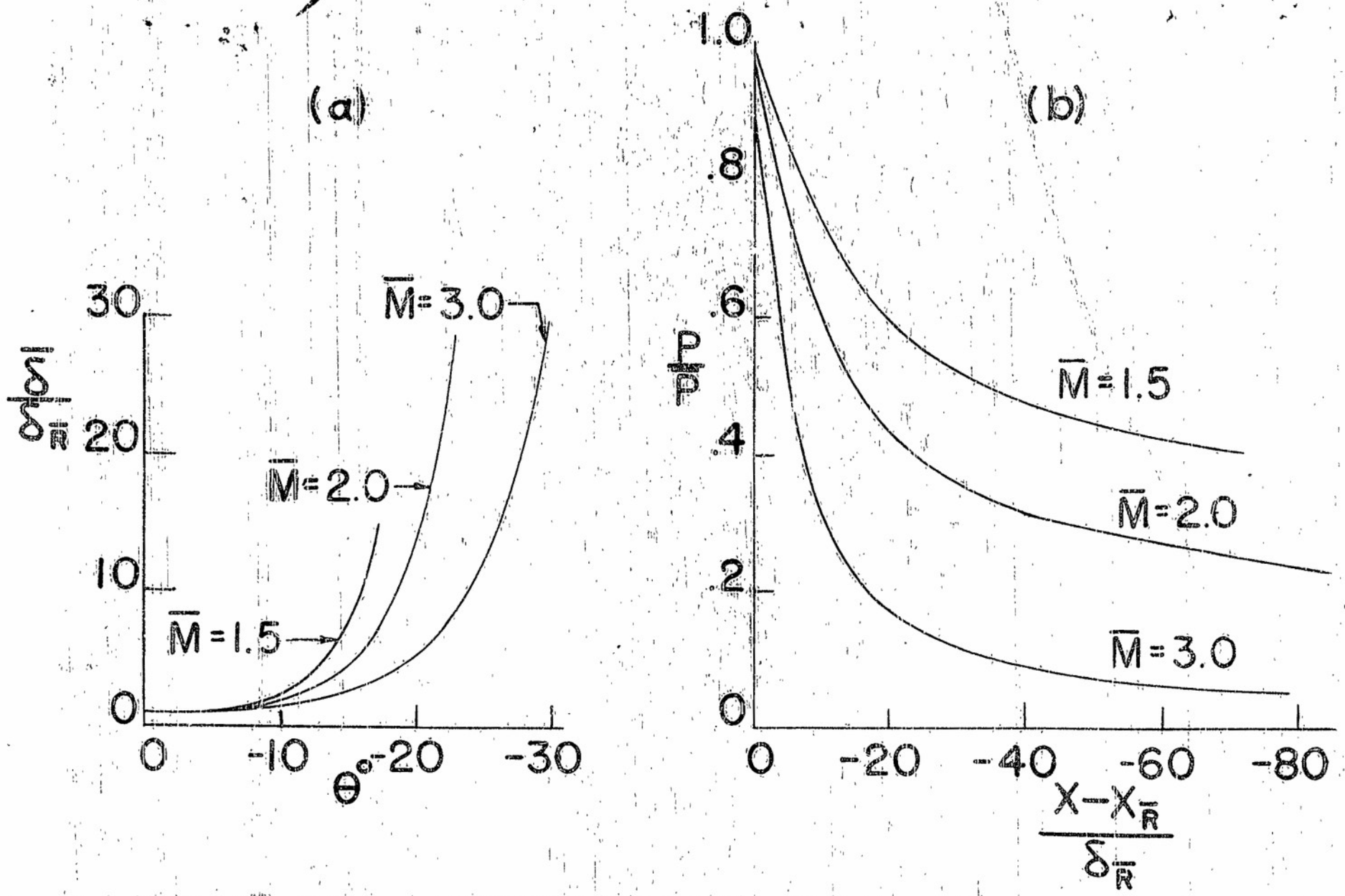

FIGURE 12. VARIATION OF THICKNESS OF DISSIPATIVE FLOW REGION AND THE STATIC PRESSURE ALONG THE AXIS IN TURBULENT WAKE. k = .03 SIMPLIFIED THEORY.

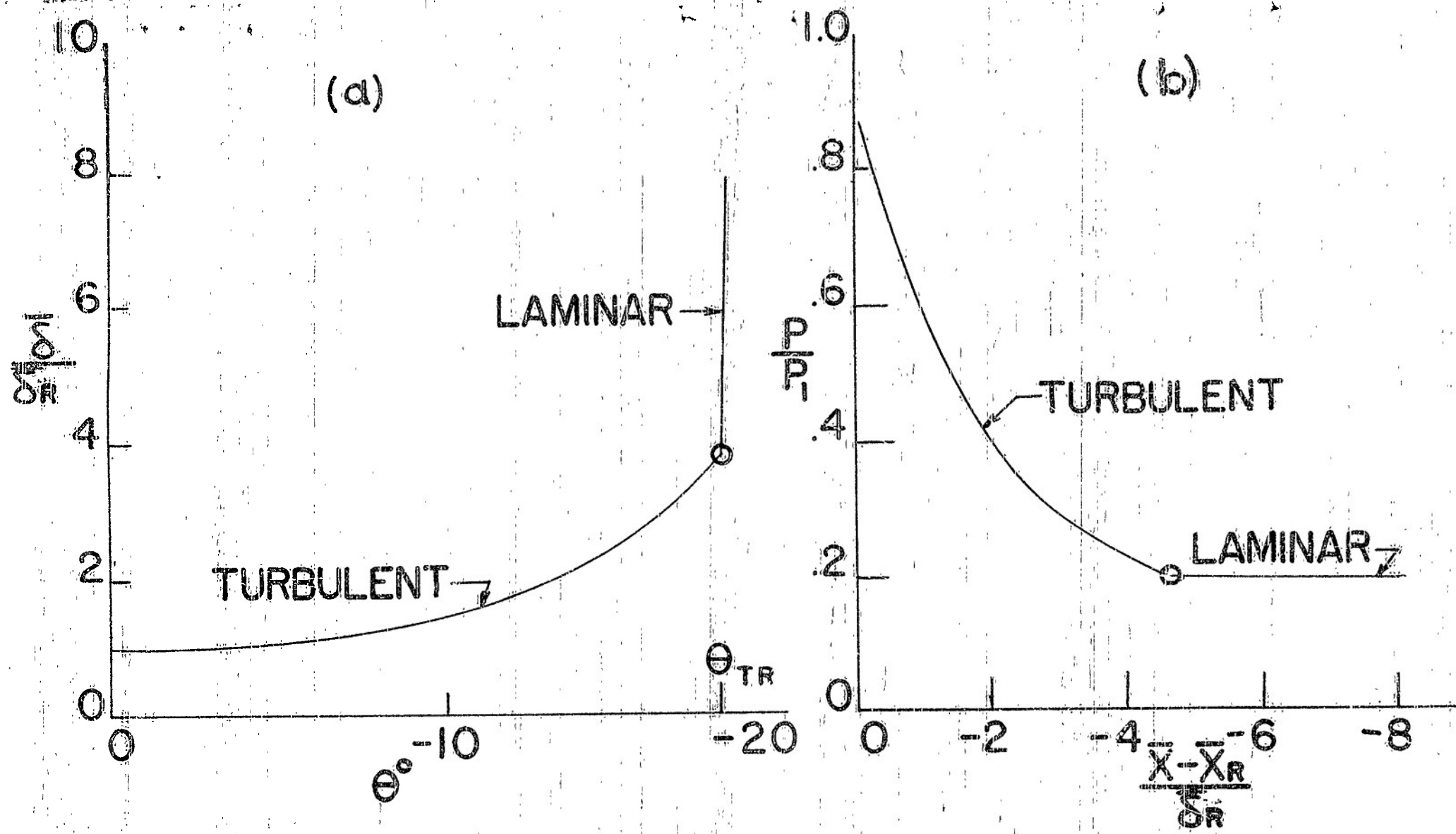

FIGURE 13. VARIATION OF THICKNESS OF DISSIPATIVE FLO REGION AND STATIC PRESSURE ALONG AXIS. TRANSITION IN WAKE

$M=3.0$, $k_{TURB}=.03$, $Re_c=2 \times 10^6$, $k_{LAM}=.00124$,

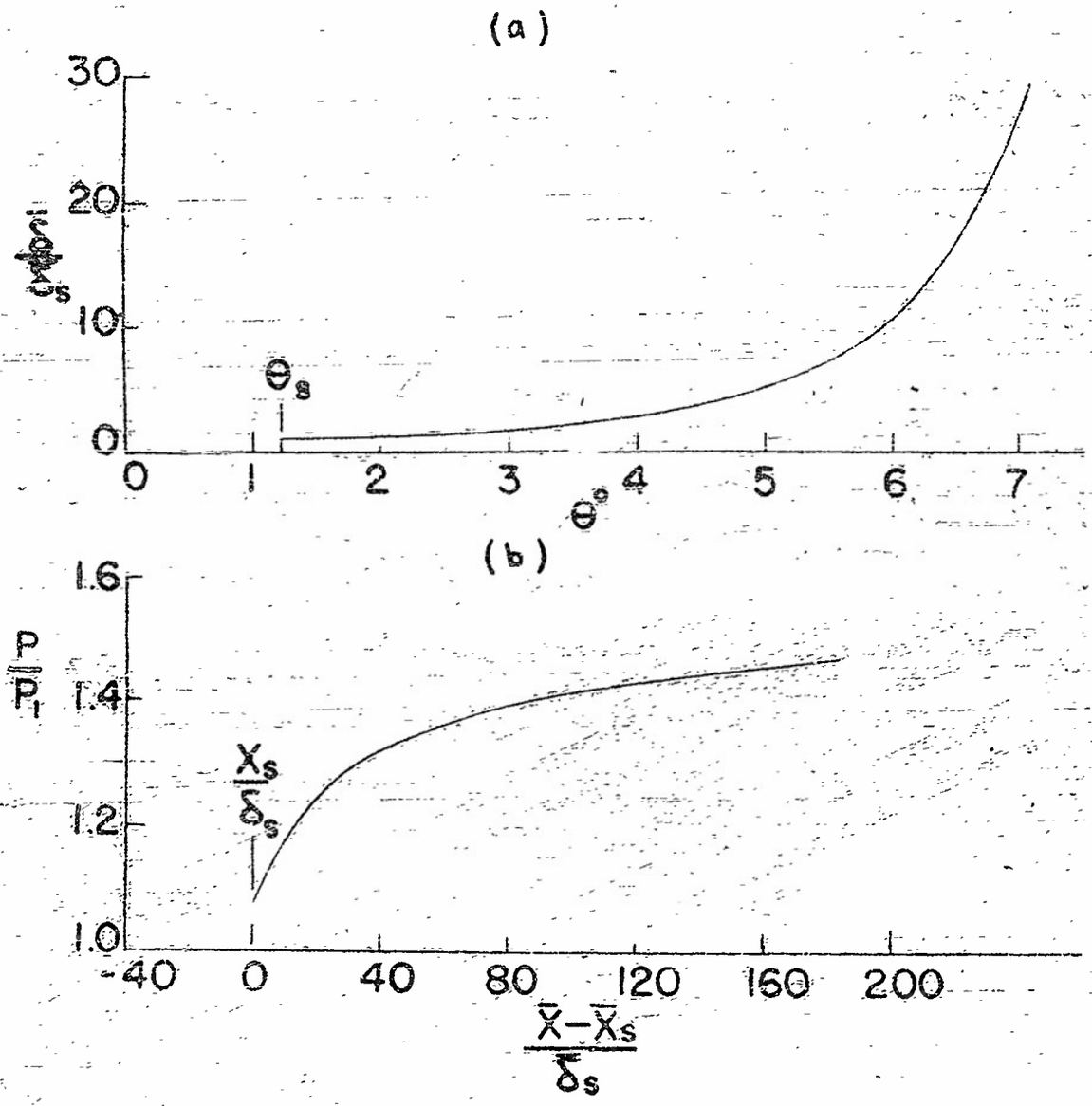

FIGURE 14. VARIATION OF THICKNESS OF SEPARATED LAMINAR FLOW REGION AND STATIC PRESSURE ALONG SURFACE. $M_1 = 2.0$, $Re_{x_s} = 110{,}000$, $k_{LAM} = .0055$, $\theta_s = 1.23°$

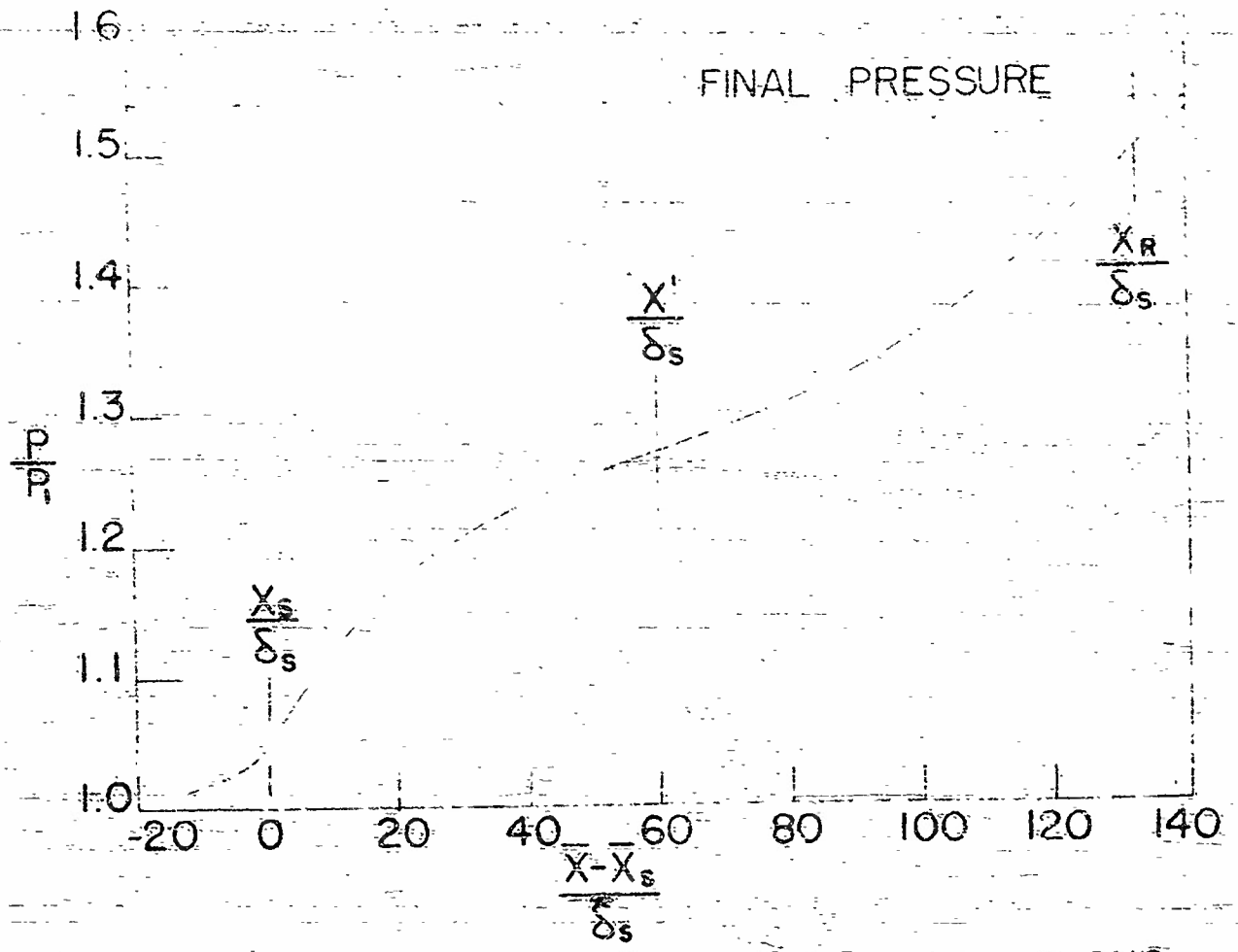

FIGURE 15. STATIC PRESSURE DISTRIBUTION ALONG SURFACE FOR LAMINAR BOUNDARY LAYER — SHOCK WAVE INTERACTION.

$M_{-\infty} = M_1 = 2.0$, $\theta_w = 4^\circ$, $Re_{x_s} = 250{,}000$

$k_{LAM} = .0037$

SIMPLIFIED THEORY

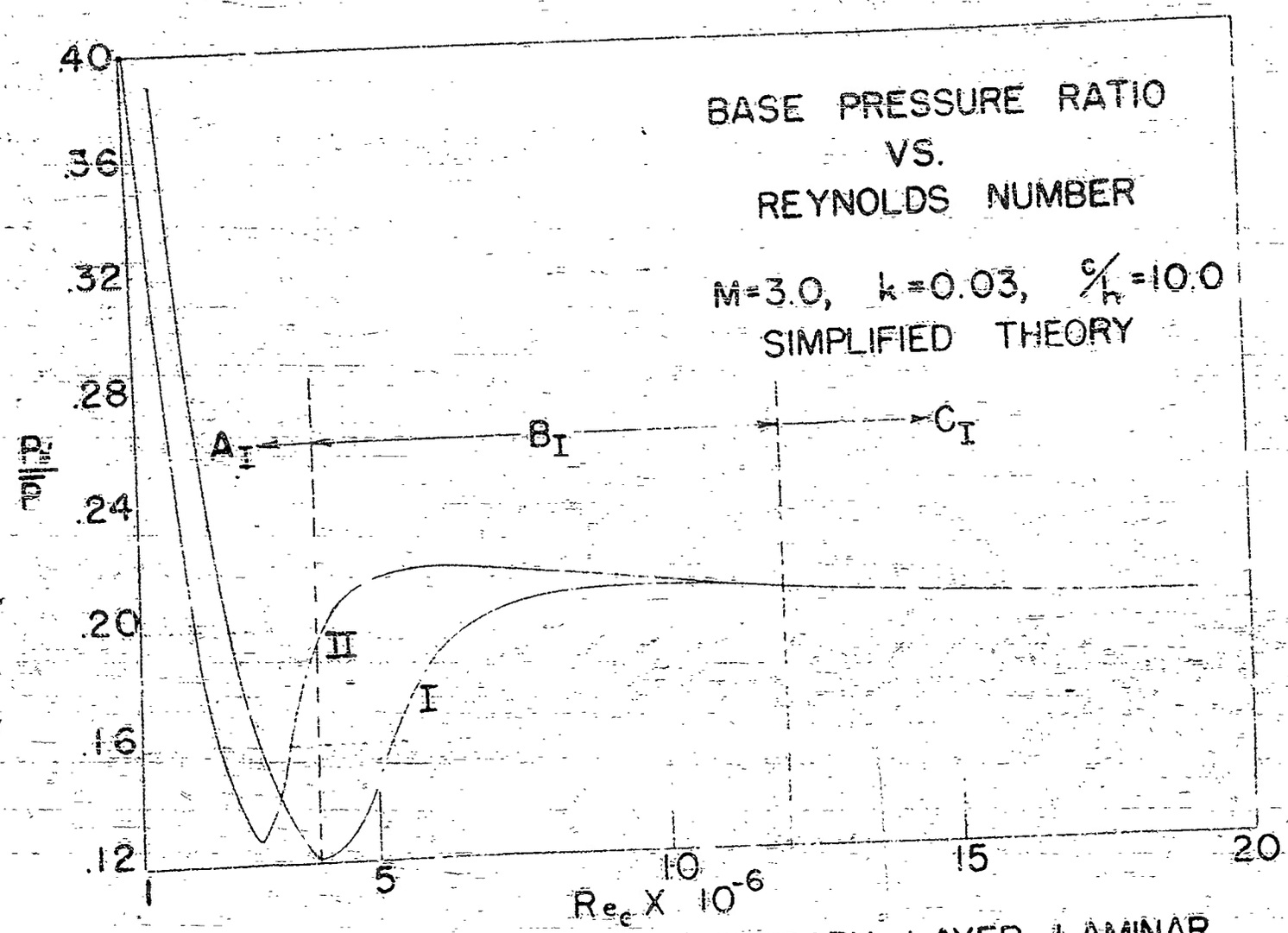

FIGURE 16. REGION A_I - BODY BOUNDARY LAYER LAMINAR, TRANSITION IN WAKE

REGION B_I - TURBULENT WAKE, TRANSITION ON BODY

REGION C_I - FULLY TURBULENT

I & II REFER TO THE TWO DIFFERENT ASSUMED TRANSITION CURVES

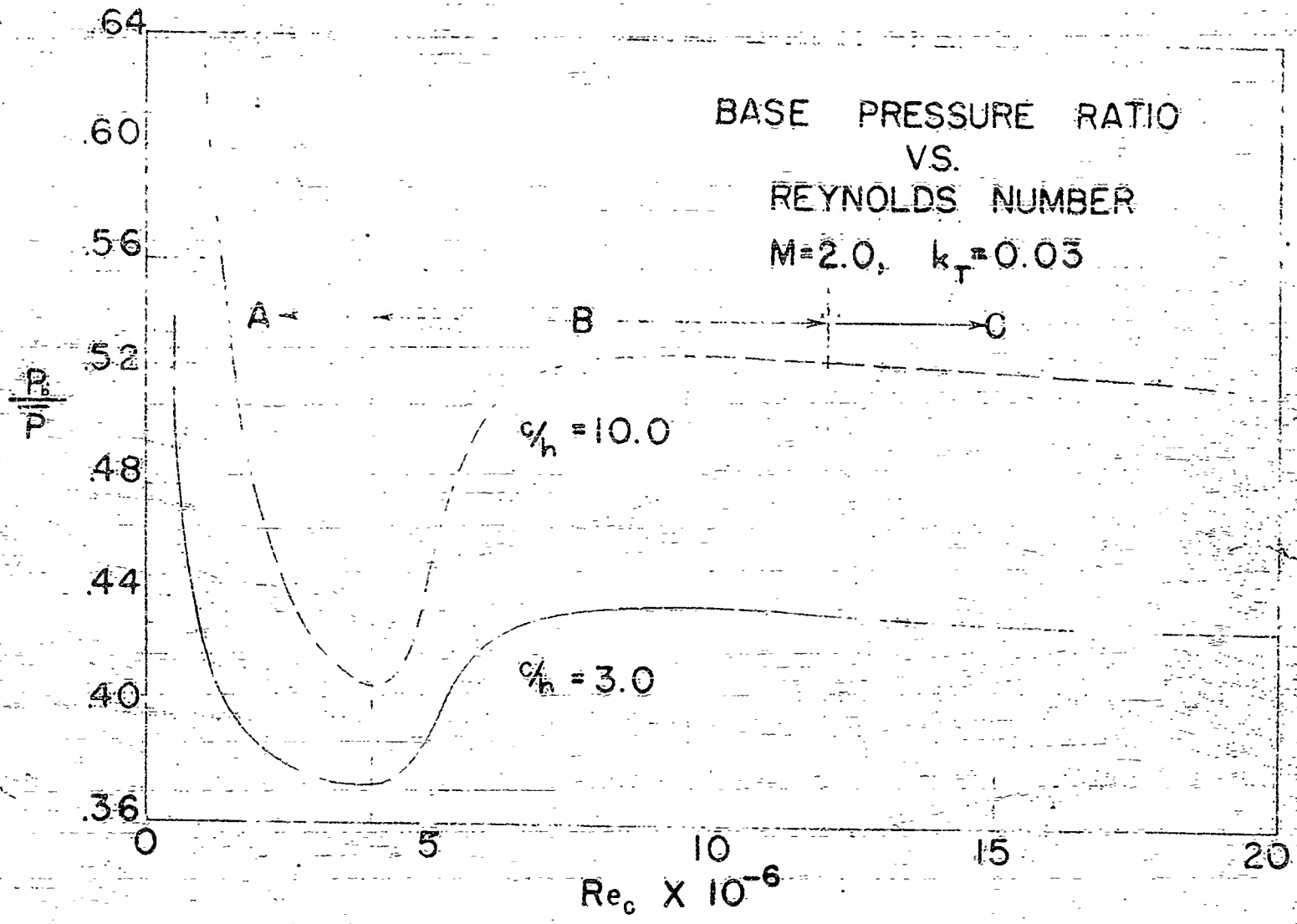

FIGURE 17. REGION A – BODY BOUNDARY LAYER LAMINAR, TRANSITION IN WAKE

REGION B – TURBULENT WAKE, TRANSITION ON BODY

REGION C – FULLY TURBULENT

SIMPLIFIED THEORY – TRANSITION CURVE I

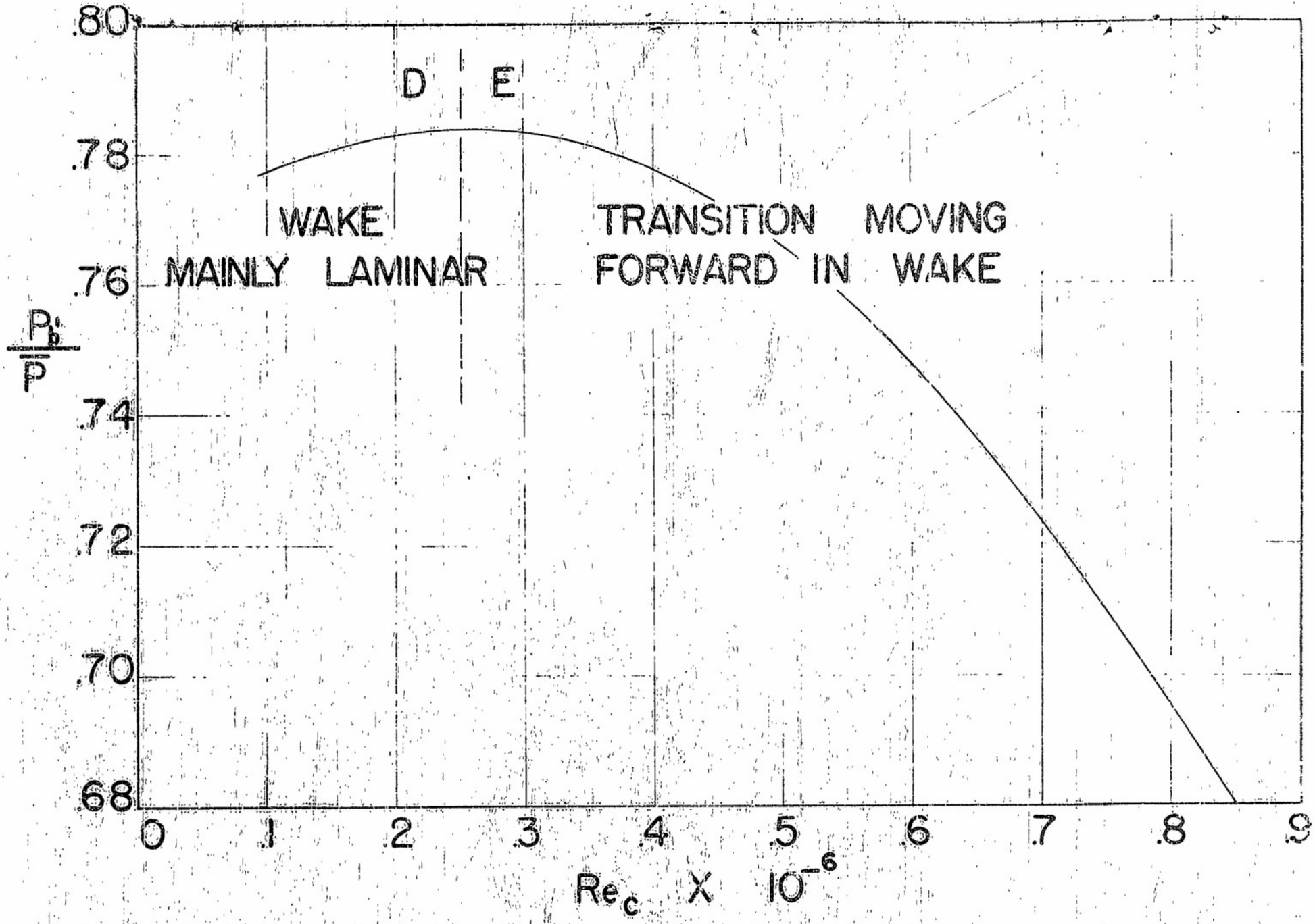

FIGURE 18. BASE PRESSURE RATIO VS. REYNOLDS NUMBER IN LOW REYNOLDS NUMBER REGION. M=2.0, k_T=0.03, δ/h=10.0

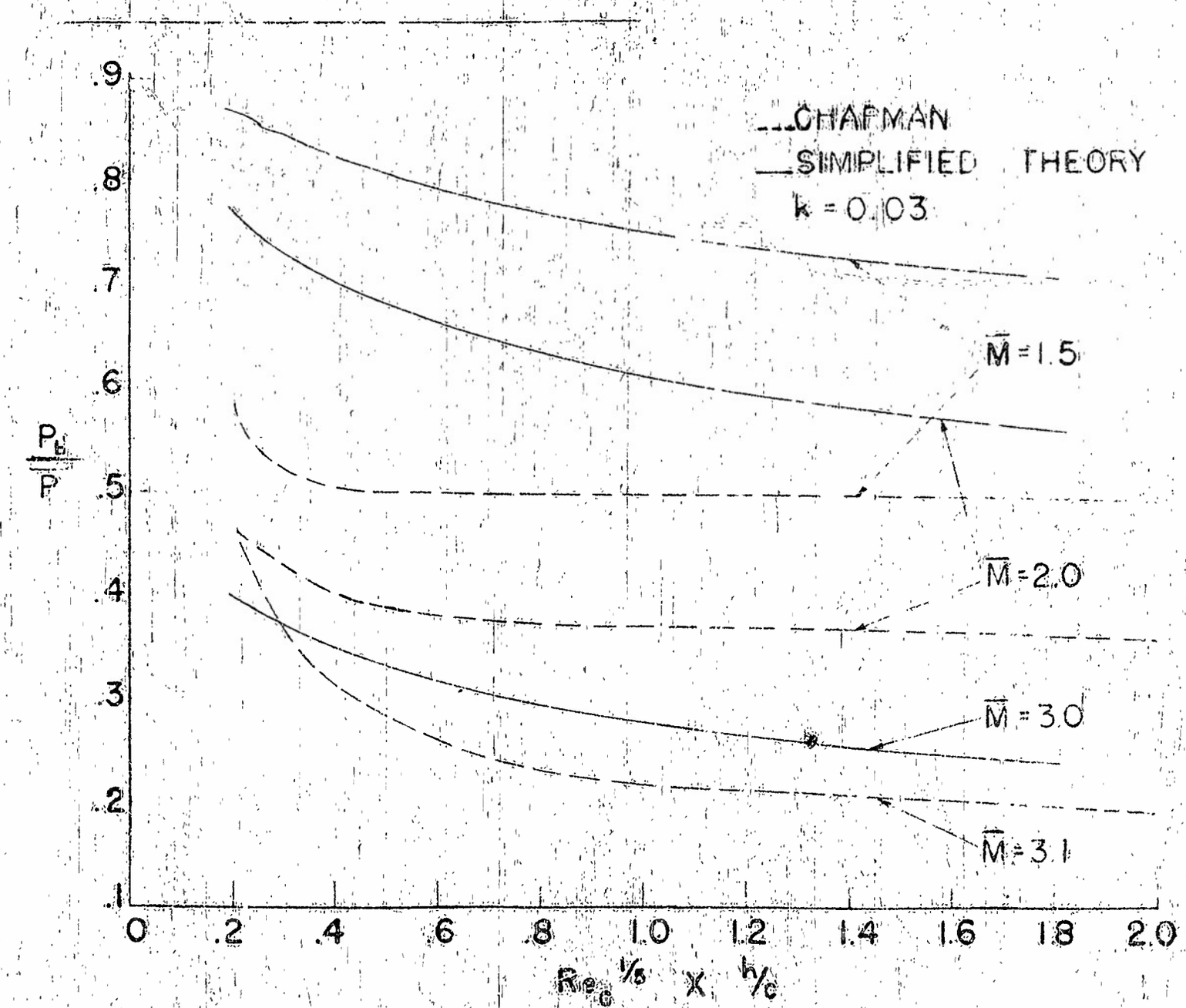

FIGURE 19. BASE PRESSURE IN FULLY TURBULENT REGION.

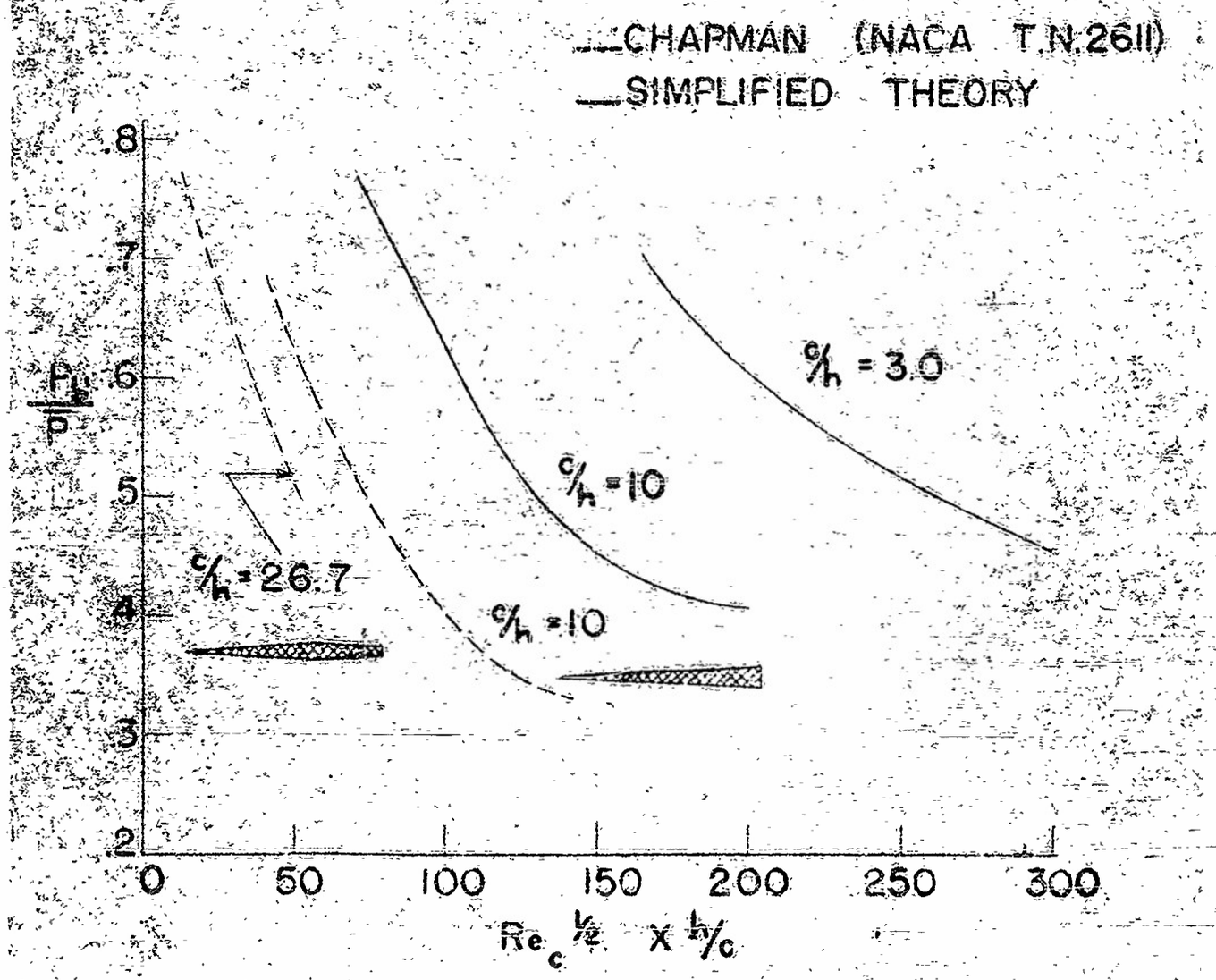

FIGURE 20. TRANSITION IN WAKE, AIRFOIL BOUNDARY LAYER LAMINAR, SHOWING DEPENDENCE OF BASE PRESSURE ON c/h. M=2.0